Quelle physique à l'ILC ?

Prolégomènes

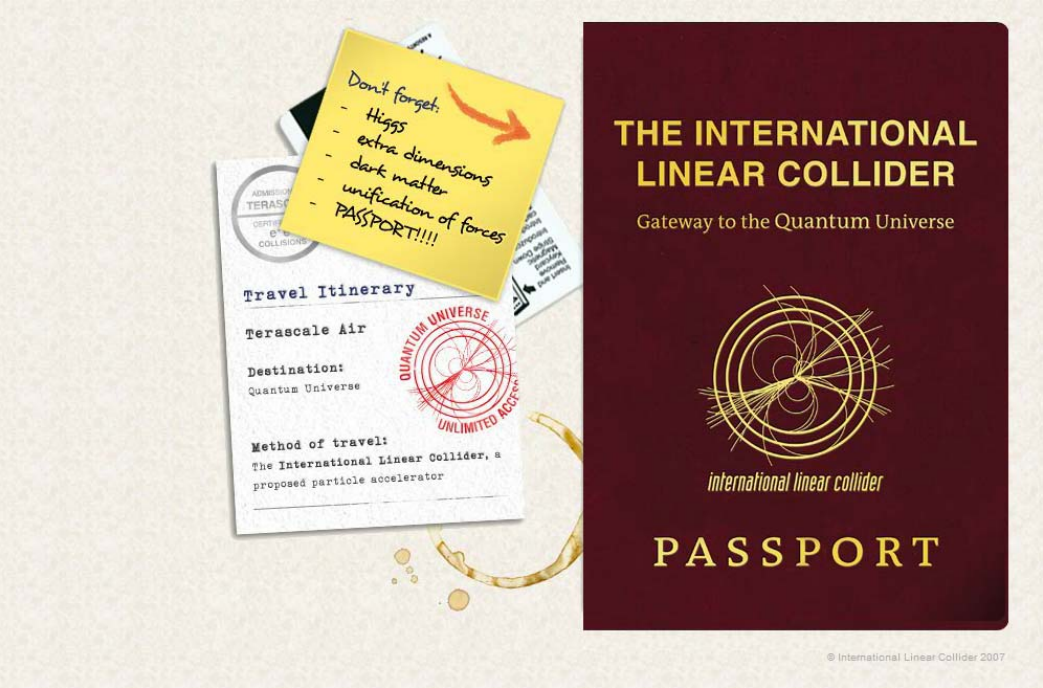

Plan

- Contexte général
- La machine
- Les détecteurs et le contexte expérimental
- Physique
  - Higgs
  - quark top
  - SUSY
  - 2 fermions
  - W/Z
  - Secteurs de Higgs étendus
  - Aspects cosmologiques

Du mouvement...

Martinet noir juin 2013

...et un cap

Du mouvement...

- Passé: 20 ans de R & D
  - Premières idées LC : 1965
  - Première réalisation SLC (SLAC): 1988-98
  - 2004: choix de la technologie froide
  - 2007: ILC Reference Design Report
  - 2009: Lettre d'intentions (LOI) concepts détecteurs ⇨ SiD et ILD
- 2013 dans le monde
  - Début 2013: « mini-TDR » détecteurs (dit DBD)
  - 12 juin 2013: remise officielle du TDR machine.
- 2013 au Japon
  - Annonce de la communauté japonaise de son intention de construire l'ILC
  - Déclaration du 1er Ministre japonais
  - Création d'un groupe de travail de députés en faveur de l'ILC
  - Négociations Japon / USA
  - Choix du site japonais: été 2013.
- 2013 en Europe:
  - Déclarations de soutien des communautés allemandes et espagnoles
- Calendrier possible:
  - Fin 2013: engagement du Japon
  - 2013-2015: négociations intergouvernements
  - ~ 2015: décision
  - ~2016/18 démarrage de la construction

...et un cap: ~2026-27: commissioning.

Qu'est-ce que l'ILC ?

- Collisionneur Linéaire International: e^+ e^-
  - Baseline: $\sqrt{s}$ = 500 GeV
    - Phase à 250 GeV (usine à Higgs)
    - Options : 90 GeV (GigaZ), e^-e^-, $\gamma\gamma$, $e^-\gamma$
    - Upgrade: 1 TeV
  - 2 détecteurs en « push pull » (un seul point de collision)
    - ILD et SiD
  - Luminosité:
    - 1.8 x 10^{34} cm^{-2} s^{-1}
    - 500 fb^{-1} (4 ans)
  - Polarisation: e^- = 80% ; e^+ = 30% (upgrade 60%)

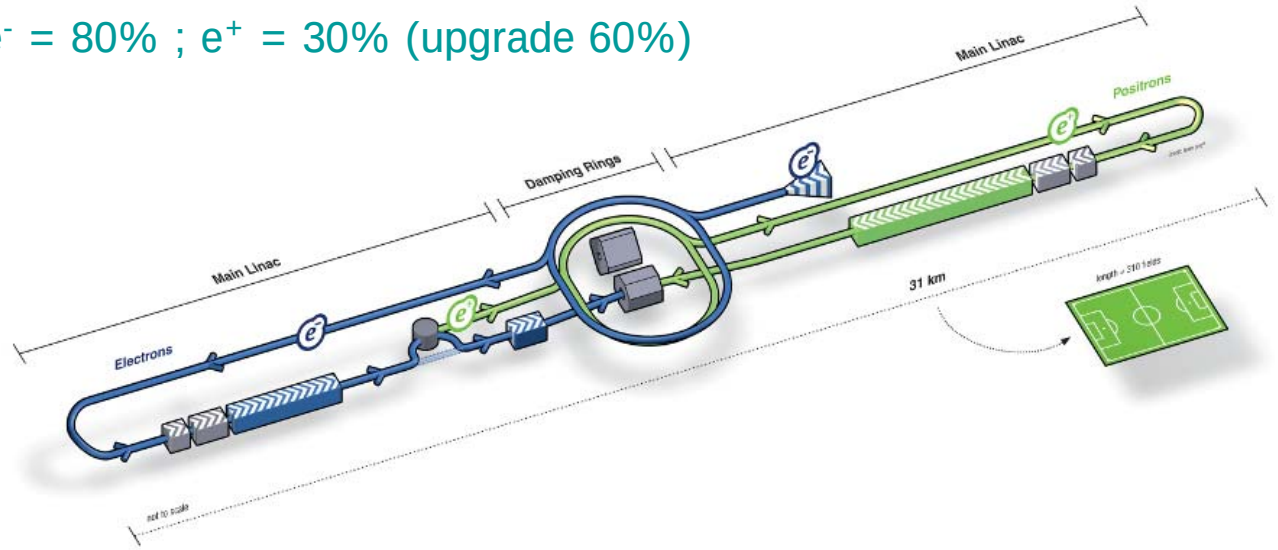

Serious hope for the long awaited miracle to come

almost certain to happen
high likelihood
unclear

Indicated dates are very rough

The GAP Zone

12 13 14 15 16 17 18 19 20 21 22 23 24 25 26 27 28 29 30 31 32 33 34 35 36 37 38 39 40 41 42

Europe
LHC — planned
HL-LHC — planned
HE-LHC — considered
CLIC — considered
Americas
muColl — considered
Asia
BEPC — planned
superKeKB — planned
ILC

Long standing R&R TDR level Global project

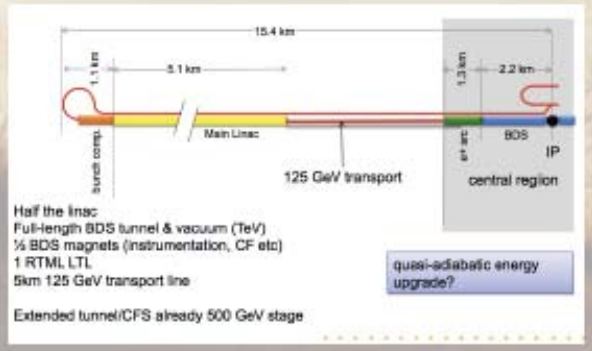

(F.Lediberder)

Collisionneur Linéaire

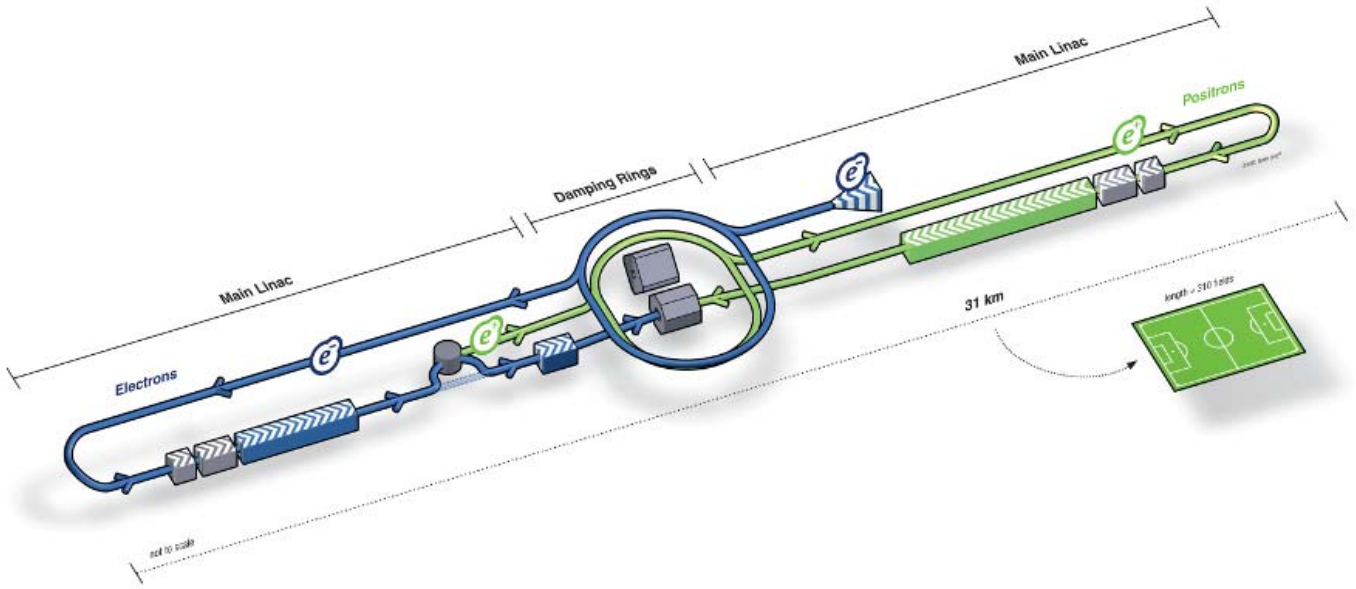

L'accélérateur

• 5/10 Hz train
• polarised e^-

1) e^- source

7) e^+ Ring to main linac system

• ⇨ 5GeV

2) e^- damping ring

• Bunch compressor

3) e^- Ring to main linac system

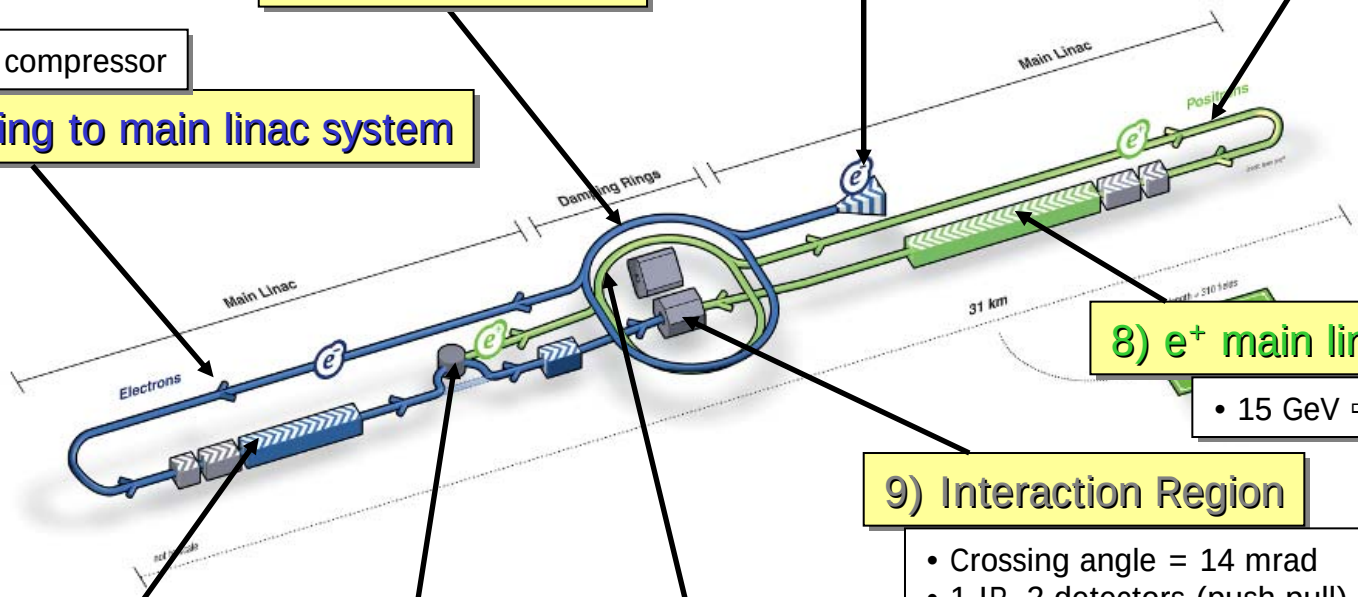

8) e^+ main linac

• 15 GeV ⇨ 250 GeV

9) Interaction Region

• Crossing angle = 14 mrad
• 1 IP, 2 detectors (push pull)

4) e^- main linac

• 15 GeV ⇨ 250 GeV

5) e^+ source

• ondulator ⇨ γ ⇨ target ⇨ e^+

6) e^+ damping ring

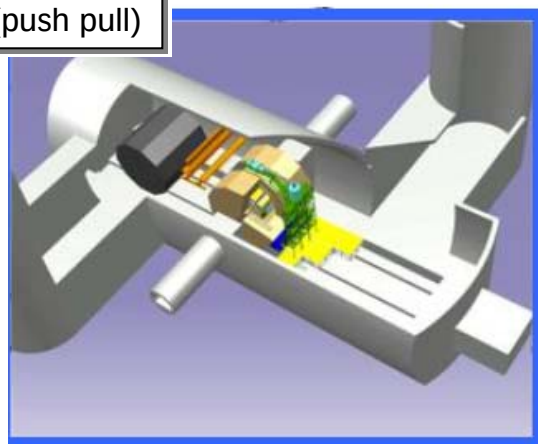

Structure des faisceaux

- Structure « discontinue »
  - 5 trains/s;
  - Nombre de paquets: 1312-2625 /train
    - 2x10^{10} e-/paquet
  - Temps entre les paquets: 554/366ns
  - Temps d'un train ~ 1 ms
  - Temps entre les trains ~ 200ms
    - Long temps mort entre les trains
    - Possibilité de « power cycling » pour minimiser P_{diss}
    - Possibilité de read-out entre les trains

Parameters	Value
C.M. Energy	500 GeV
Peak luminosity	1.8 x10^{34} $cm^{-2}s^{-1}$
Beam Rep. rate	5 Hz
Pulse duration	0.73 ms
Average current	5.8 mA (in pulse)
E gradient in SCRF acc. cavity	31.5 MV/m +/-20% Q_0 = 1E10

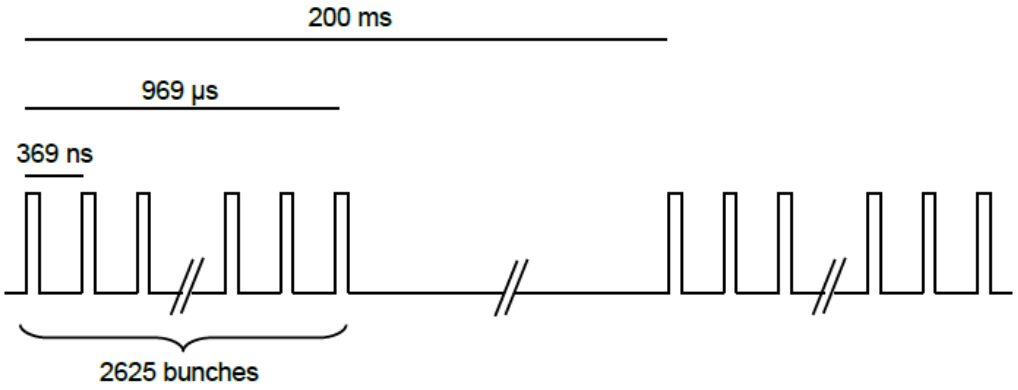

ILC paramètres

			Baseline 500 GeV Machine			1st Stage	L Upgrade	E_{CM} Upgrade	
								A	B
Centre-of-mass energy	E_{CM}	GeV	250	350	500	250	500	1000	1000
Collision rate	f_{rep}	Hz	5	5	5	5	5	4	4
Electron linac rate	f_{linac}	Hz	10	5	5	10	5	4	4
Number of bunches	n_b		1312	1312	1312	1312	2625	2450	2450
Bunch population	N	$\times 10^{10}$	2.0	2.0	2.0	2.0	2.0	1.74	1.74
Bunch separation	Δt_b	ns	554	554	554	554	366	366	366
Pulse current	I_{beam}	mA	5.8	5.8	5.8	5.8	8.8	7.6	7.6
Main linac average gradient	G_a	MV m^{-1}	14.7	21.4	31.5	31.5	31.5	38.2	39.2
Average total beam power	P_{beam}	MW	5.9	7.3	10.5	5.9	21.0	27.2	27.2
Estimated AC power	P_{AC}	MW	122	121	163	129	204	300	300
RMS bunch length	σ_z	mm	0.3	0.3	0.3	0.3	0.3	0.250	0.225
Electron RMS energy spread	$\Delta p/p$	%	0.190	0.158	0.124	0.190	0.124	0.083	0.085
Positron RMS energy spread	$\Delta p/p$	%	0.152	0.100	0.070	0.152	0.070	0.043	0.047
Electron polarisation	P_-	%	80	80	80	80	80	80	80
Positron polarisation	P_+	%	30	30	30	30	30	20	20
Horizontal emittance	$\gamma\epsilon_x$	µm	10	10	10	10	10	10	10
Vertical emittance	$\gamma\epsilon_y$	nm	35	35	35	35	35	30	30
IP horizontal beta function	β_x^*	mm	13.0	16.0	11.0	13.0	11.0	22.6	11.0
IP vertical beta function	β_y^*	mm	0.41	0.34	0.48	0.41	0.48	0.25	0.23
IP RMS horizontal beam size	σ_x^*	nm	729.0	683.5	474	729	474	481	335
IP RMS veritcal beam size	σ_y^*	nm	7.7	5.9	5.9	7.7	5.9	2.8	2.7
Luminosity	L	$\times 10^{34}$ cm^{-2}s^{-1}	0.75	1.0	1.8	0.75	3.6	3.6	4.9
Fraction of luminosity in top 1%	$L_{0.01}/L$		87.1%	77.4%	58.3%	87.1%	58.3%	59.2%	44.5%
Average energy loss	δ_{BS}		0.97%	1.9%	4.5%	0.97%	4.5%	5.6%	10.5%
Number of pairs per bunch crossing	N_{pairs}	$\times 10^3$	62.4	93.6	139.0	62.4	139.0	200.5	382.6
Total pair energy per bunch crossing	E_{pairs}	TeV	46.5	115.0	344.1	46.5	344.1	1338.0	3441.0

½ gradient
Initial Higgs factory

Baseline

½ longueur
(Option 1e phase)

Lumi
upgrade

1TeV upgrade

Figure 2.1
Schematic layout of the ILC complex for 500 GeV CM.

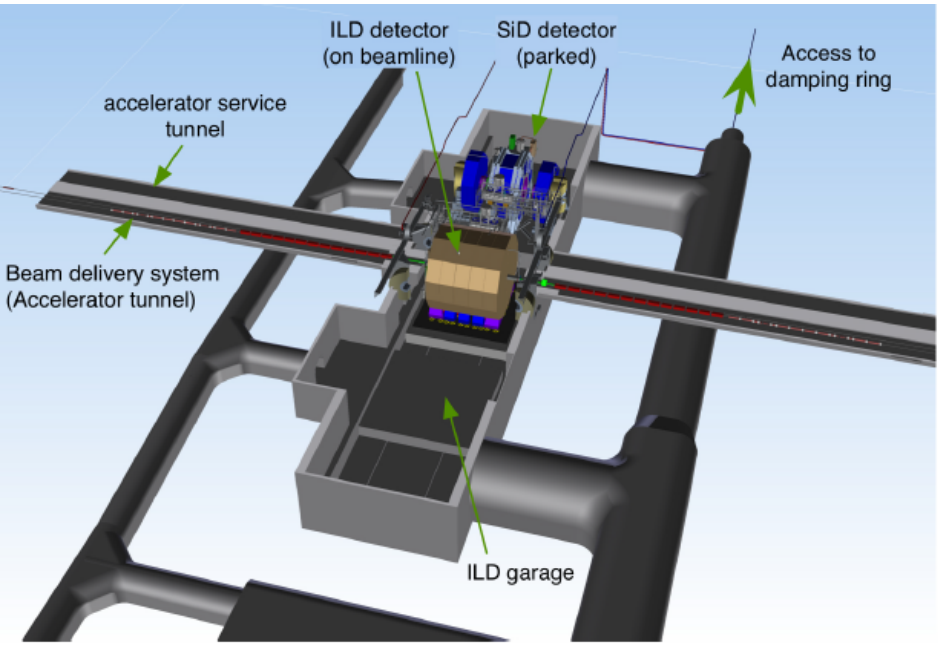

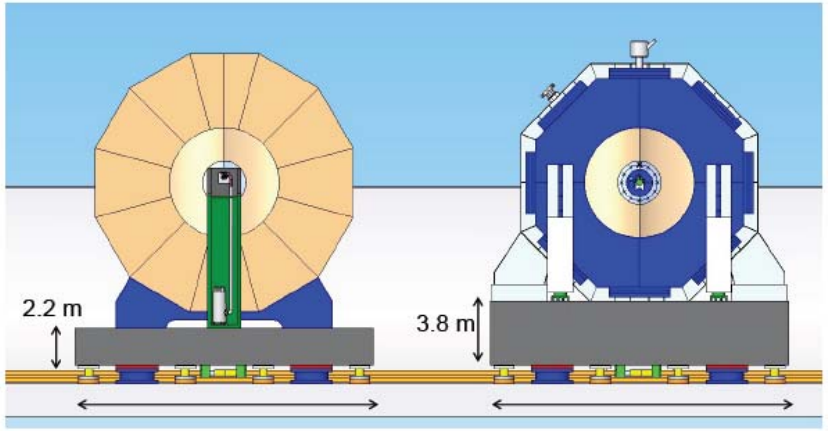

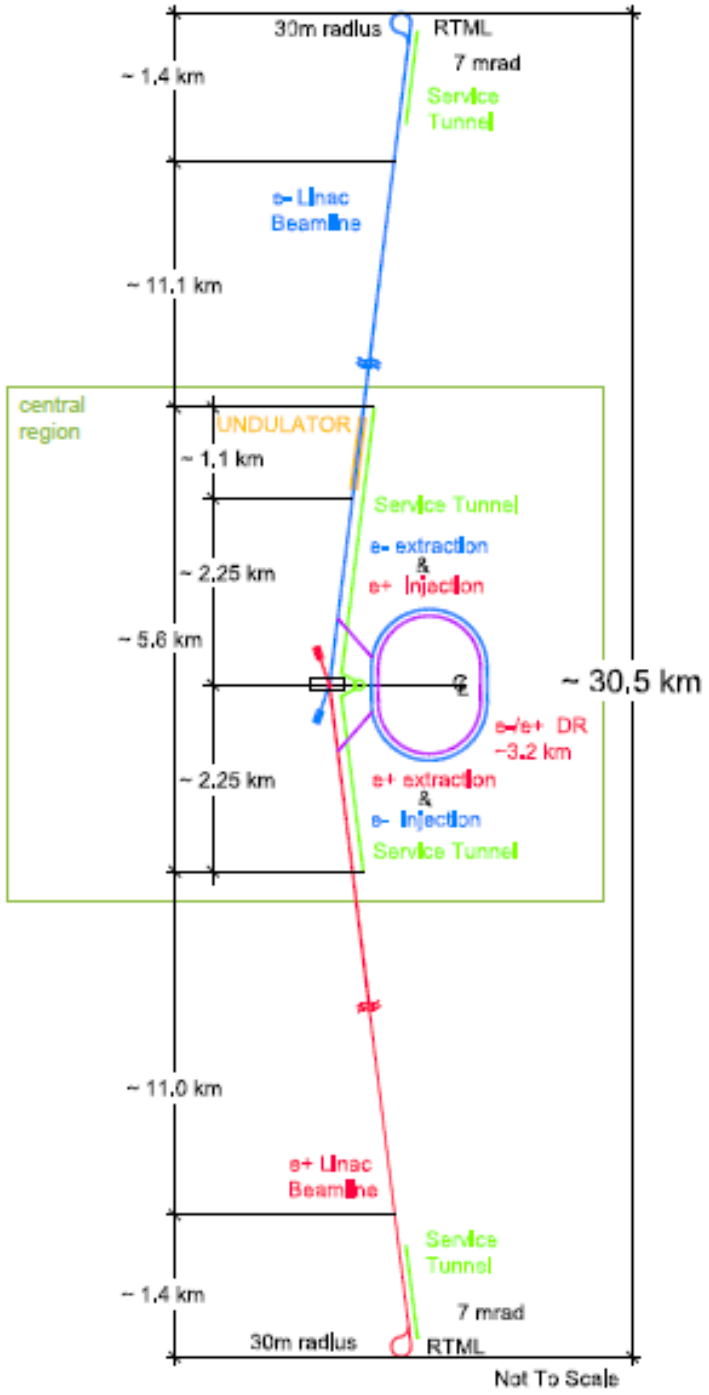

Facteur de qualité Q_0 d'une cavité supra

- Puissance à fournir pour une cavité:
  - $P_{RF} \sim P_{faisceau} + P_{cavité}$
- Enjeu:
  - maintenir $Q_0 \geq 10^{10}$ et un gradient élevé, sans Quench

$$P_{cavité} \sim (E_{acc} \times L_{acc})^2 / ((r/Q)Q_0)$$

1 klystron pour 13 cavités

1 Cryomodule (12m) = 8-9 cavités

P_{RF} (via coupleur de puissance)

e^-

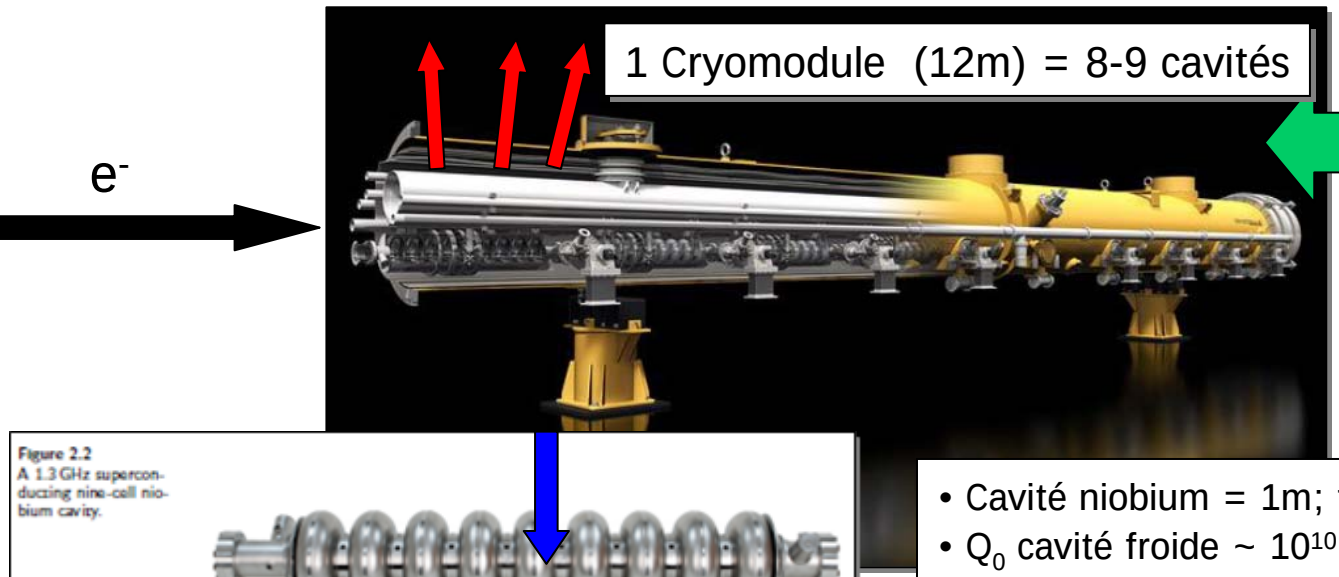

- Cavité niobium = 1m; fonctionnement à 2K.
- Q_0 cavité froide ~ 10^{10} / Q_0 cavité chaude ~ qqs 10^4
- r/Q = ~1000 Ω
- Fréquence 1.3 GHz: taille cavité ∝ 1/f
- Gradient 31.5 MV/m ⇨ longueur ~ 11km (250GeV)

$$P_{faisceau} = \Delta U \times I_{faisceau}$$

$I \sim 5.8$ mA ; $\Delta U \sim 31.5$ MV

⇨ $P_{faisceau} \sim 0.18$ MW / cavité

Cavités

- Enjeu: production en série
  - 7400 cavités à construire
    - (~850 cryomodules)
    - Rendement / cout
    - Gradient: 31.5 MV/m ± 20%
    - Objectifs (GDE) atteints
  - Expérience acquise
    - après 20 ans de R&D

    (DESY, KEK, FNAL, etc.)
    - La technologie est prête.

Progress in SCRF Cavity Gradient

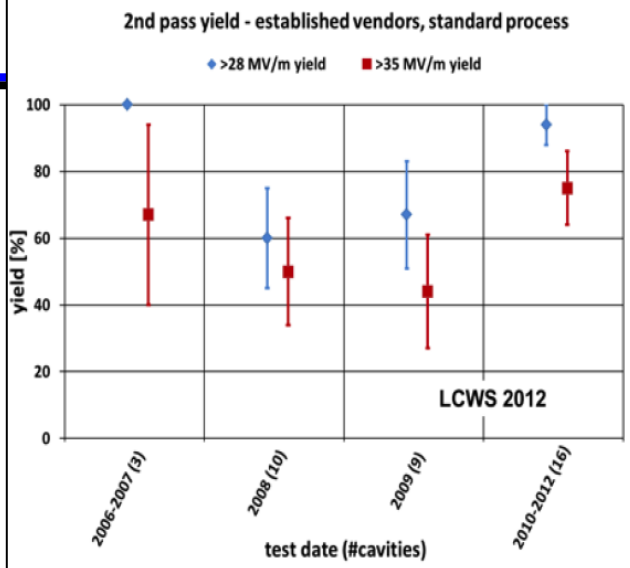

Production yield:
94 % at > 28 MV/m,

Average gradient:
37.1 MV/m

reached (2012)

15 A. Yamamoto, 13/05/27 ILC Technical Status

Figure 2.20
L-band SCRF niobium-cavity-gradient envelope and gradient R&D impact on SCRF linacs.

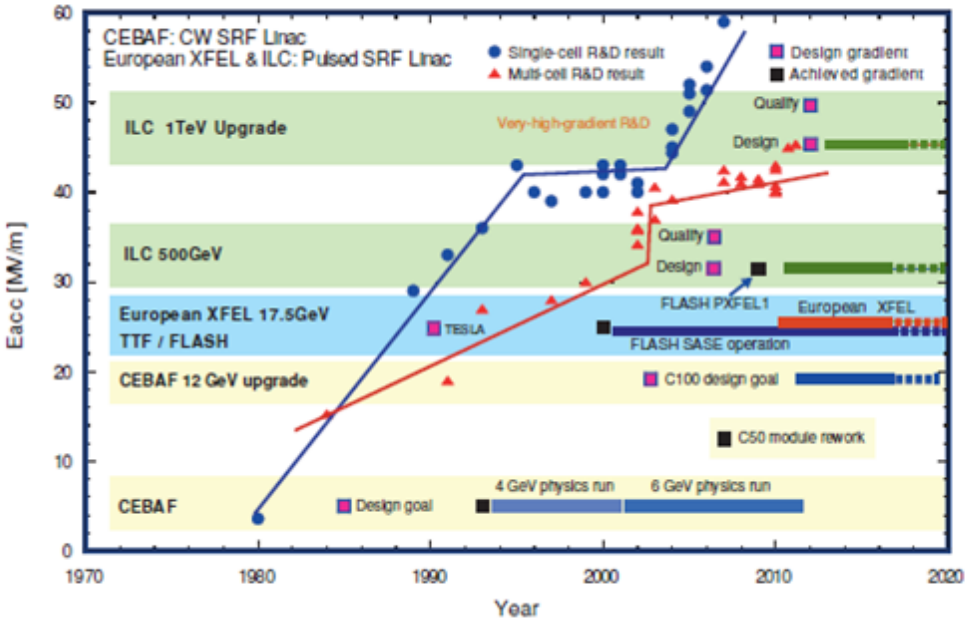

Interaction faisceau-faisceau et Beamstrahlung

- Pinch effect ~ Luminosité x2

Perte d'energie moyenne des faisceaux δ_{BS}

$$\delta_{BS} \approx 0.86 \frac{e r_e^3}{2 m_0 c^2} \left(\frac{E_{cm}}{\sigma_z} \right) \frac{N^2}{(\sigma_x + \sigma_y)^2}$$

Luminosité

$$L = \frac{n_b N^2 f_{rep}}{4\pi \sigma_x \sigma_y} H_D$$

- Beamstrahlung
  - Paquets $e^{\pm}$ subissent le champs intense du faisceau opposé
    - Rayonnement de γ
    - ⇨e^-e^+ de faible impulsion transverse
    - Négligeable @ LEP
  - Conséquences
    - Conversions en paires e^+e^-
    - Responsable de l'essentiel de l'occupation des premières couches des détecteurs: jusqu'à ~ 6 hits/cm^2/BX
    - Responsable de l'essentiel des radiations ~ 10^s krad/an, 10^{11} n_{eq}(1MeV)/an
    - Perte d'énergie des faisceaux $\delta_{BS} \propto \sqrt{s}$

Breit-Wheeler

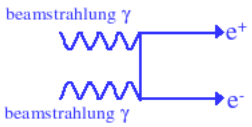

Bethe-Heitler

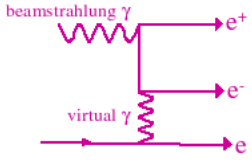

Landau-Lifshitz

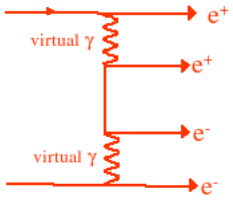

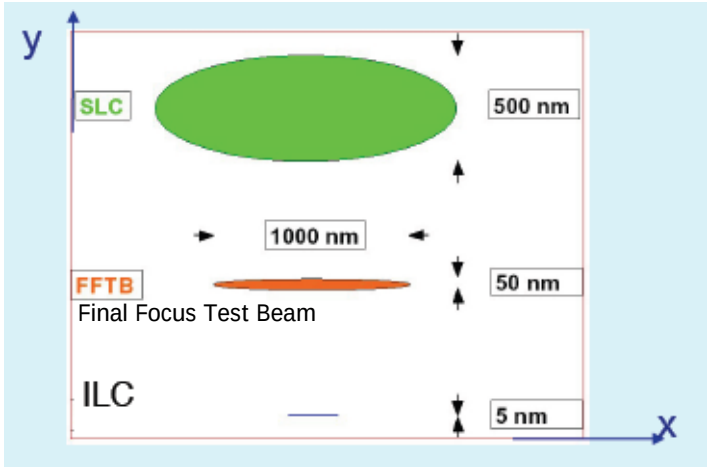

- Minimisation
  - Faisceau « plat » minimise cet effet
  - Taille transverse du faisceau: σ^*_x = 5.9 nm ; σ^*_y = 474 nm

Beamstrahlung: effet sur E_{beam} ($\sqrt{s}$ = 250 GeV)

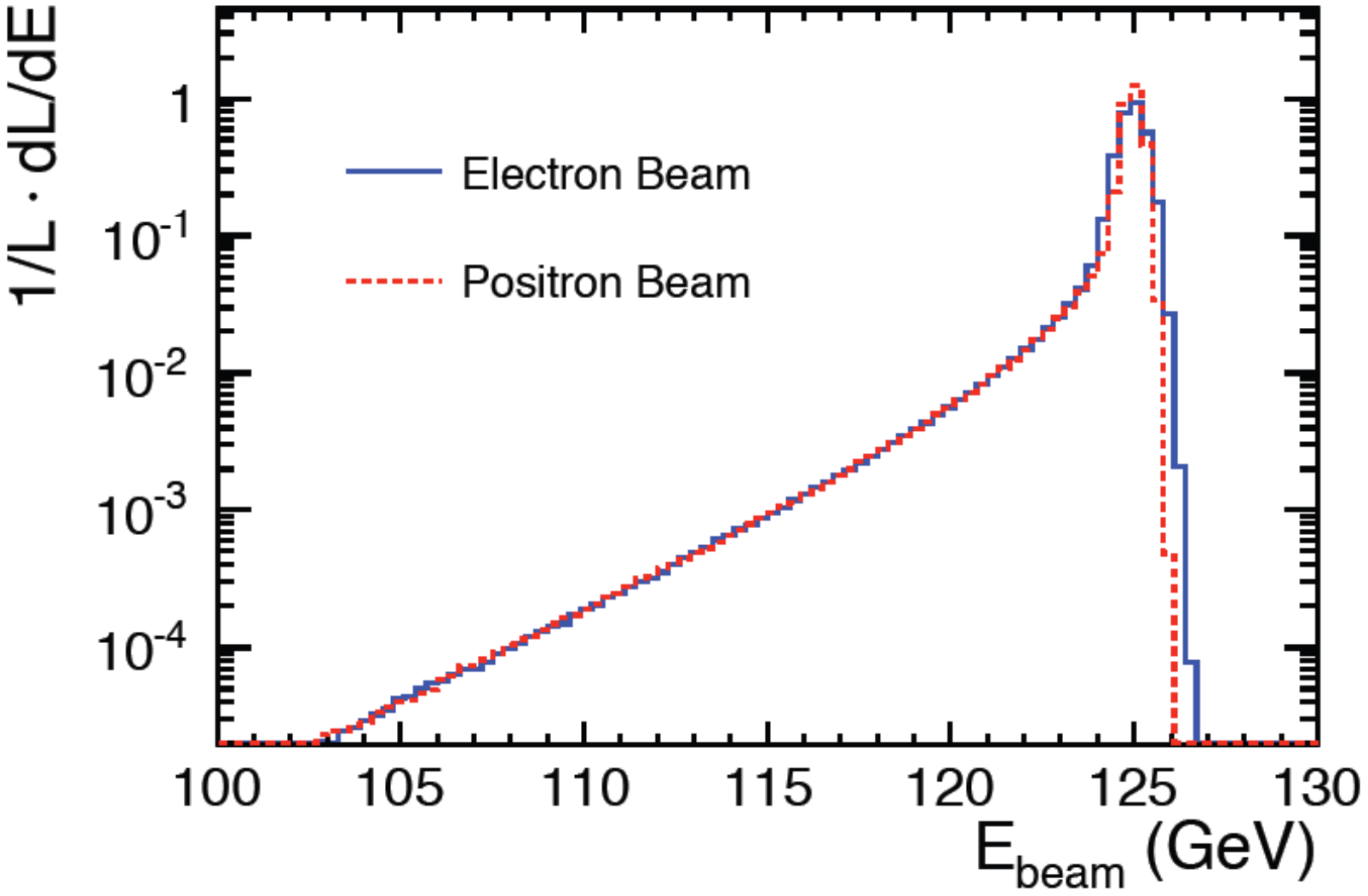

Angle de croisement: « crab crossing »

- Angle de croisement des faisceaux au point de collision
  - 14 mrad
    - Facilite l'extraction après la collision
    - Perte de luminosité sans crab crossing

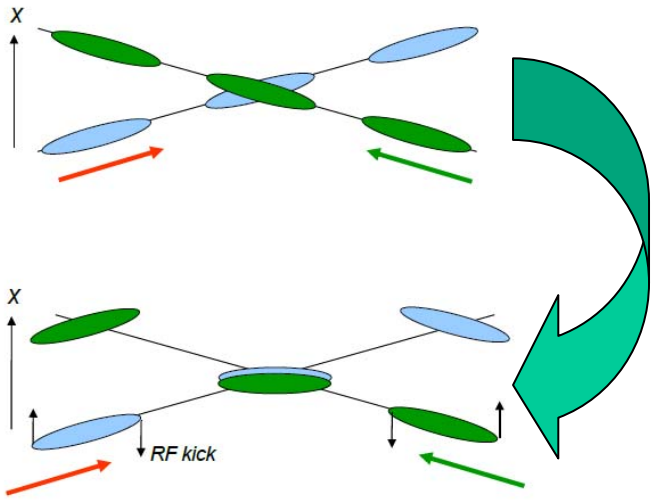

Luminosité x Facteur 10 !

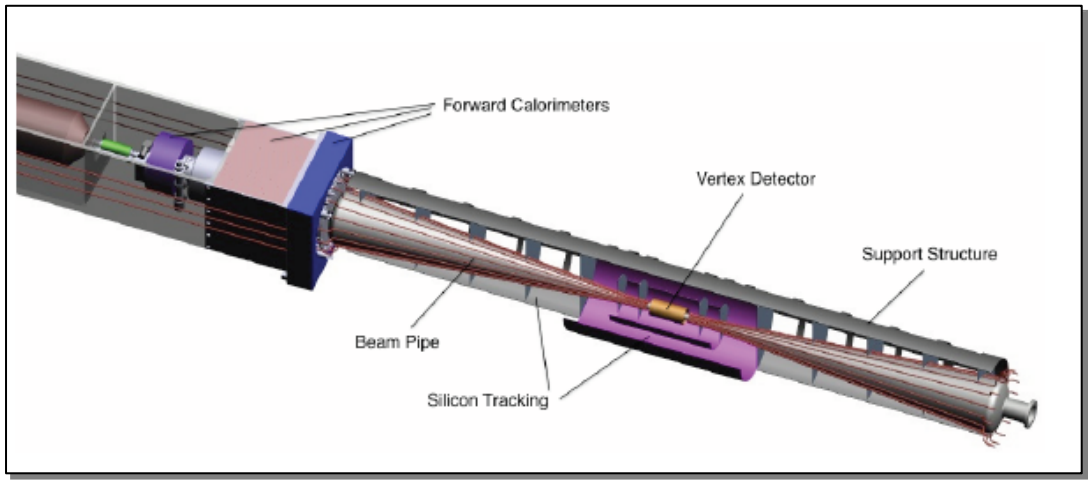

Mais pourquoi ce cap ?

Pourquoi un collisionneur linéaire e^+e^- ? (1)

- Énergie dans le centre de masse bien définie
  - beamstrahlung: RMS energy loss: δ_{BS} ~ 1% @ $\sqrt{s}$ = 250 GeV ⇨ 90% de la luminosité a moins de 1% d'écart vs $\sqrt{s}$.
- Énergie dans le centre de masse ajustable
  - Flexibilité, balayages aux seuils de production ⇨ détermination des masses (top,...)
- Faisceaux polarisés (e^- : 80%, e^+ : 30%)
  - Ouvre ou ferme certains canaux.
- ILC: Bruit de fond modéré
  - ILC: Background principal: beamstrahlung. = (~ 5 part/cm^2/BX sur la première couche)
    - particules de faible pT, Pas de bruit de fond QCD, pas d'empilement d'événements.
  - Pas de trigger ⇨ simplification, aucun biais (pas de « turn on »)

⇨ Environnement « propre », événements « pleinement reconstructibles »

  - Cahier des charges
    - Saveur des jets, Lepton ID, herméticité, Particle flow
- LHC: environnement totalement différent
  - total cross section = ~ 100mb, BX time 50ns, 30 collisions pp/BX
    - donnant chacun des centaines de traces de hauts pT
    - Tenue au rayonnement impose certains choix technologiques
    - Flux de particules impose des vitesses de lecture élevées
    - Trigger obligatoire
    - Calorimétrie: plus « profond » (X_0 / λ) pour contenir les gerbes ⇨ solénoïde a l'intérieur
- Performances globales:
  - Gain d'un facteur 10 sur la résolution du trajectographe
  - Gain d'un facteur 3 sur la résolution des jets.
  - Excellent étiquetage des b et taus et capacités a étiqueter les c.

Sections efficaces comparées

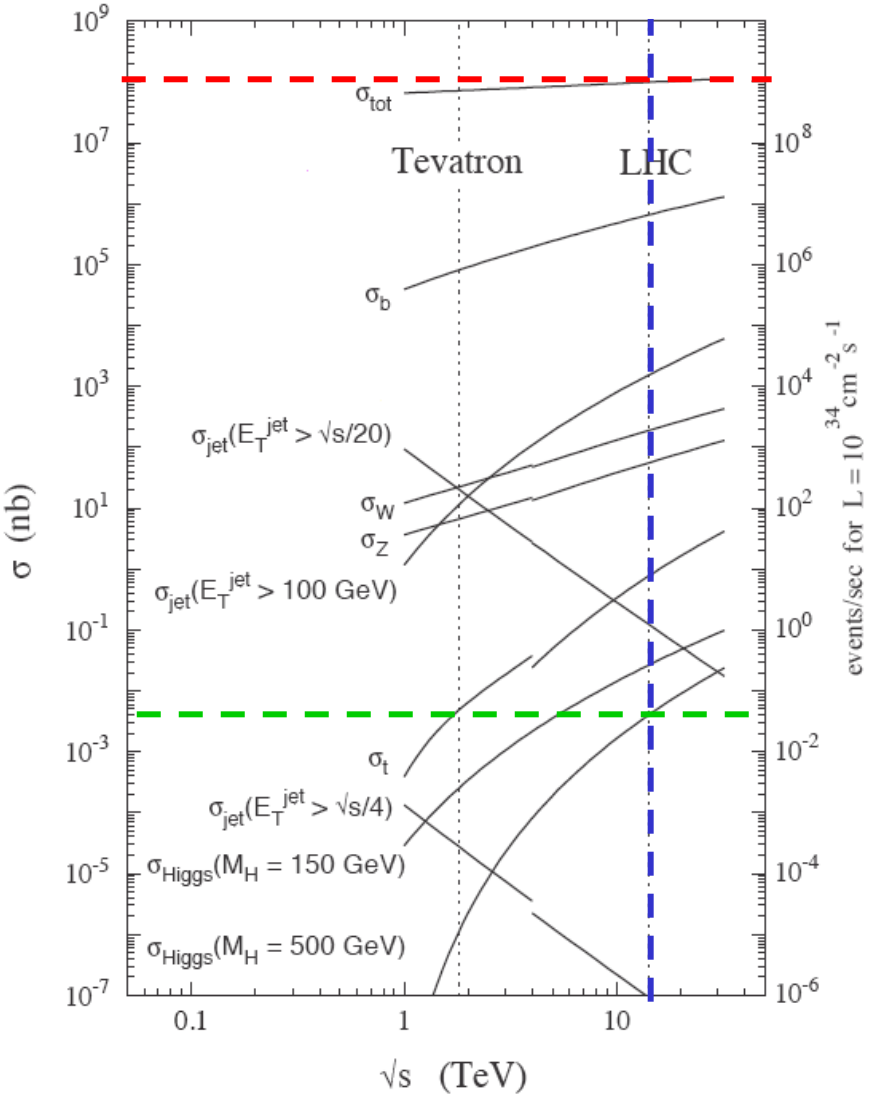

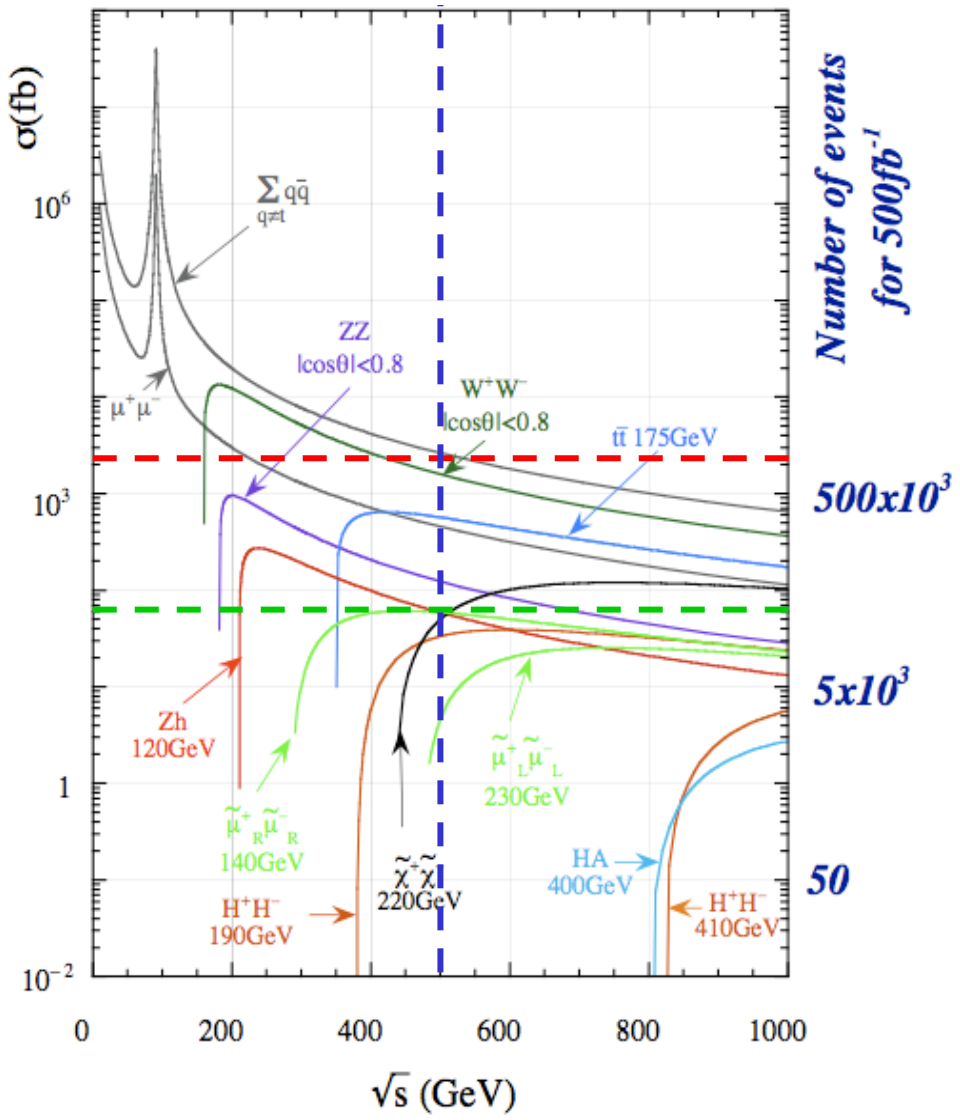

Pourquoi un collisionneur linéaire e^+e^- ? (2)

- Production démocratique
  - Production d'un Higgs au LHC : 1 evt / 10 000 000 000
    - Nécessité absolue d'un trigger au LHC
    - Accent sur les canaux riches en particules facilement identifiables/(e-, μ, γ, etc.)
    - Résolution sur l'énergie des photons cruciale
  - Production d'un Higgs a l'ILC : 1 evt / 100
    - Pas de trigger !

- Sections efficaces
  - Globalement faibles à l'ILC (ZH ~ 100 fb) $\neq$ LHC (~100pb)
    - Etudier tous les canaux (même hadroniques)
    - Résolution sur l'énergie des jets cruciale

- Précision et faisabilité des calculs
  - LHC: calculs basés sur QCD
    - protons structures function systematic errors
    - Unknown Higher order QCD perturbative corrections
    - Non perturbative QCD effects
  - Incertitudes :
    - Souvent >~ 10% (NNLO)
  - ILC: collisions e+ e-
    - Corrections radiatives de l'ordre du pourcent
  - Incertitudes
    - Sous le pour mille.

Pourquoi un collisionneur lineraire e+e- ? (3) Polarisation

- Polarisation
  - Les électrons gauches et droits se couplent différemment aux composantes SU(2)xU(1) du MS.
  - Avantage d'une accélération linéaire
    - préserve la polarisation !
  - Def: P(-) et P(+) = polarisation des e- et e+
    - Exp: P(-) = -1 ⇦⇨ 100% e- gauche
- Canaux de physique
  - Z résonnance, couplage EW du quark t
    - asymétrie
  - e^+e^- annihilation
  - $e^-_L e^+_R$: augmentation de certains processus
  - $e^-_R e^+_L$: recherches au delà du SM
    - Suppression du bruit de fond SM (WW, WW fusion)

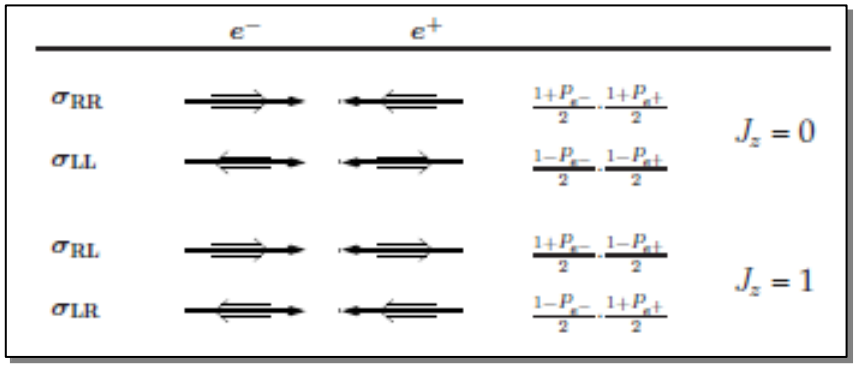

$$P_{eff} = \frac{P(-) - P(+)}{1 - P(-)P(+)} .$$

giving $P_{eff} = 89\%$ for $\mp 80\%$ e^-, $\pm 30\%$ e^+ polarisation.

$$\mathcal{L}/\mathcal{L}_0 = 1 - P(-)P(+) ,$$

giving $\mathcal{L}/\mathcal{L}_0 = 1.24$ for $\mp 80\%$ e^-, $\pm 30\%$ e^+ polarisation.

$$\mathcal{L}/\mathcal{L}_0 = (1 - P(-))(1 + P(+)) ,$$

or $\mathcal{L}/\mathcal{L}_0 = 2.34$ for -80% e^-, $+30\%$ e^+ polarisation.

Énergies de fonctionnement

Energy	Reaction	Physics Goal
91 GeV	$e^+e^- \to Z$	ultra-precision electroweak
160 GeV	$e^+e^- \to WW$	ultra-precision W mass
250 GeV	$e^+e^- \to Zh$	precision Higgs couplings
350–400 GeV	$e^+e^- \to t\bar{t}$	top quark mass and couplings
	$e^+e^- \to WW$	precision W couplings
	$e^+e^- \to \nu\bar{\nu}h$	precision Higgs couplings
500 GeV	$e^+e^- \to f\bar{f}$	precision search for Z'
	$e^+e^- \to t\bar{t}h$	Higgs coupling to top
	$e^+e^- \to Zhh$	Higgs self-coupling
	$e^+e^- \to \tilde{\chi}\tilde{\chi}$	search for supersymmetry
	$e^+e^- \to AH, H^+H^-$	search for extended Higgs states
700–1000 GeV	$e^+e^- \to \nu\bar{\nu}hh$	Higgs self-coupling
	$e^+e^- \to \nu\bar{\nu}VV$	composite Higgs sector
	$e^+e^- \to \nu\bar{\nu}t\bar{t}$	composite Higgs and top
	$e^+e^- \to \tilde{t}\tilde{t}^*$	search for supersymmetry

Détecteurs

Cahier des charges

Performances

Cahier des charges

- √s=250 GeV: Canal principal de production du boson de higgs
  - = higgsstrahlung (max @ √s=250GeV)
  - Permet une mesure absolue de g_{HZZ}
  - Mesure des Br
  - Mesure de M_H

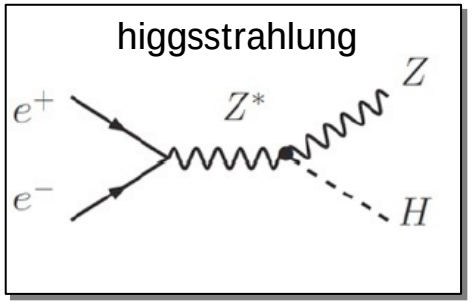

- Méthode de la masse de recul (Z→μμ; Z→ee)

$$M_H^2 = \quad M_{recoil}^2 \quad = s + M_Z^2 - 2E_Z\sqrt{s}$$

$$E_Z = \quad E_{dl} \quad = |\mathbf{P}_1| + |\mathbf{P}_2|$$
$$\mathbf{P}_Z = \quad \mathbf{P}_{dl} \quad = \mathbf{P}_1 + \mathbf{P}_2 \ ,$$
$$M_Z^2 = \quad M_{dl}^2 \quad = E_Z^2 - \mathbf{P}_Z^2$$

  - H reconstruit indépendamment de son canal de désintégration
  - « impose » les performances
    - Résolution sur l'impulsion (Z→μμ; Z→ee) (range ~ 20-90 GeV)
    - Etiquetage des saveurs (H→bb, cc, ττ)
    - H→γγ ~ seulement qqs 100^s ⇨ résolution sur les γ non cruciale

- √s=500 GeV: Canal principal de production du boson de higgs
  - = Fusion WW
  - Reconstruction H→qq
    - Reconstruction des jets

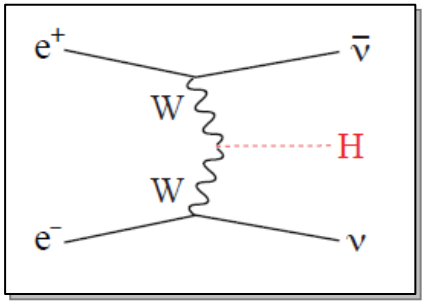

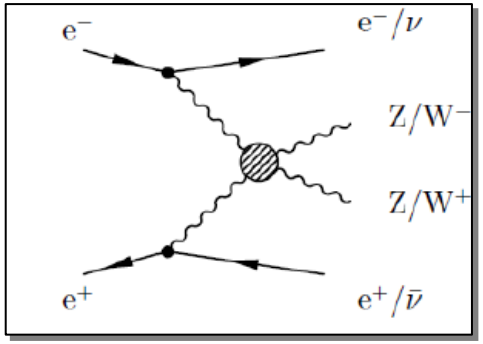

Cahier des charges

- √s=250 GeV: Canal principal de production du boson de higgs
  - higgsstrahlung (max @ √s=250GeV)
  - Permet une mesure absolue de g_{HZZ}
  - Mesure des Br
  - Mesure de M_H

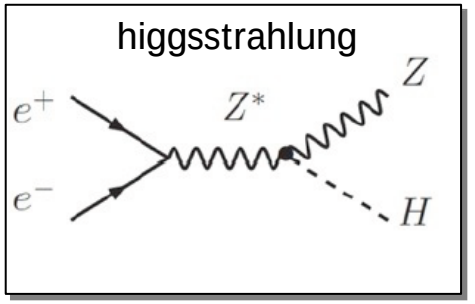

- Méthode de la masse de recul (Z→μμ; Z→ee)

$$M_H^2 = \quad M_{recoil}^2 \quad = s + M_Z^2 - 2E_Z\sqrt{s}$$

$$E_Z = \quad E_{dl} \quad = |\mathbf{P}_1| + |\mathbf{P}_2|$$
$$\mathbf{P}_Z = \quad \mathbf{P}_{dl} \quad = \mathbf{P}_1 + \mathbf{P}_2 \ ,$$
$$M_Z^2 = \quad M_{dl}^2 \quad = E_Z^2 - \mathbf{P}_Z^2$$

  - H reconstruit indépendamment de son canal de désintégration
  - « impose » les performances
    - Resolution sur l'impulsion (Z→μμ; Z→ee) (range ~ 20-90 GeV)
    - Etiquetage des saveurs (H→bb, cc, ττ)
    - H→γγ ~ seulement qqs 100^s ⇨ resolution sur les γ non cruciale

- √s=500 GeV: Canal principal de production du boson de higgs
  - Fusion WW
  - Reconstruction H→qq
    - Reconstruction des jets

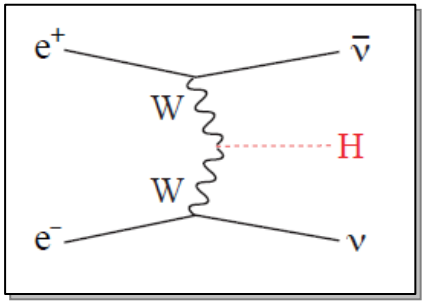

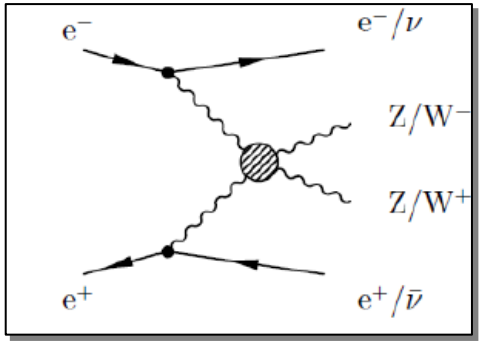

Performances requises

- Vertex
  - Résolution sur le paramètre d'impact
  - Résolution spatiale ~ 3 μm
  - Budget de matière 0.15/0.2 % X0 / couche
- Trajectographie
  - Résolution sur l'impulsion transverse

$$\delta(1/p_T) \simeq 2 \times 10^{-5}/\mathrm{GeV}/c$$

- Résolution sur l'énergie des jets
  - Séparation des WW/ZZ à ~ 2.5 σ
    - Résolution $\Delta E_{Jet}/E_{Jet} \sim 3.5\%$
    - LEP ~ 6% (2-jets events principalement)
    - meilleure acceptance à l'ILC

$$\sigma_b < 5 \oplus 10/p\beta \sin^{3/2}\theta \ \mu\mathrm{m}$$

Détecteur à pixel multicouche
1ere couche au rayon le plus petit possible
Diffusion multiple: budget de matière minimisé

Trajectographe de haute résolution
Champ magnétique intense

Algorithmes particle flow
Calorimètre de haute granularité
Calorimètre hadronique important
Calorimètre dans le solénoïde
Barrel plus court % LHC (boost plus faible)

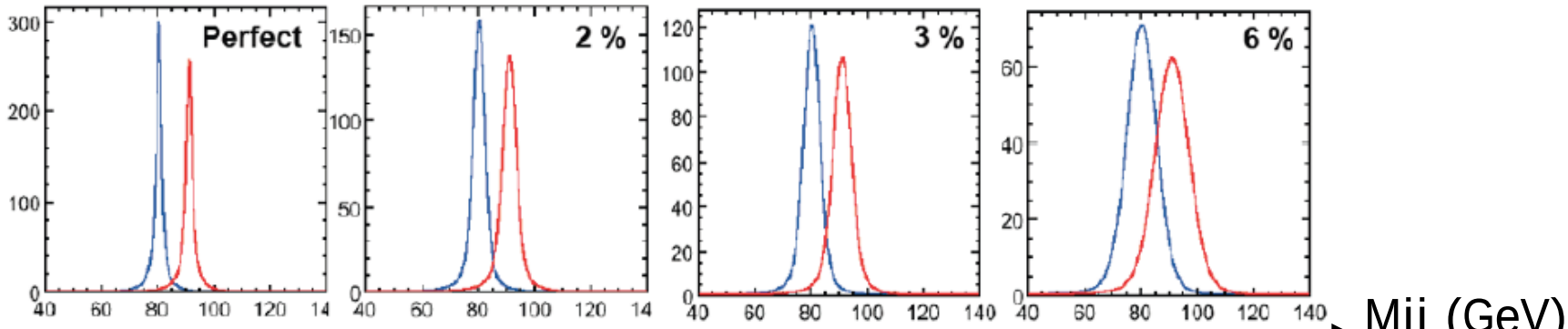

Quelques performances

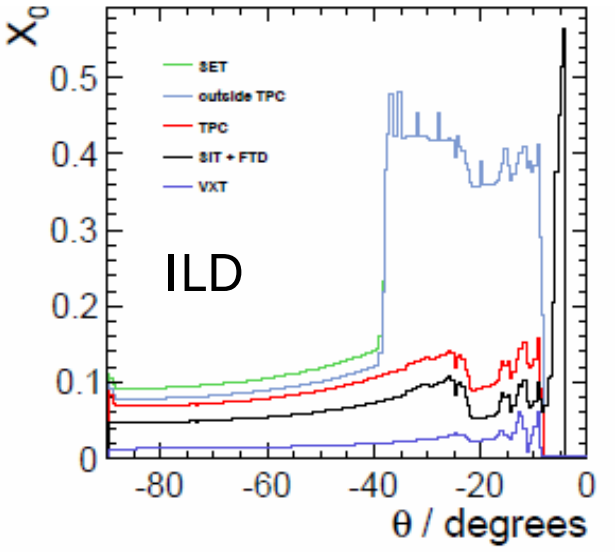

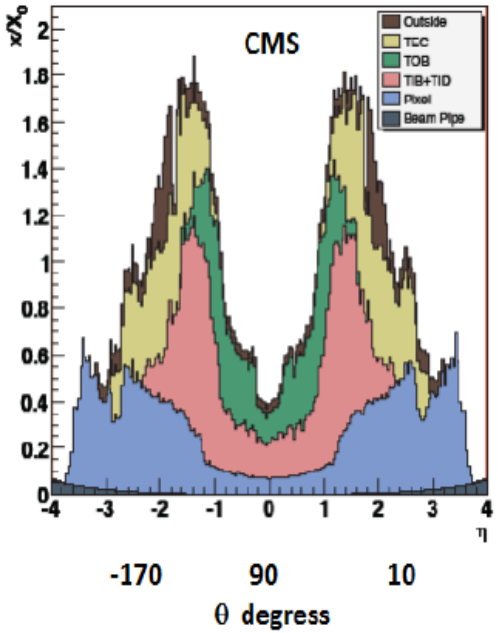

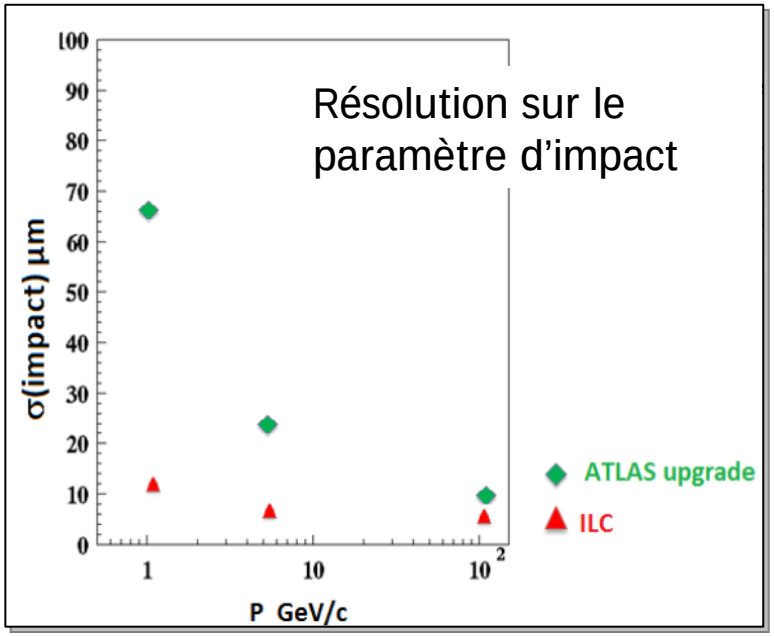

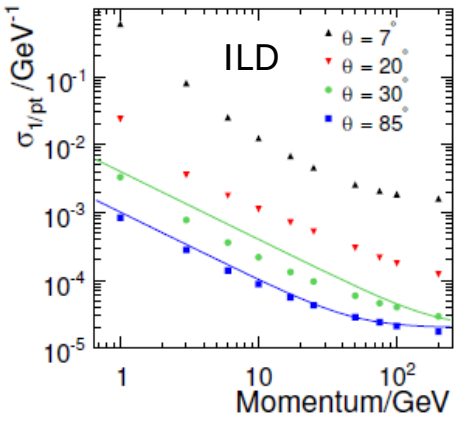

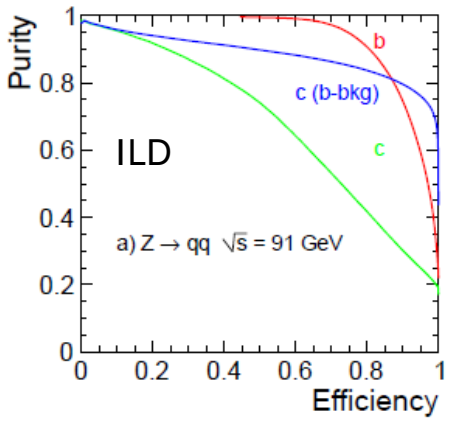

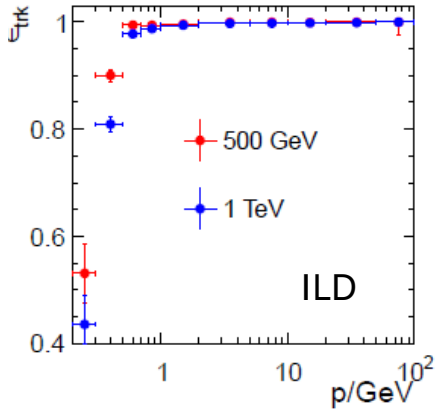

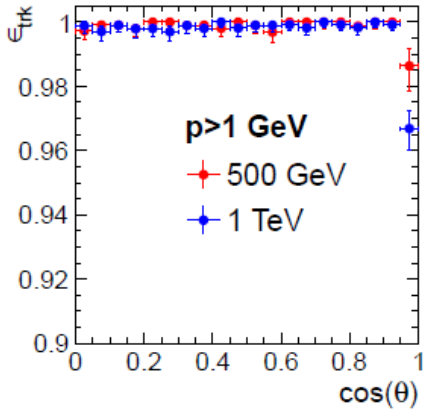

Efficacité de tracking (tt-> 6 jets)

Particle Flow Algorithm (PFA) (1)

- Principe
  - E jet = $E_{\text{hadron chargés}}$ (65%) + E_{photon} (25%) + $E_{\text{hadrons neutres}}$(10%)
    - Mesurer l'énergie de chaque composante des jets avec le détecteur le plus précis
    - Reconstruire individuellement chaque particule
    - Risque de confusion (double comptage)

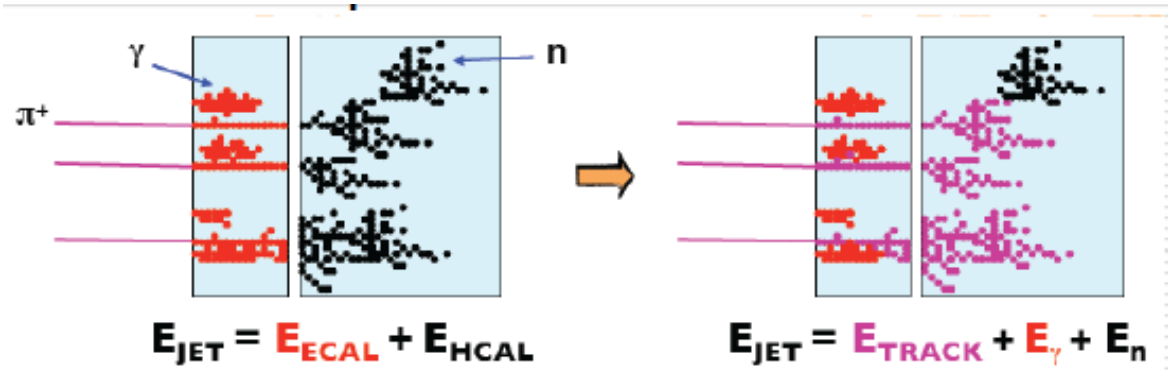

- $\sigma^2(E_{jet}) = \sigma^2(E_{charged}) + \sigma^2(E_{photons}) + \sigma^2(E_{neutral\ hadr.}) + \sigma^2_{confusion}$

- Conséquences
  - Optimisations du PFA et limitation
    - Confusion plus importante que la résolution du calorimètre
    - Design optimisé pour la granularité
    - Calorimètre compact nécessaire (extension radiale de la gerbe)
    - Efficacité de reconstruction des traces > 99%
    - Budget de matière avant le calorimètre
    - Calorimètre dans le solénoïde (appariement traces / Energie calo)

Particle Flow Algorithm (PFA) (2)

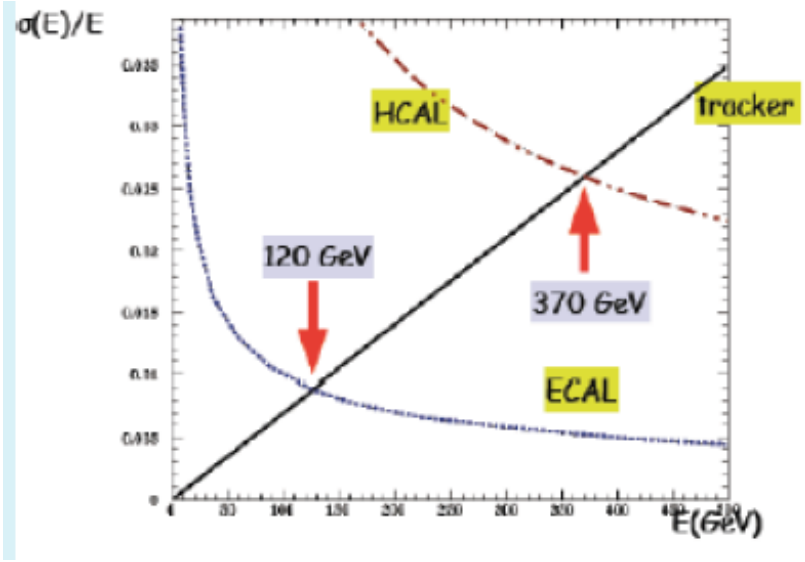

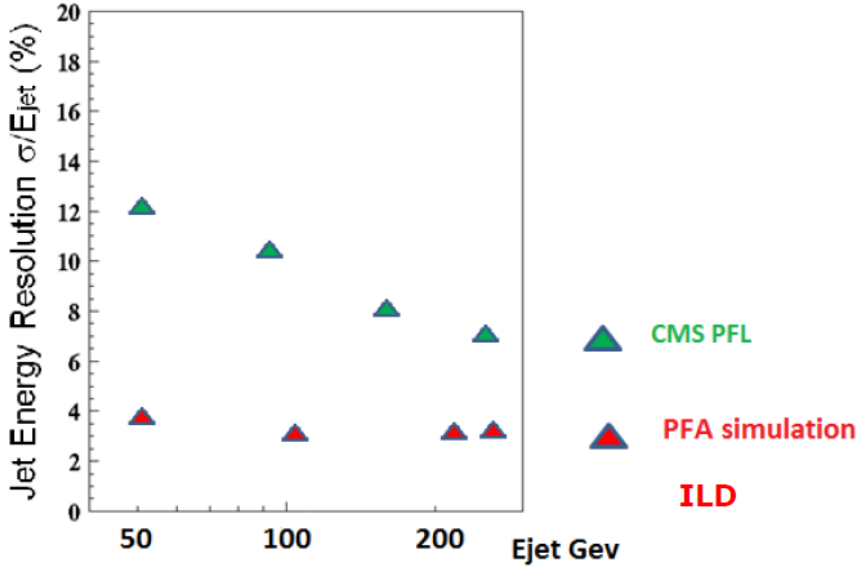

Séparation ννWW / ννZZ

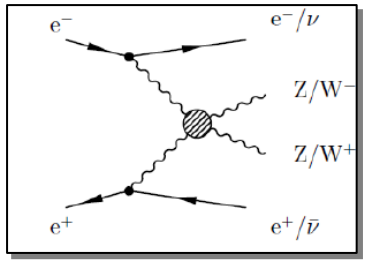

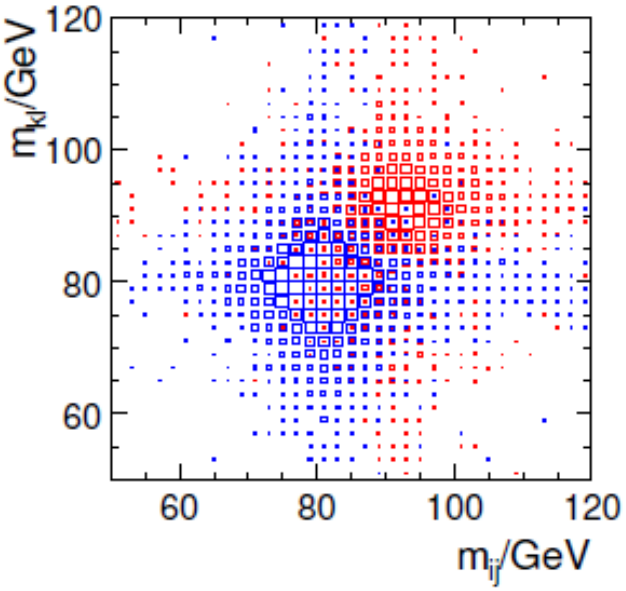

Masse di-jet reconstruite
Evenements ννWW (bleu)
Evenements ννZZ (rouge)
@ √s = 1 TeV

ILD - The Overview

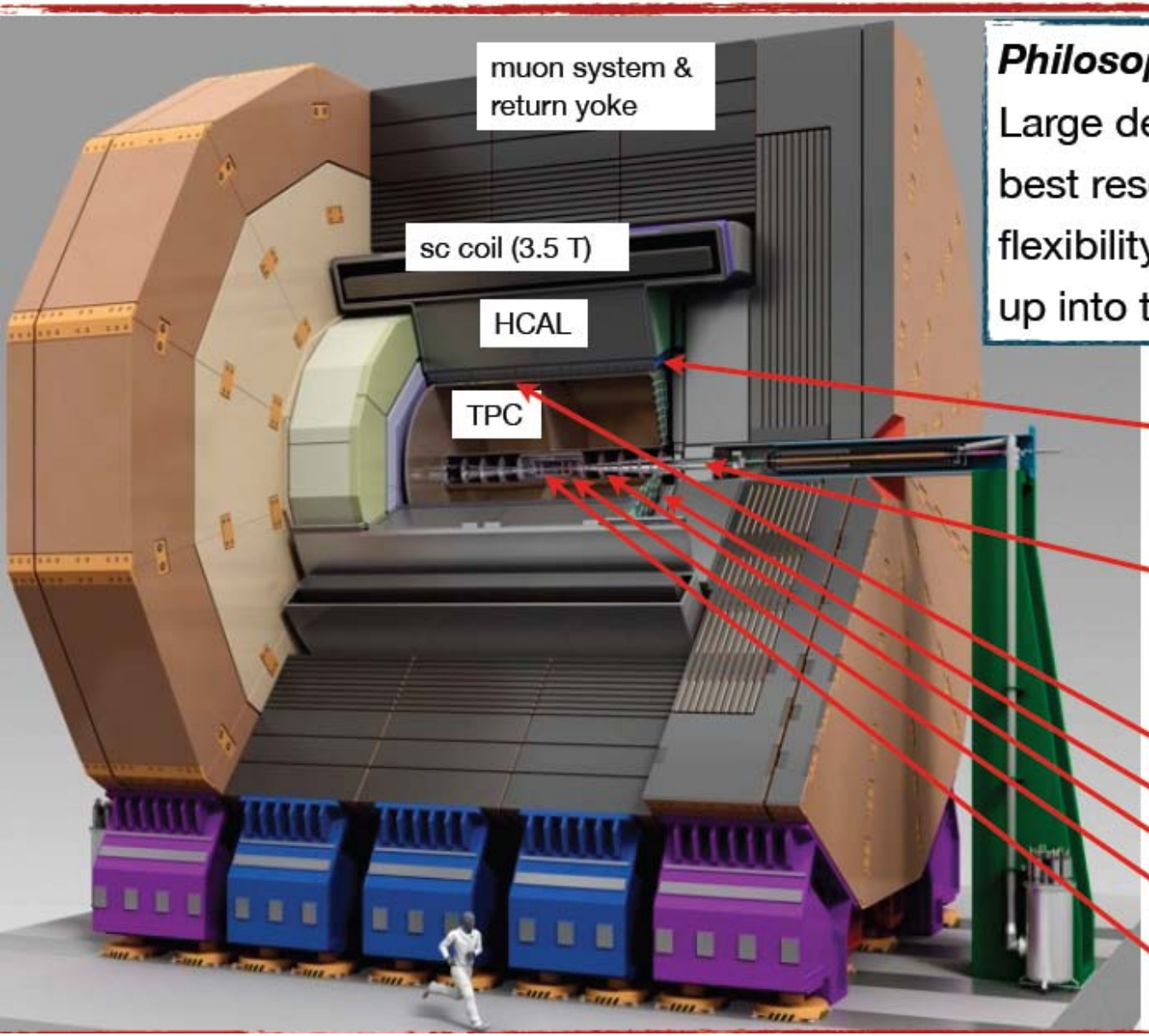

Philosophy:

Large detector optimized for best resolution, providing flexibility for higher energies up into the TeV range

ECAL

forward calorimeters
LumiCAL
BeamCAL, LHCAL

silicon tracking
Silicon **E**xternal **T**racker
Endplate **T**racking **D**etector
Forward **T**racking **D**isks
Silicon **I**nner **T**racker

VerTeX Detector

The Detectors in ILC

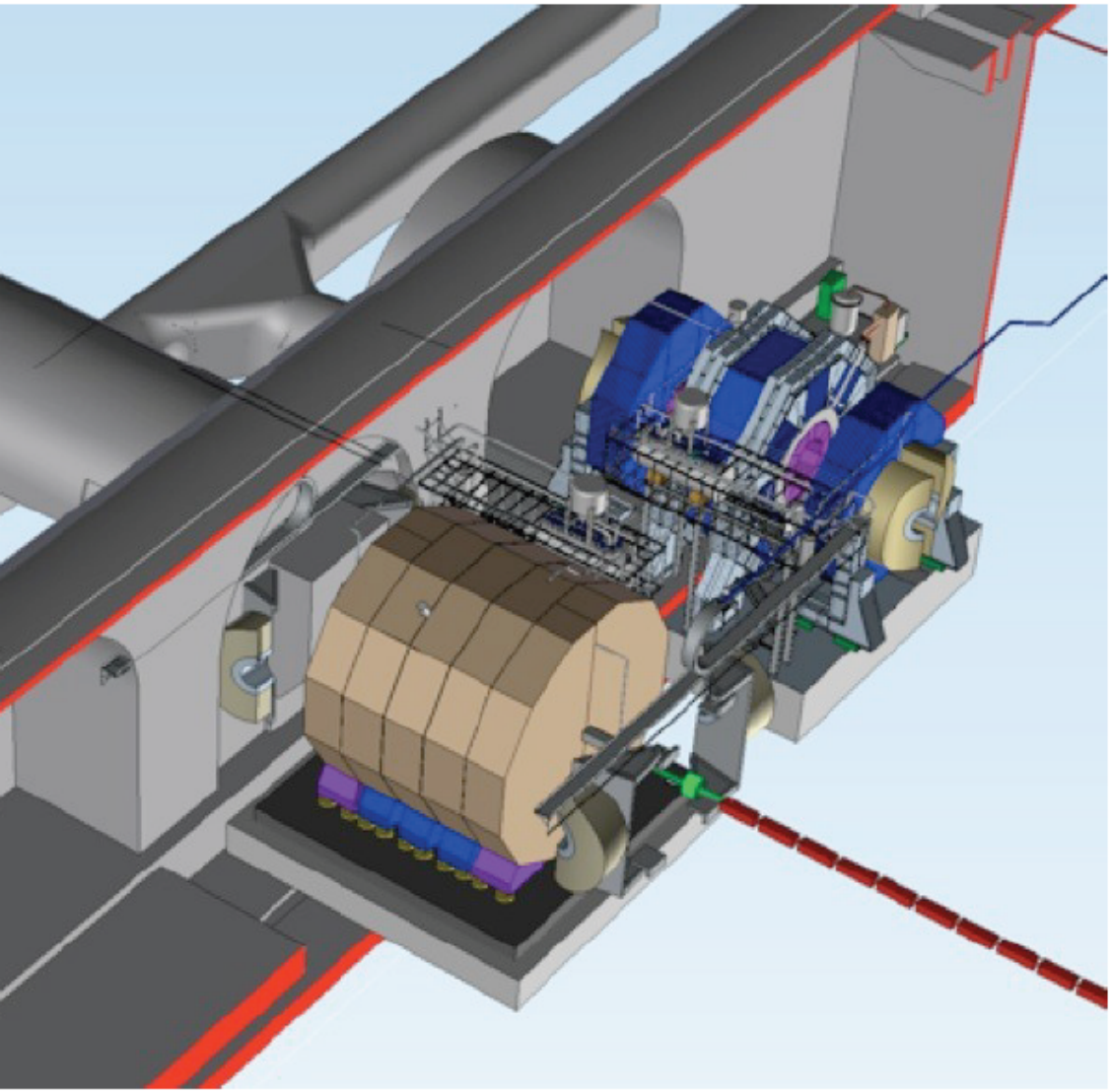

- Current concept: Two detectors share one interaction region - Exchange by push-pull on air-cushioned platforms
- Requires well designed integration & services

NB: Here two detectors do not increase the total integrated luminosity - The gain is in systematics (and sociological aspects!)

Performances: résumé

Table I-1.2. Detector performance needed for key ILC physics measurements.

Physics Process	Measured Quantity	Critical System	Physical Magnitude	Required Performance
Zhh $Zh \to q\bar{q}b\bar{b}$ $Zh \to ZWW^*$ $\nu\overline{\nu}W^+W^-$	Triple Higgs coupling Higgs mass $B(h \to WW^*)$ $\sigma(e^+e^- \to \nu\overline{\nu}W^+W^-)$	Tracker and Calorimeter	Jet Energy Resolution $\Delta E/E$	3% to 4%
$Zh \to \ell^+\ell^- X$ $\mu^+\mu^-(\gamma)$ $Zh + h\nu\overline{\nu} \to \mu^+\mu^- X$	Higgs recoil mass Luminosity weighted E_{cm} BR($h \to \mu^+\mu^-$)	μ detector Tracker	Charged particle Momentum Resolution $\Delta p_t/p_t^2$	$5 \times 10^{-5}(GeV/c)^{-1}$
$Zh, h \to b\bar{b}, c\bar{c}, b\bar{b}, gg$	Higgs branching fractions b-quark charge asymmetry	Vertex	Impact parameter	$5\mu m \oplus$ $10\mu m/p(\mathrm{GeV/c})\sin^{3/2}\theta$
SUSY, eg. $\tilde{\mu}$ decay	$\tilde{\mu}$ mass	Tracker Calorimeter μ detector	Momentum Resolution Hermeticity	

Bon mais alors et la physique ?

Brout-Englert-Higgs

MS: Secteur électrofaible / Higgs.

$$\mathcal{L}_{EW}^{SM} = -\frac{1}{4}W^a_{\mu\nu}W_a^{\mu\nu} - -\frac{1}{4}B_{\mu\nu}B^{\mu\nu}$$
$$+\bar{L}\gamma^\mu\left(i\partial_\mu - \frac{1}{2}g\tau_a W^a_\mu - \frac{1}{2}g'YB_\mu\right)L$$
$$+\bar{R}\gamma^\mu\left(i\partial_\mu - -\frac{1}{2}g'YB_\mu\right)R$$
$$-\left|\left(i\partial_\mu - \frac{1}{2}g\tau_a W^a_\mu - \frac{1}{2}g'YB_\mu\right)\Phi\right|^2$$
$$+\mu^2|\Phi|^2 - \lambda|\Phi|^4$$
$$-(\sqrt{2}\lambda_d\bar{L}\Phi R + \sqrt{2}\lambda_u\bar{L}\Phi_c R + h.c.)$$

$$V_H = \mu^2\Phi^\dagger\Phi + \frac{1}{2}\lambda(\Phi^\dagger\Phi)^2\ ;\quad \lambda = \frac{M_H^2}{v^2} \text{ and } \mu^2 = -\frac{1}{2}M_H^2$$

⇨ Masse des bosons de jauge
⇨ Couplages aux bosons de jauge

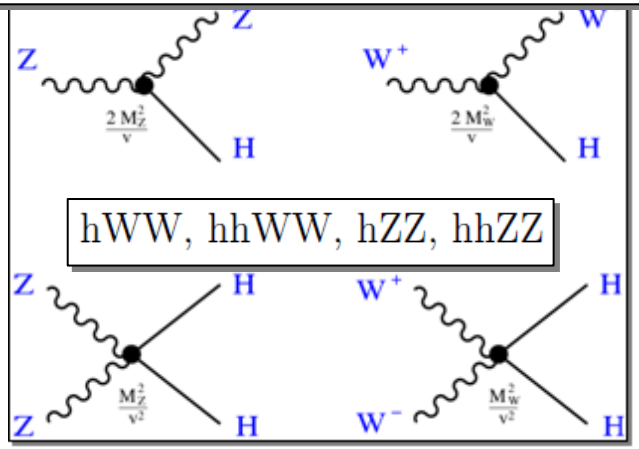

⇨ paramètre μ
⇨ Masse du Higgs

$$\mu^2 = -\frac{1}{2}M_H^2$$

⇨ paramètre λ
⇨ autocouplage du Higgs

$$\lambda = \frac{M_H^2}{v^2}$$

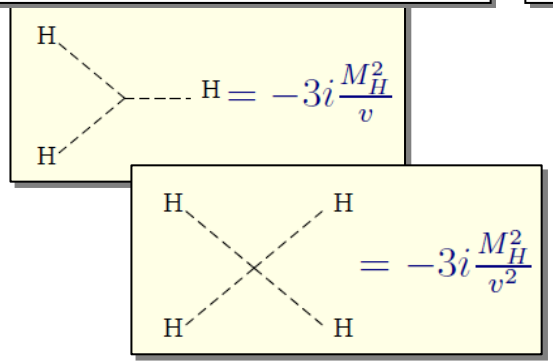

⇨ Couplages de Yukawa ∝ masses fermions
⇨ 9 paramètres libres

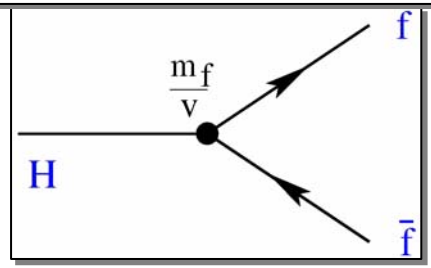

« physics case » : le pourquoi de ces mesures

- Boson découvert au LHC.
  - C'est un boson, probablement de spin 0 (voire 2 ?)
    - Mesure de son spin
  - Il se couple aux fermions et aux bosons

prefer J=0 over 2 and CP + over - at few σ level
LHC will do good job here

- Mesures:
  - Masse: stabilité du vide ?
  - Spin, CP
- 3 types de couplages
  - Couplage aux fermions:
    - établir le « mécanisme » de Yukawa
    - Couplage up / down ? Couplage quarks / leptons ? Couplage aux 3 générations ?
  - Couplage aux bosons:
    - établir le mécanisme de Higgs
  - Autocouplage:
    - établir la forme du potentiel de Higgs
- Questions:
  - Est-il complètement « standard » ?
    - Quid du problème des corrections radiatives et de l'ajustement fin ?
  - Est-il inclut dans une théorie au delà du modèle standard ?
    - Élémentaire ou composite ?
    - Doublet(s) supplémentaire(s) ?
    - SUSY: est-ce vraiment le higgs léger h ?

Brisure spontanée de la symétrie électrofaible

- Pas d'explication de cette brisure de symétrie dans le modèle standard
- 3 classes de modèles
  - Brisure due a la présence d'une nouvelle interaction « forte » à l'échelle du TeV
    - Observables clefs : études des bosons W/Z.
  - Higgs field composite a plus haute énergie
    - Randall-Sudrum models, Little Higgs models, etc.
    - Observables clefs: couplages W/Z/ t au Higgs
  - Supersymétrie
    - Observables clefs: Recherches de jauginos et des Higgs supplémentaires
    - Déviations des Br % SM.

Production du boson H à l'ILC

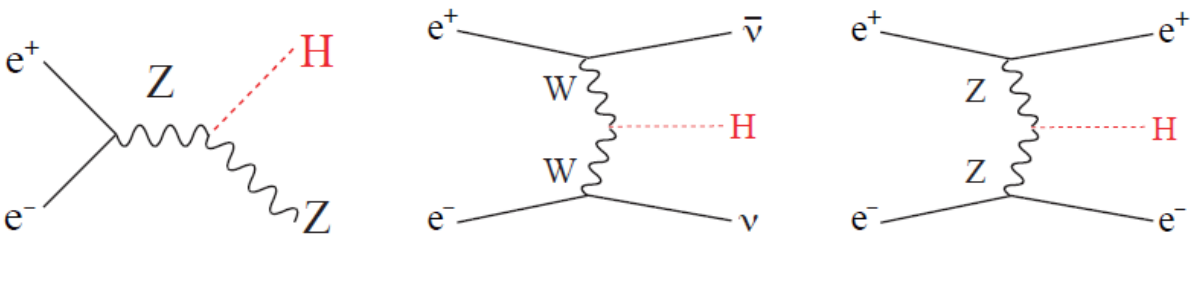

Figure 8: Feynman diagrams for the three major Higgs production processes at the ILC: $e^+e^- \to Zh$ (left), $e^+e^- \to \nu\bar{\nu}H$ (center), and $e^+e^- \to e^+e^-H$ (right).

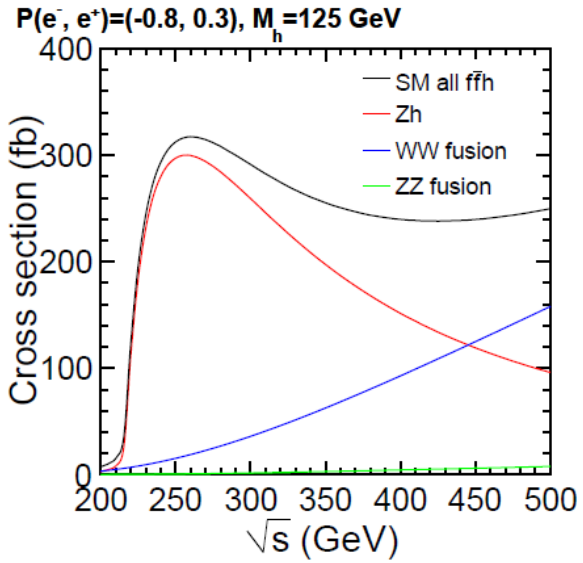

Figure 9: Production cross section for the $e^+e^- \to Zh$ process as a function of the center of mass energy for $m_h = 125\,\text{GeV}$, plotted together with those for the WW and ZZ fusion processes: $e^+e^- \to \nu\bar{\nu}H$ and $e^+e^- \to e^+e^-H$.

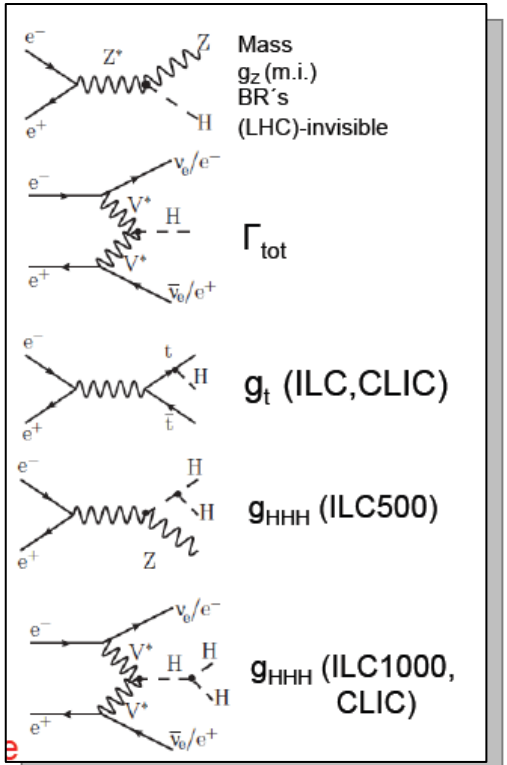

Retour sur la méthode de la masse de recul

$$M_H^2 = \quad M_{recoil}^2 \quad = s + M_Z^2 - 2E_Z\sqrt{s}$$

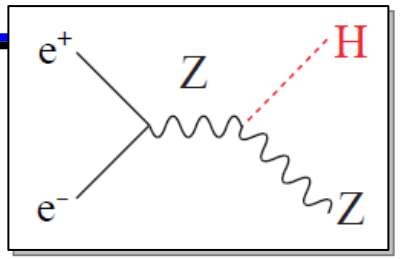

- Avantages:
  - Mesure de la masse mH — LHC goal
    ILC: → $\Delta m_H \approx 30$ MeV — → $\Delta m_H \approx 100$ MeV (syst. limited)
  - Mesure de la section efficace totale σ_{ZH} $\Delta\sigma_{ZH}/\sigma_{ZH} = 2.5\%$
    - Mesure absolue du couplage g_{HZZ}
  - Mesure absolue des rapports de branchement indépendante du modèle
    - $BR_{(H\to XX)} = (\sigma_{ZH} \times BR_{(H\to XX)})_{meas} / (\sigma_{ZH})_{meas}$
    - + Mesure accès au BR invisible

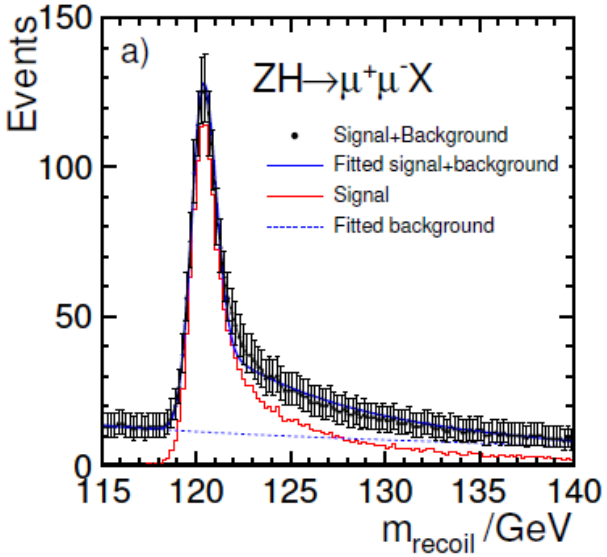

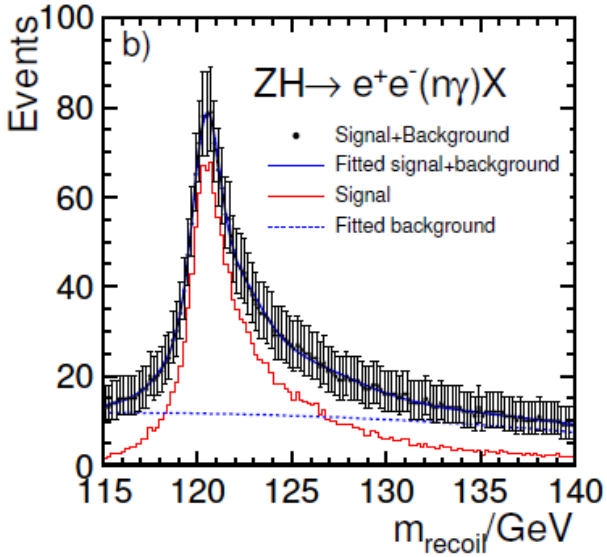

Rapport de Branchement théoriques du boson de BEH

A. Denner, S. Heinemeyer, I. Puljak, D. Rebuzzi and M. Spira, Eur. Phys. J. C 71, 1753 (2011) [arXiv:1107.5909 [hep-ph]].

sample. The ILC, including its eventual 1 TeV stage, will allow measurement of the Higgs boson couplings to W, Z, b, c, τ, and μ, plus the loop-induced couplings to gg, $\gamma\gamma$, and γZ. The regularity of the SM that the Higgs couplings are precisely proportional to mass can thus be verified or refuted through measurements of many couplings spanning a large dynamic range.

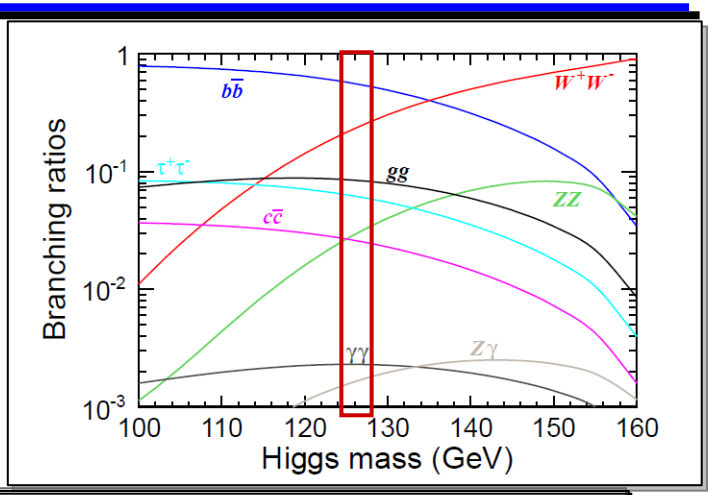

M_H [GeV]	$H \to b\bar{b}$	$H \to \tau^+\tau^-$	$H \to \mu^+\mu^-$	$H \to c\bar{c}$
124.5	$5.84E{-}01^{+3.2\%}_{-3.2\%}$	$6.39E{-}02^{+5.8\%}_{-5.7\%}$	$2.22E{-}04^{+6.0\%}_{-5.9\%}$	$2.95E{-}02^{+12.2\%}_{-12.2\%}$
125.0	$5.77E{-}01^{+3.2\%}_{-3.3\%}$	$6.32E{-}02^{+5.7\%}_{-5.7\%}$	$2.20E{-}04^{+6.0\%}_{-5.9\%}$	$2.91E{-}02^{+12.2\%}_{-12.2\%}$
125.5	$5.69E{-}01^{+3.3\%}_{-3.3\%}$	$6.24E{-}02^{+5.7\%}_{-5.6\%}$	$2.17E{-}04^{+6.0\%}_{-5.8\%}$	$2.87E{-}02^{+12.2\%}_{-12.2\%}$
126.0	$5.61E{-}01^{+3.3\%}_{-3.4\%}$	$6.15E{-}02^{+5.6\%}_{-5.6\%}$	$2.14E{-}04^{+5.9\%}_{-5.8\%}$	$2.83E{-}02^{+12.2\%}_{-12.2\%}$
126.5	$5.53E{-}01^{+3.4\%}_{-3.4\%}$	$6.08E{-}02^{+5.6\%}_{-5.5\%}$	$2.11E{-}04^{+5.9\%}_{-5.7\%}$	$2.79E{-}02^{+12.2\%}_{-12.2\%}$

M_H [GeV]	$H \to gg$	$H \to \gamma\gamma$	$H \to Z\gamma$	$H \to WW$	$H \to ZZ$	Γ_H [GeV]
124.5	$8.61E{-}02^{+10.3\%}_{-10.0\%}$	$2.28E{-}03^{+5.0\%}_{-4.9\%}$	$1.49E{-}03^{+9.1\%}_{-8.9\%}$	$2.07E{-}01^{+4.3\%}_{-4.2\%}$	$2.52E{-}02^{+4.4\%}_{-4.2\%}$	$4.00E{-}03^{+4.0\%}_{-4.0\%}$
125.0	$8.57E{-}02^{+10.2\%}_{-10.0\%}$	$2.28E{-}03^{+5.0\%}_{-4.9\%}$	$1.54E{-}03^{+9.0\%}_{-8.8\%}$	$2.15E{-}01^{+4.3\%}_{-4.2\%}$	$2.64E{-}02^{+4.3\%}_{-4.2\%}$	$4.07E{-}03^{+4.0\%}_{-3.9\%}$
125.5	$8.52E{-}02^{+10.2\%}_{-9.9\%}$	$2.28E{-}03^{+4.9\%}_{-4.8\%}$	$1.58E{-}03^{+8.9\%}_{-8.8\%}$	$2.23E{-}01^{+4.2\%}_{-4.1\%}$	$2.76E{-}02^{+4.3\%}_{-4.1\%}$	$4.14E{-}03^{+3.9\%}_{-3.9\%}$
126.0	$8.48E{-}02^{+10.1\%}_{-9.9\%}$	$2.28E{-}03^{+4.9\%}_{-4.8\%}$	$1.62E{-}03^{+8.9\%}_{-8.8\%}$	$2.31E{-}01^{+4.1\%}_{-4.1\%}$	$2.89E{-}02^{+4.2\%}_{-4.0\%}$	$4.21E{-}03^{+3.9\%}_{-3.8\%}$
126.5	$8.42E{-}02^{+10.1\%}_{-9.8\%}$	$2.28E{-}03^{+4.8\%}_{-4.7\%}$	$1.66E{-}03^{+8.8\%}_{-8.7\%}$	$2.39E{-}01^{+4.1\%}_{-4.0\%}$	$3.02E{-}02^{+4.1\%}_{-4.0\%}$	$4.29E{-}03^{+3.8\%}_{-3.8\%}$

Exemples de déviation % au Modèle Standard

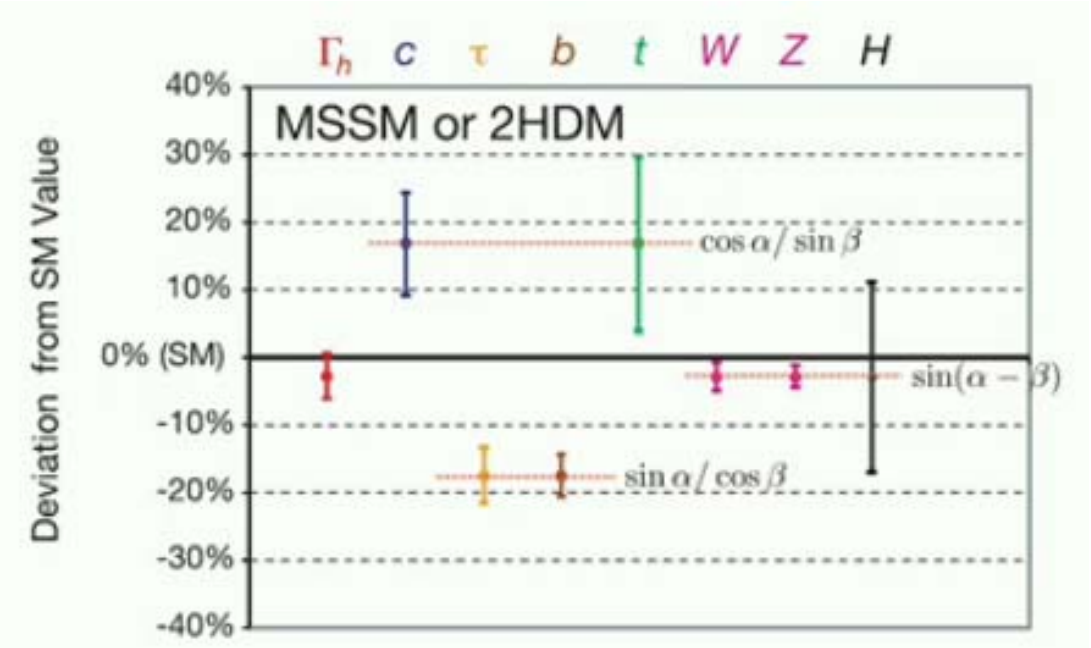

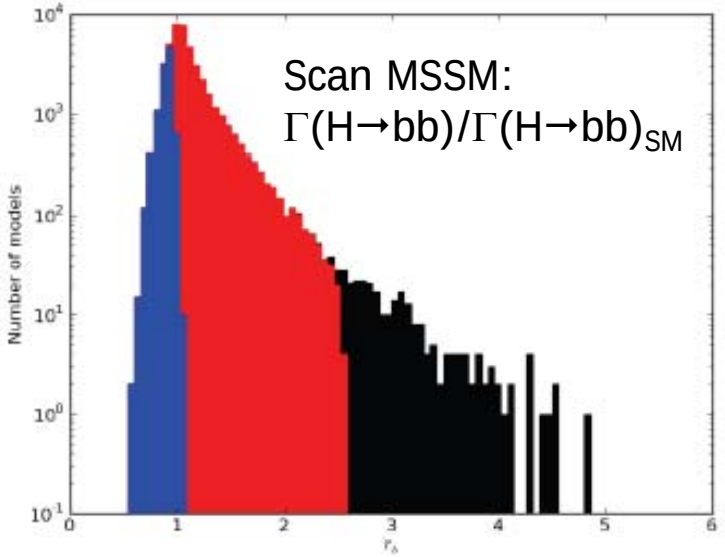

Maximum Deviation	ΔhVV	$\Delta h\bar{t}t$	$\Delta h\bar{b}b$
Mixed-in Singlet	6%	6%	6%
Composite Higgs	8%	tens of %	tens of %
Minimal Supersymmetry	< 1%	3%	10%, 100%

$\tan\beta > 20$ no superpartners — all other cases

- Ordre de grandeur:
  - Différence SM/BSM de quelques pourcents très souvent. (5-10%)
  - Nécessité de mesure avec une précision de cet ordre.

Higgs: nombre d'événements attendus

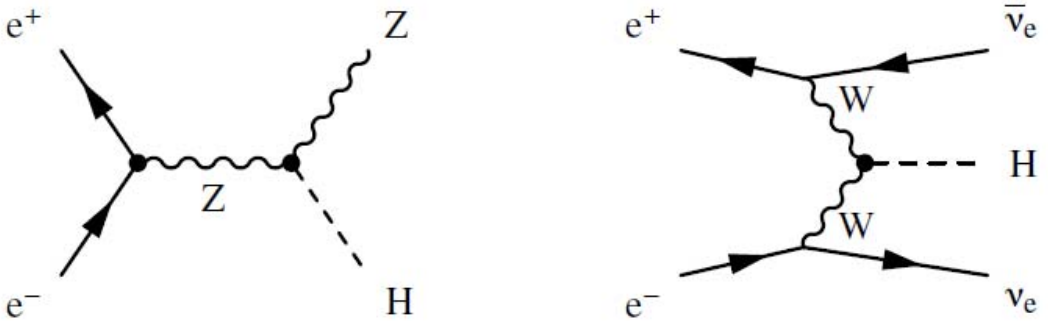

Figure 1: The two main Higgs production processes at a LC.

	250 GeV	350 GeV	500 GeV	1 TeV	1.5 TeV	3 TeV
$\sigma(e^+e^- \to ZH)$	240 fb	129 fb	57 fb	13 fb	6 fb	1 fb
$\sigma(e^+e^- \to H\nu_e\bar{\nu}_e)$	8 fb	30 fb	75 fb	210 fb	309 fb	484 fb
Int. $\mathcal{L}$	250 fb^{-1}	350 fb^{-1}	500 fb^{-1}	1000 fb^{-1}	1500 fb^{-1}	2000 fb^{-1}
# ZH events	60,000	45,500	28,500	13,000	7,500	2,000
# $H\nu_e\bar{\nu}_e$ events	2,000	10,500	37,500	210,000	460,000	970,000

HHH coupling

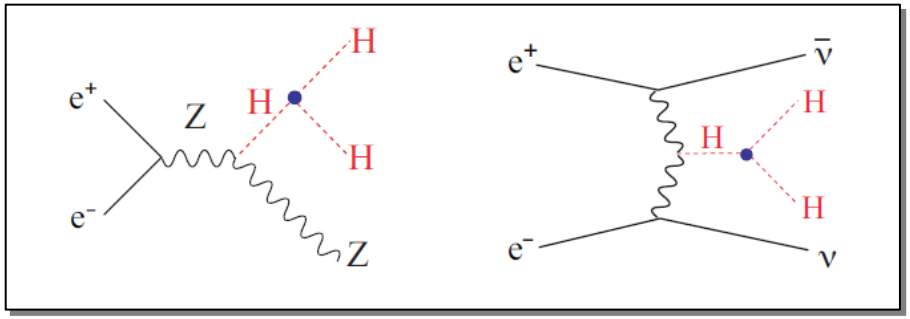

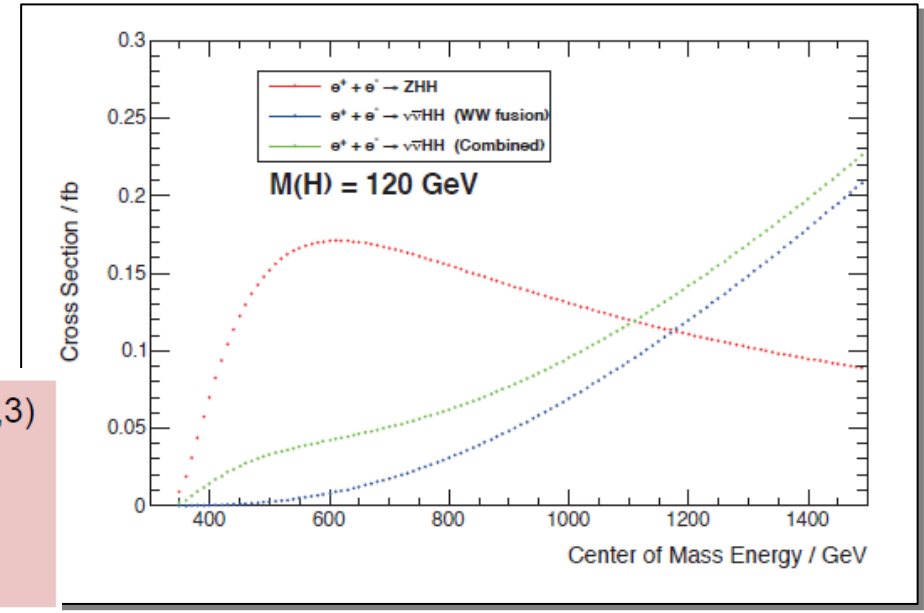

ZHH	500 GeV 2 ab^{-1} P=(-0,8,0,3)
significance for HH prod.	5.0σ
Δσ(ZHH)/σ(ZHH)	27%
Δλ/λ	44%

state-of-the-art today

	Δλ/λ
ILC 500/2ab^{-1}	44%
ILC 1000/2ab^{-1}	18%
CLIC1400/1.5 ab^{-1}	22%
CLIC3000/2 ab^{-1}	11%

Très haute luminosité requise

- key algorithms: b-tag, lepton-finder, jet-finder.
- lots of efforts are ongoing for the further improvement.

Signal efficiencies $\lesssim$ 10% → room for improvement? (e.g. jet finding, jetless vtx?)

production tth et top Yukawa coupling (√s = 1000 GeV)

$e^+e^- \to bq\bar{q}\,\bar{b}q\bar{q}\,b\bar{b}$ (hadronic)
$e^+e^- \to bl\nu\,\bar{b}q\bar{q}\,b\bar{b}$ (semi lep)
$e^+e^- \to bl\nu\,\bar{b}l\nu\,b\bar{b}$ (leptonic)

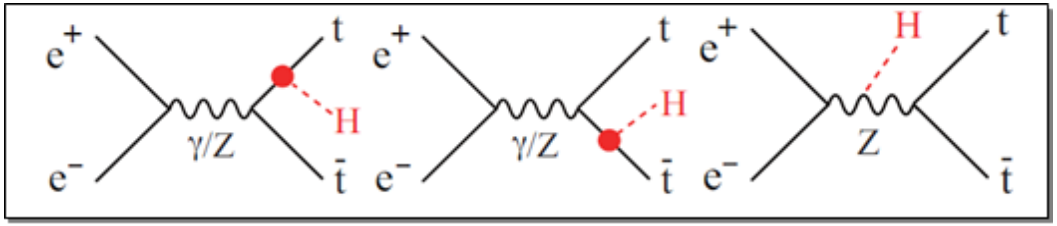

Top Yukawa Coupling @ 500 GeV

R. Yonamine, T. Tanabe, K. Fujii

6 jet + lep	tth (6J+L)	bb4f	ttZ	ttbb	Sig
No Selection	246	9.09×10^5	1910	1060	
Cut-based	32	39	21	15	3.1
Likelihood	39	58	29	22	3.2

Semi Leptonic [E_{CM}=500 GeV, L=1 ab^{-1}, Pol=(-0.8,+0.3)]

8 jet	tth (8J)	bb4f	ttZ	ttbb	Sig
No Selection	235	9.09×10^5	1910	1060	
Cut-based	38	41	25	16	3.5
Likelihood	78	241	63	46	3.8

Hadronic [E_{CM}=500 GeV, L=1 ab^{-1}, Pol=(-0.8,+0.3)]

6 jet & 8 jet modes	Combined Sig	$\left(\frac{\Delta g_{ttH}}{g_{ttH}}\right)_{stat}$
Cut-based	4.7	11 %
Likelihood	5.0	10 %

1 TeV SiD analysis

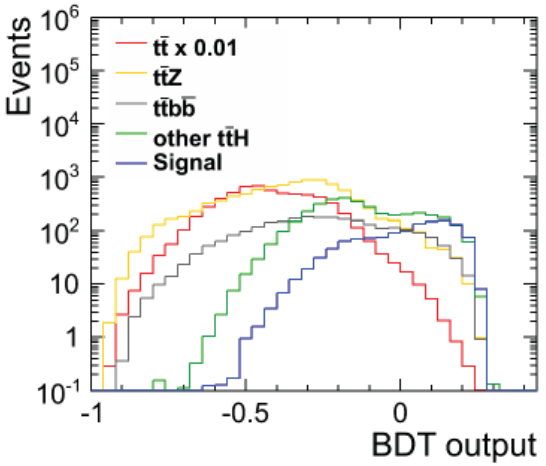

	500 GeV/ 1 ab^{-1}	1000 GeV/ 2 ab^{-1}
$\Delta g_{ttH}/g_{ttH}$	10%	4.6%

note: σ(520 GeV)/σ(500) GeV ~ 2 (!)

Couplages: résumé

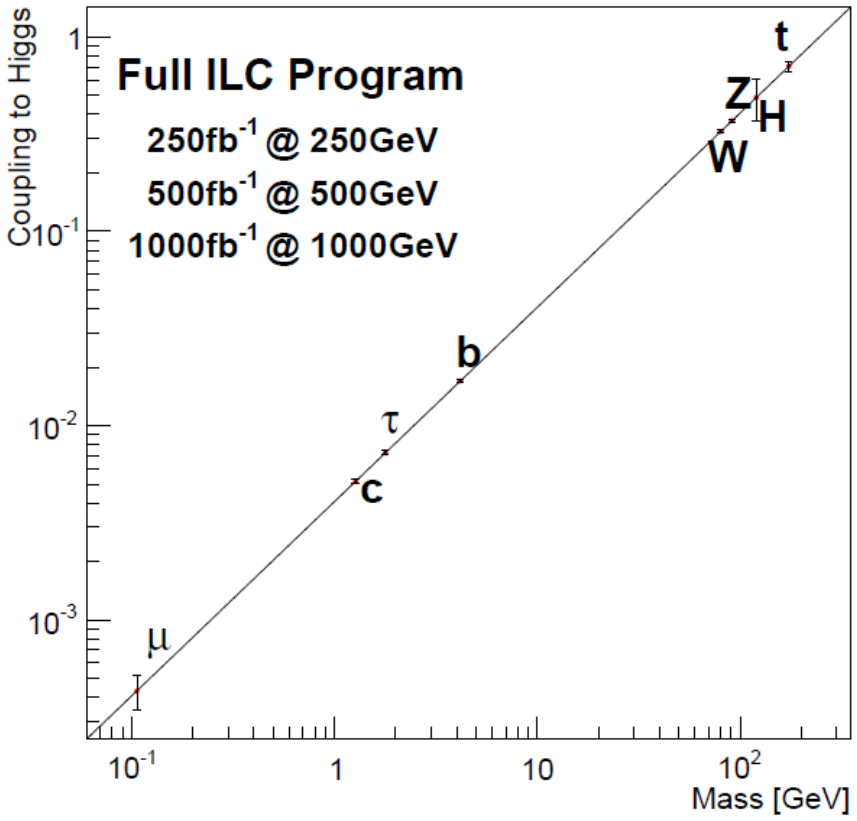

Figure 23: Expected precision from the full ILC program of tests of the Standard Model prediction that the Higgs coupling to each particle is proportional to its mass.

	$\Delta(\sigma \cdot BR)/(\sigma \cdot BR)$				
$\sqrt{s}$ and $\mathcal{L}$ (P_{e^-}, P_{e^+})	250 fb^{-1} at 250 GeV (-0.8,+0.3)		500 fb^{-1} at 500 GeV (-0.8,+0.3)		1 ab^{-1} at 1 TeV (-0.8,+0.2)
mode	Zh	$\nu\bar{\nu}h$	Zh	$\nu\bar{\nu}h$	$\nu\bar{\nu}h$
$h \to b\bar{b}$	1.1%	10.5%	1.8%	0.66%	0.47%
$h \to c\bar{c}$	7.4%	-	12%	6.2%	7.6%
$h \to gg$	9.1%	-	14%	4.1%	3.1%
$h \to WW^*$	6.4%	-	9.2%	2.6%	3.3%
$h \to \tau^+\tau^-$	4.2%	-	5.4%	14%	3.5%
$h \to ZZ^*$	19%	-	25%	8.2%	4.4%
$h \to \gamma\gamma$	29-38%	-	29-38%	20-26%	7-10%
$h \to \mu^+\mu^-$	100%	-	-	-	32%

process	$\sqrt{s}$ [GeV]	$\mathcal{L}$ [fb^{-1}]	(P_{e^-}, P_{e^+})	$\Delta(\sigma \cdot BR)/(\sigma \cdot BR)$	$\Delta g/g$
$t\bar{t}h$	500	500	(-0.8,+0.3)	35%	18%
Zhh	500	500	(-0.8,+0.3)	64%	104%
$t\bar{t}h$	1000	1000	(-0.8,+0.2)	8.7%	4.0%
$\nu\bar{\nu}hh$	1000	1000	(-0.8,+0.2)	38%	28%

Couplage: comparaison ILC/LHC

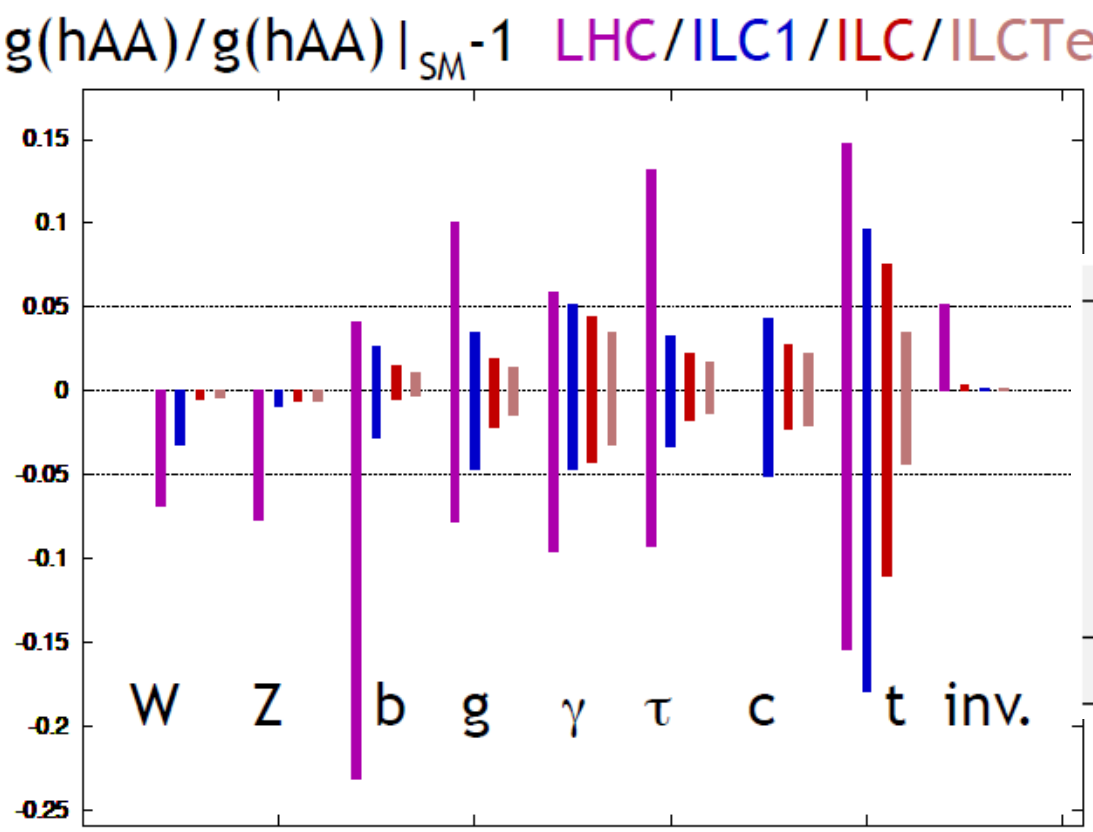

LC(250GeV)
_C(500GeV)
= ILC(1TeV)

Mode	LHC	ILC(250)	ILC500	ILC(1000)
WW	4.1 %	1.9 %	0.24 %	0.17 %
ZZ	4.5 %	0.44 %	0.30 %	0.27 %
$b\bar{b}$	13.6 %	2.7 %	0.94 %	0.69 %
gg	8.9 %	4.0 %	2.0 %	1.4 %
$\gamma\gamma$	7.8 %	4.9 %	4.3 %	3.3 %
$\tau^+\tau^-$	11.4 %	3.3 %	1.9 %	1.4 %
$c\bar{c}$	–	4.7 %	2.5 %	2.1 %
$t\bar{t}$	15.6 %	14.2 %	9.3 %	3.7 %
$\mu^+\mu^-$	–	–	–	16 %
self	–	–	104%	26 %
BR(invis.)	$< 9\%$	< 0.44 %	< 0.30 %	< 0.26 %
$\Gamma_T(h)$	20.3%	4.8 %	1.6 %	1.2 %

Figure 2.20. Estimate of the sensitivity of the ILC experiments to Higgs boson couplings in a model-independent analysis. The plot shows the 1 σ confidence intervals as they emerge from the fit described in the text. Deviation of the central values from zero indicates a bias, which can be corrected for. The upper limit on the WW and ZZ couplings arises from the constraints (2.31). The bar for the invisible channel gives the 1 σ upper limit on the *branching ratio*. The four sets of errors for each Higgs coupling represent the results for LHC (300 fb^{-1}, 1 detector), the threshold ILC Higgs program at 250 GeV, the full ILC program up to 500 GeV, and the extension of the ILC program to 1 TeV. The methodology leading to this figure is explained in [65].

top

Et autres mesures de précision

Quark top

- Top a l'ILC:
  - Rôle crucial dans la brisure de symétrie EW ?
  - Production EW
  - Erreurs théoriques faibles
  - Mesure de la masse
    - Stabilité du vide
  - Asymétries
    - Structure chirale du MS.
  - Corrections radiatives: ⇨m_t
  - Nouvelle physique susceptible d'apparaitre dans les mesures de précision du secteur du top.
    - Recherche de nouvelles physique

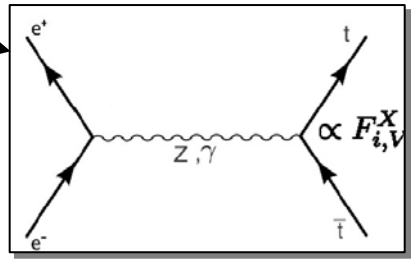

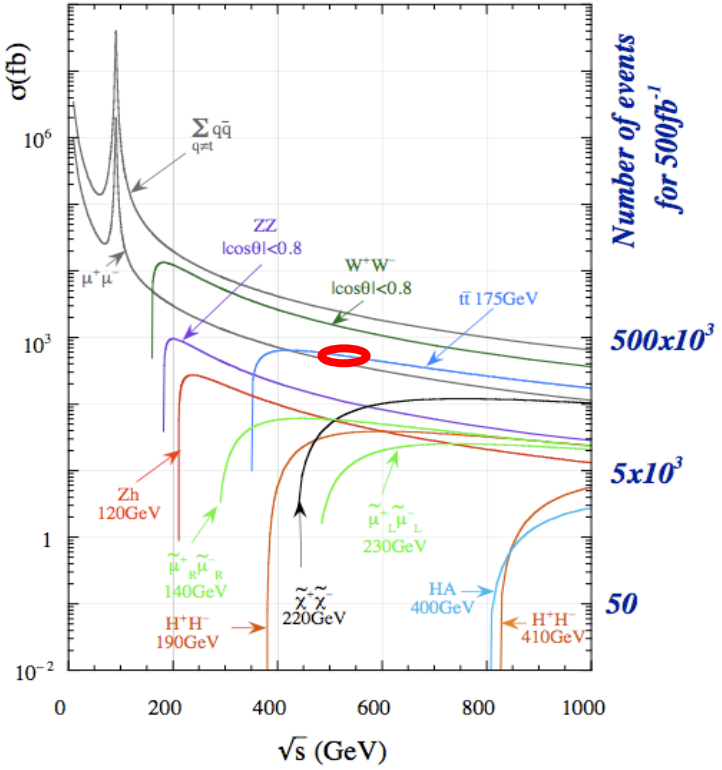

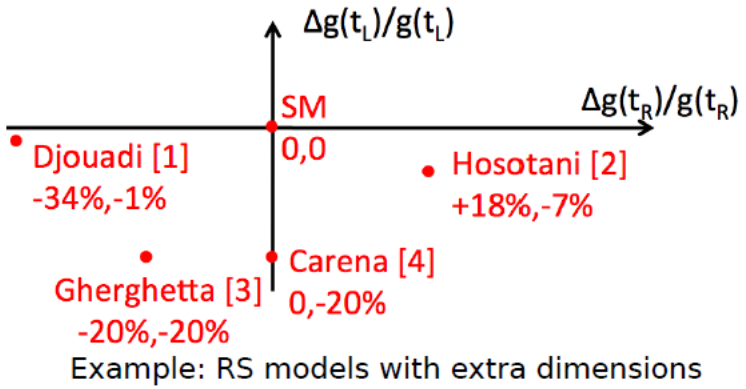

Masse du top: « threshold scan »

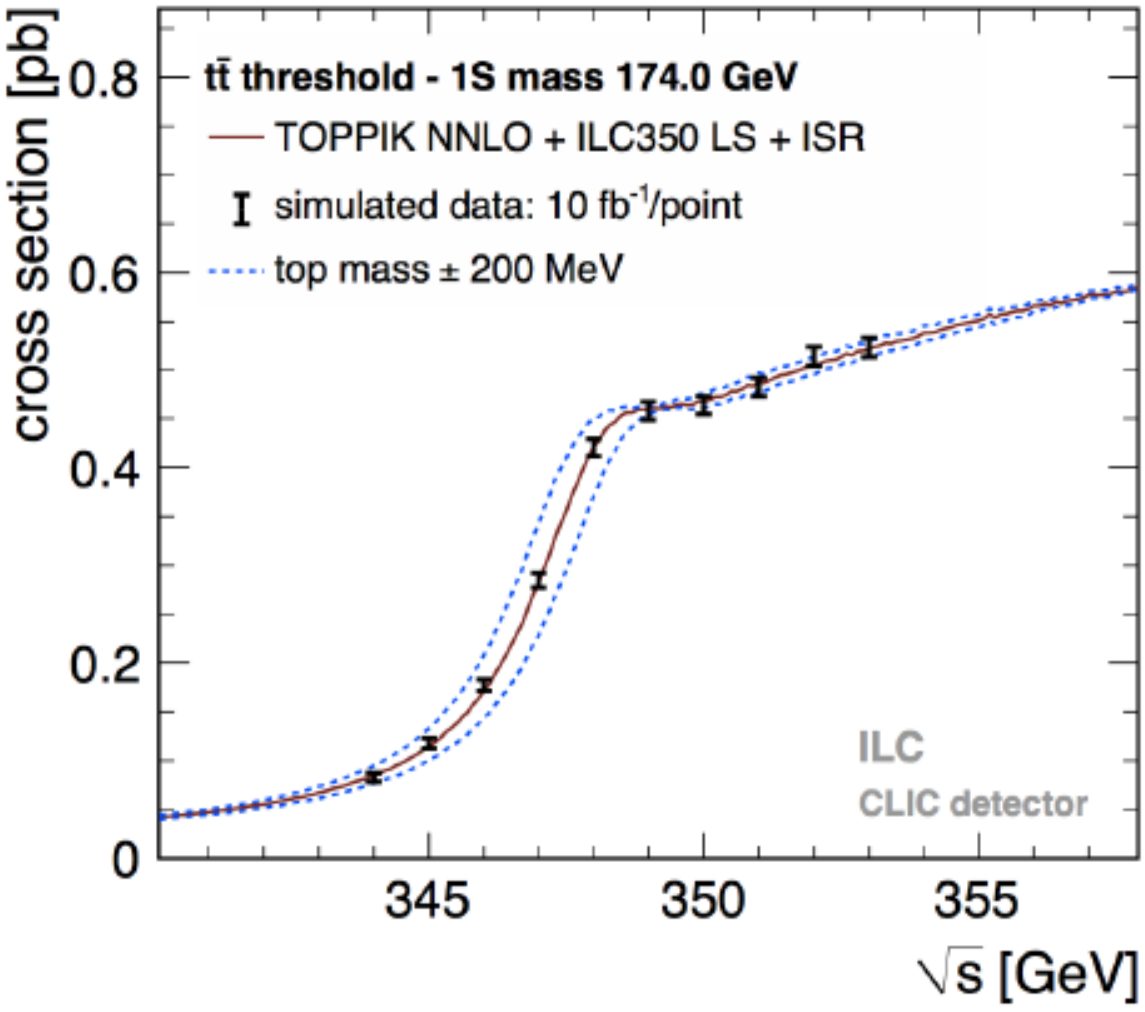

Top quark mass with ~100 MeV precision

Stabilité du potentiel de higgs.

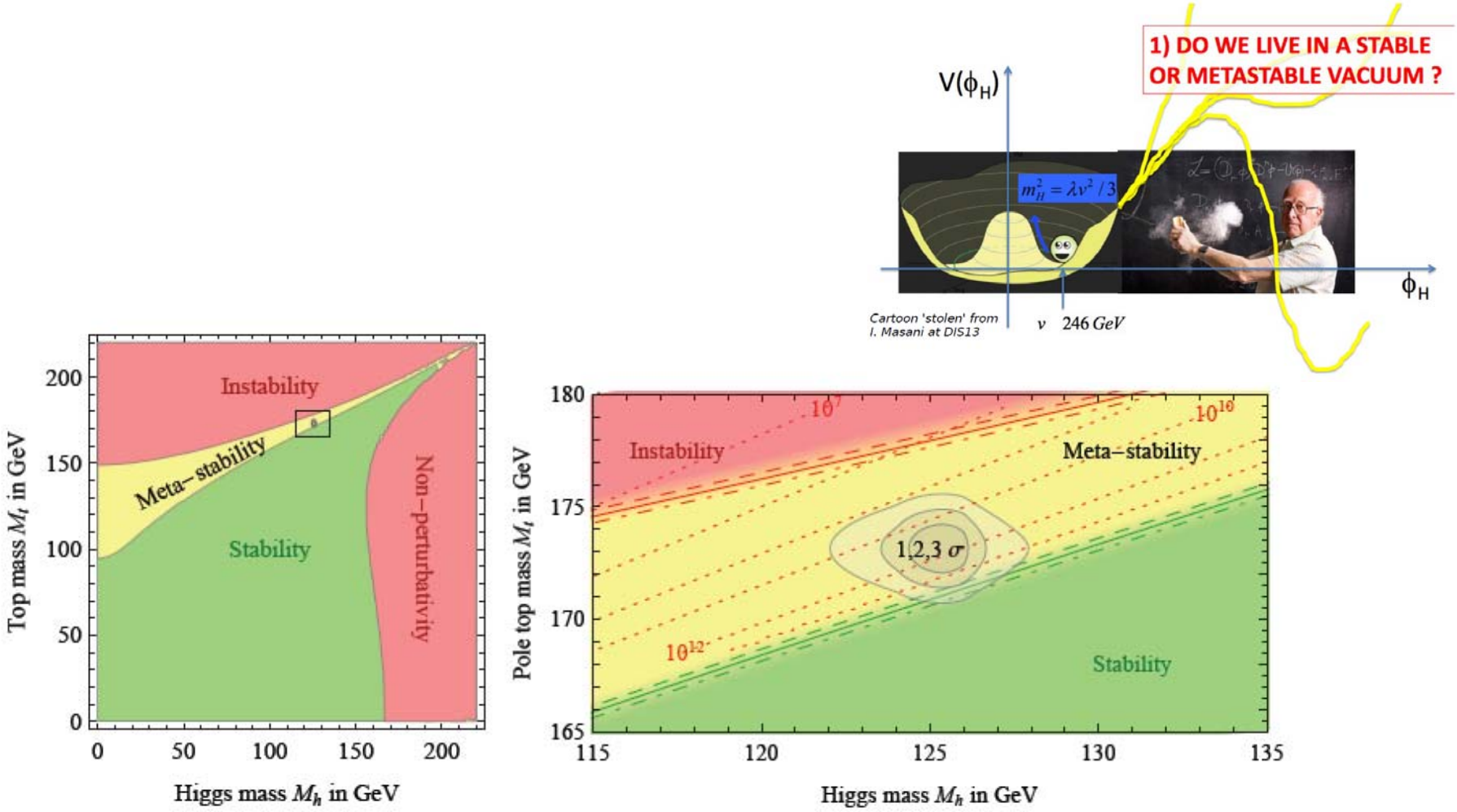

Figure 4: Regions of stability and instability for the Higgs potential of the Standard Model, in the plane of m_h vs. m_t, from [14]. The right-hand figure show the 1, 2, and 3 σ contours corresponding to the currently preferred values of the Higgs boson and top quark masses.

W physics

W pair production

Single W production

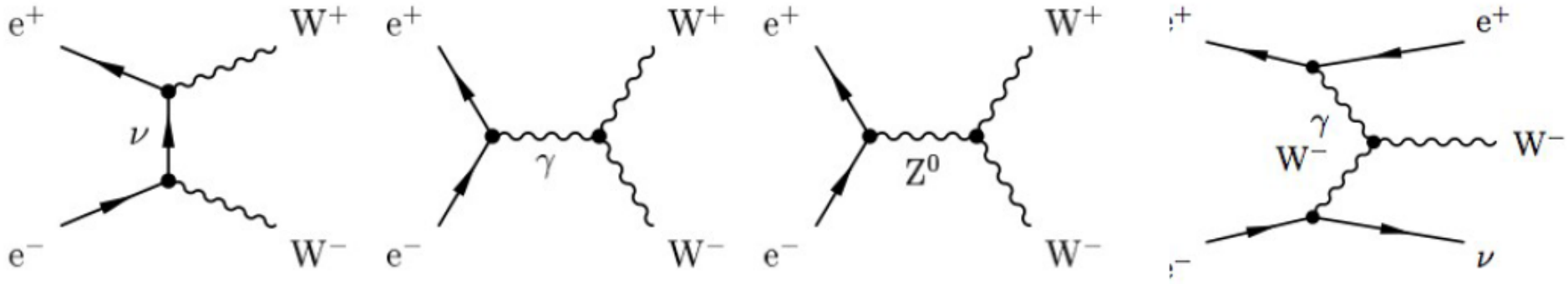

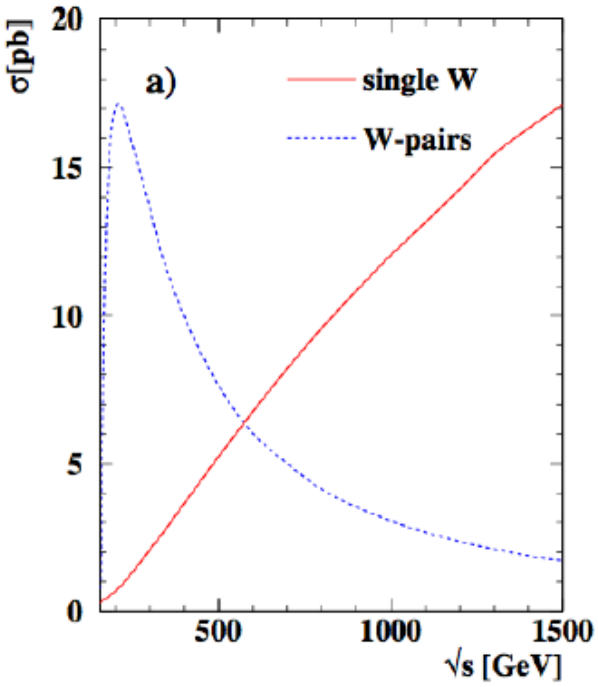

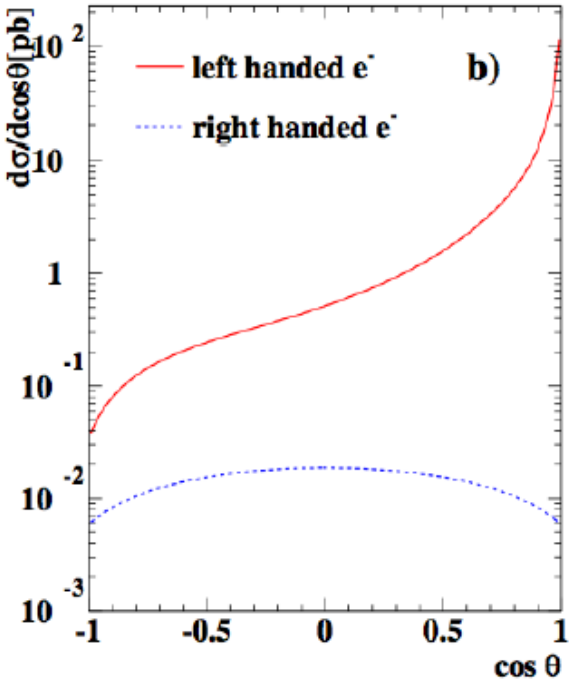

- Sensitivity to Triple and quartic gauge Boson couplings (TGC and QGC)

- Observables depend strongly on beam polarisation

=> Enrich different helicity modes of W
=> in situ measurement of beam polarisation

Au delà du Modèle Standard

exemples

Recherche de Z'

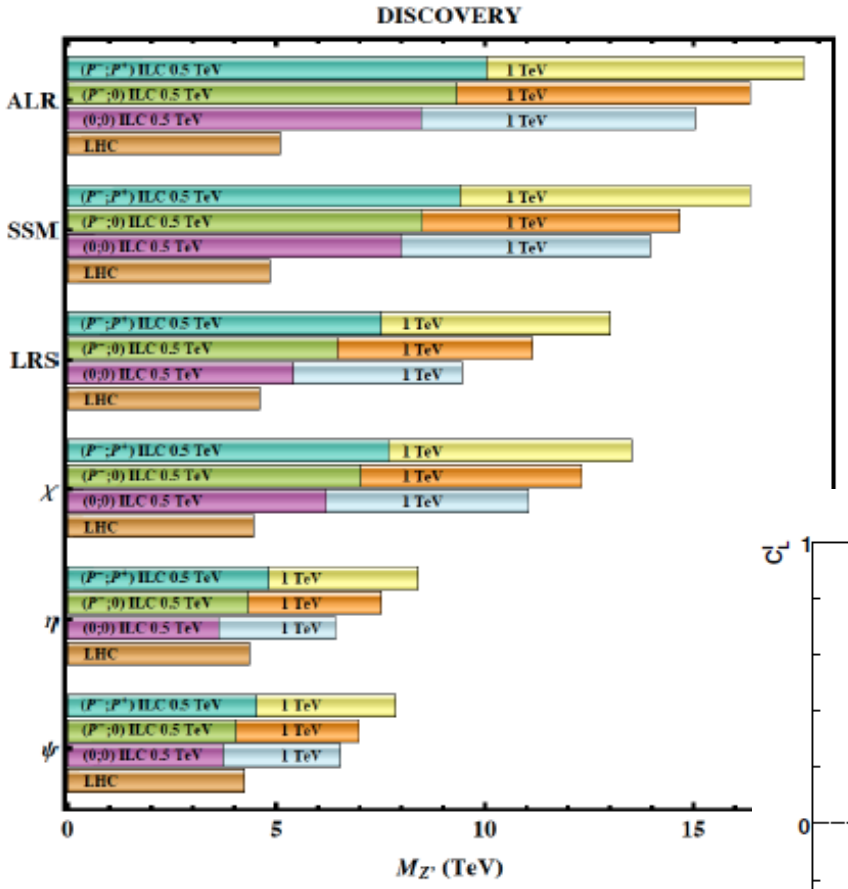

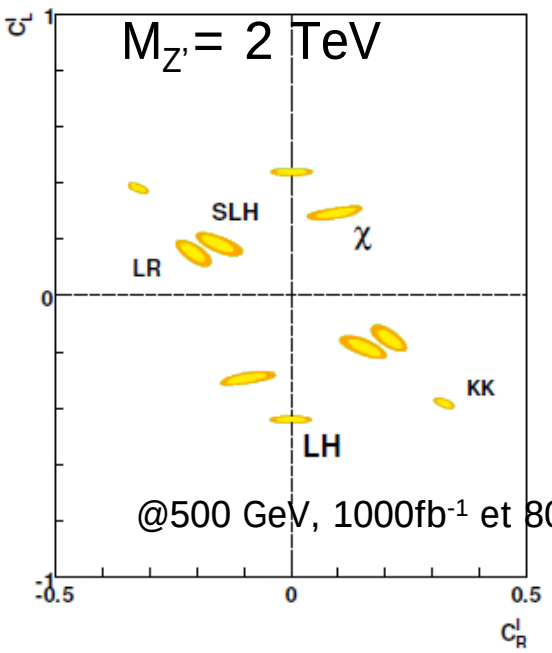

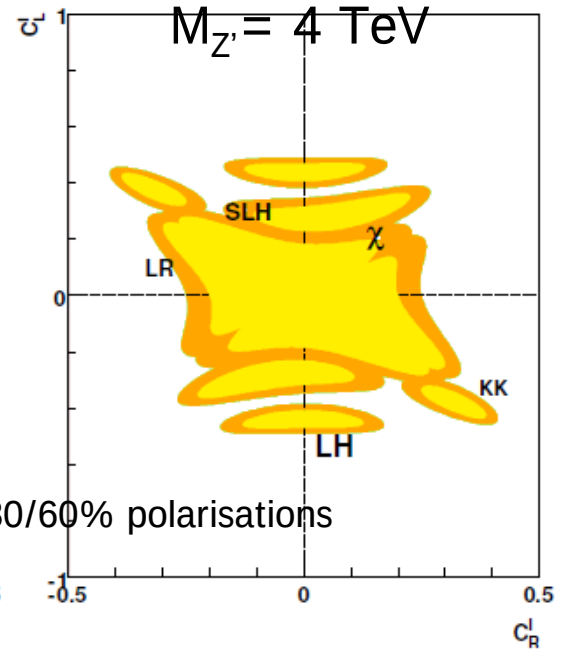

@500 GeV, 1000fb^{-1} et 80/60% polarisations

Supersymétrie

- LHC:
  - Recherches squarks/gluinos
  - Masse du Higgs
    - Difficile d'éviter un ajustement fin (~%)

These bounds are not "robust" and don't exclude weak scale SUSY but call for non-minimal models

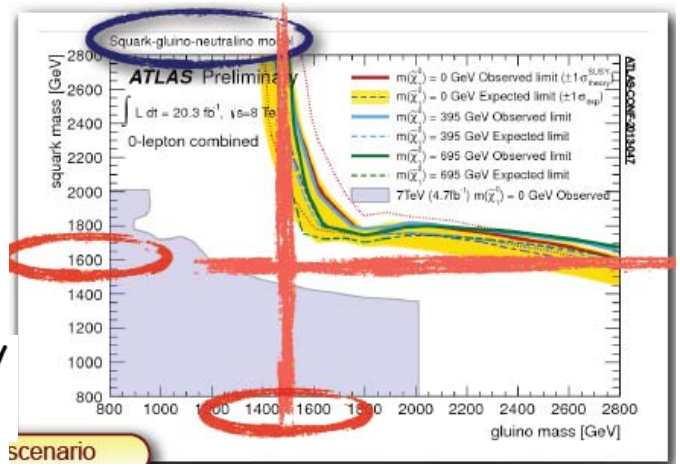

  - Hiérarchie des masses des sparticules « moins classiques »
- ILC
  - Capacités secteurs sleptons / jauginos
    - Mesures des masses O(%)
    - Mesure des spins
  - En cas de découvertes
    - Energie, polarisation
    - Détermination précise des propriétés des particules susy découvertes

Figure 7.3 Measurement of the chargino mixing angles at the ILC at 500 GeV from the production cross-sections using e^-Le^+R and $e^-_Re^+_L$ polarized beams. From [104].

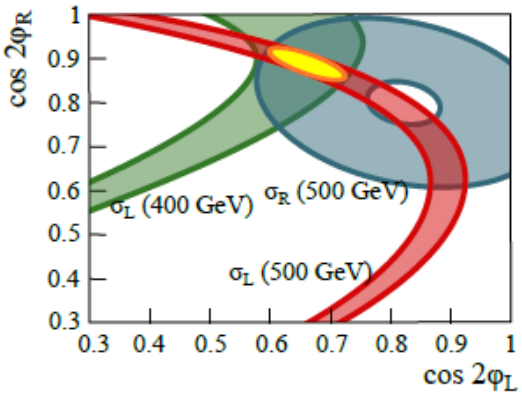

Matière sombre

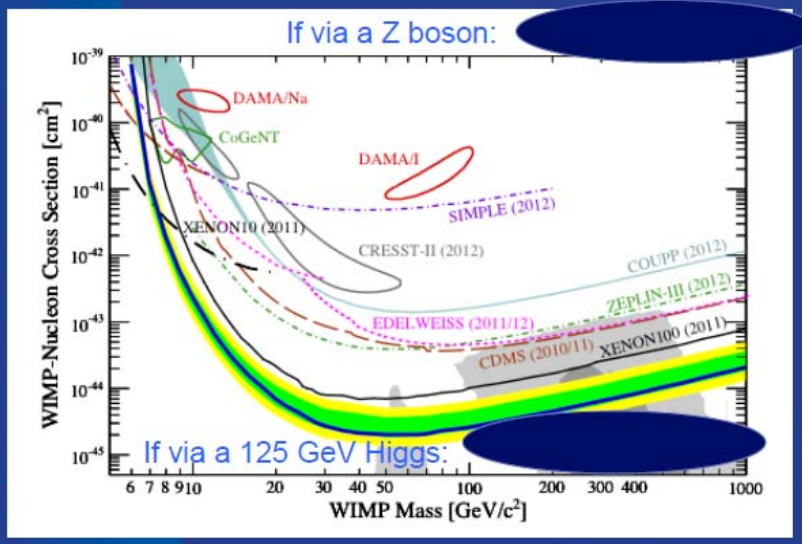

Next generation DM experiments can see this

Adapted from AAAS slide by N. Weiner

ILC and dark matter

- If the DM is light enough, ILC will produce it directly
- Or from decays of partners (e.g. charginos, sleptons)
- Or from Higgs decays

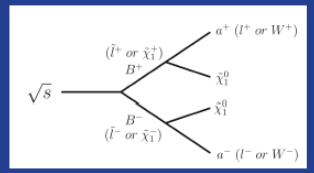

Together with results from direct + indirect detection + LHC, ILC can "close the circle" on dark matter

- Do measured DM properties account for its relic density?
- What is the relation of dark matter to ordinary matter?

Giga Z option

	LEP/SLC/Tev/world av. [49]	ILC
$\sin^2\theta^\ell_{\rm eff}$	0.23146 ± 0.00017	$\leq \pm 0.00001$
M_Z	91.1876 ± 0.0021 GeV	± 0.0016 GeV
Γ_Z	2.4952 ± 0.0023 GeV	± 0.0008 GeV
$\alpha_s(m_Z^2)$	0.1184 ± 0.0007	± 0.0005
$\Delta\rho_\ell$	$(0.55 \pm 0.10) \cdot 10^{-2}$	$\pm 0.05 \cdot 10^{-2}$
N_ν	2.984 ± 0.008	± 0.004
$\mathcal{A}_b$	0.923 ± 0.020	± 0.001
$R_{\rm b}^0$	0.21653 ± 0.00069	± 0.00014
M_W	80.385 ± 0.015 GeV	± 0.006 GeV

Table 16: Precision of several SM observables that can be achieved at the ILC from a high-luminosity low-energy run (GigaZ option). The left column gives the present status together with possible expectations from the LHC experiments. The values given for the $\Delta\rho$ parameter as well as for the determination of the strong coupling constant assume $N_\nu = 3$.

Conclusion

- La découverte d'un boson au LHC en 2012 justifie plus que jamais le programme de physique de l'ILC.
- La R & D sur l'ILC a démontré la faisabilité technique du projet.
- Le projet ILC rentre dans une période cruciale.
  - 2013-2016

> Whatever might be added from LHC discoveries later in this decade, the Higgs is there. The ILC capabilities are perfectly matched to the needs of an experimental program of precision measurements on the 125 GeV Higgs boson. It is the right time, in direct response to the discovery, to call for the construction of this machine.

Michael Peskin

- Proposition japonaise:
  - Opportunité unique à saisir de la part de la communauté
  - L'avenir de la discipline se prépare aujourd'hui.

Saisir l’opportunité...

Saisir l’opportunité...

...c’est déclencher une réaction au bon moment !

Back up

Bibliographie sommaire

- TDR (june 2013)
  - http://www.linearcollider.org/ILC/Publications/Technical-Design-Report
- Letters of Intent
  - http://www.linearcollider.org/physics-detectors/Detectors/Detector-LOIs
- Reference Design report (Aout 2007)
  - http://www.linearcollider.org/about/Publications/Reference-Design-Report
- Detector Baseline Document (draft dec 2012)
  - http://www-flc.desy.de/dbd/
- LHC/ILC interplay
  - http://arxiv.org/abs/hep-ph/0410364
- LC notes:
  - http://www-flc.desy.de/lcnotes/
- Calendrier:
  - http://www.linearcollider.org/Calendar
- Workshop, conferences recentes
  - ILD workshop 2012: http://epp.phys.kyushu-u.ac.jp/ildws2012/
  - European strategy for Particle Physics: http://espp2012.ifj.edu.pl/
  - Journees LC France
  - ECFA Desy.
- Sites
  - ILC: http://www.linearcollider.org/
  - News: http://newsline.linearcollider.org/
  - ILD: http://ilcild.org/
  - SID: https://silicondetector.org/display/SiD/home

Incertitudes sur les rapports de branchement du Higgs

A. Denner, S. Heinemeyer, I. Puljak, D. Rebuzzi and M. Spira, Eur. Phys. J. C 71, 1753 (2011) [arXiv:1107.5909 [hep-ph]].

Comparaisons entre les collisionneurs e^+e^-

e^+e^- colliders

Table 2.2: Overview of electron-positron colliders (*different scenarios).

Facility	Year	E_{cm} [GeV]	Luminosity $[10^{34}\,cm^{-2}s^{-1}]$	Tunnel length [km]
ILC 250	≪2030	250	0.75	
ILC 500		500	1.8	∼ 30
ILC 1000		1000	4.9	∼ 50
CLIC 500	>2030	500	2.3 (1.3)*	∼ 13
CLIC 1400		1400 (1500)*	3.2 (3.7)*	∼ 27
CLIC 3000		3000	5.9	∼ 48
LEP3	>2024?	240	1	LEP/LHC
TLEP	>2030	240	5	80 (ring)
TLEP		350	0.65	80 (ring)

from European Strategy „Briefing Book“ (red stuff added by KD)

Higgs Physics at CLIC

- Currently working towards a comprehensive assessment of the full SM Higgs programme
- $\sqrt{s} = 350\,\text{GeV}$:
  - Model-independent mass and cross section from recoil method
  - $H \to b\bar{b}$, $H \to c\bar{c}$, $H \to gg$, $H \to \tau^+\tau^-$, $H \to WW^*$
- $\sqrt{s} = 1.4\,\text{TeV}$:
  - $H \to b\bar{b}$, $H \to c\bar{c}$, $H \to gg$, $H \to \tau^+\tau^-$, $H \to WW^*$, $H \to Z\gamma$, $H \to \gamma\gamma$, $H \to \mu^+\mu^-$
  - top Yukawa coupling from the $t\bar{t}H$ cross section
  - Higgs self-coupling from $HH\nu\bar{\nu}$ cross section (improvements expected)
  - Higgs production in ZZ-fusion
- $\sqrt{s} = 3.0\,\text{TeV}$:
  - $H \to b\bar{b}$, $H \to c\bar{c}$, $H \to gg$, $H \to WW^*$, $H \to \mu^+\mu^-$
  - Higgs self-coupling from $HH\nu\bar{\nu}$ cross section (improvements expected)
- Final results expected in summer

M_h=120 GeV to 125 GeV

Cross sections at each energy

Calculate by whizard 1.95

E_{cm}	M_h	beam pol	σ(ffh)	σ(vvh)	σ(eeh)	σ(Zh)	beam param
250	120	P(-0.8,+0.3)	319.6	15.7	0.7	303.1	4 (RDR_ISR_on)
250	125	P(-0.8,+0.3)	319.4	15.9	0.5	303.0	22 (TDR_ws)
500	120	P(-0.8,+0.3)	269.3	159.7	8.6	101.1	2 (RDR)
500	125	P(-0.8,+0.3)	257.7	149.5	7.8	100.4	21 (TDR_ws)
1000	120	P(-0.8,+0.2)	458.5	409.6	22.9	26.0	18 (1000_B1b_ws)
1000	125	P(-0.8,+0.2)	447.5	399.5	22.4	25.6	18 (1000_B1b_ws)

Almost same cross section including beam parameter difference

Branching ratios (120 GeV w/ Pythia, 125 GeV w/ LHC Handbook BRs)

Mh (GeV)	bb	cc	gg	WW*	ZZ*	ττ	γγ	μμ	Zγ	ss
120 (LOI)	65.7%	3.6%	5.5%	15.0%	1.72%	8.0%	0.29%	0.03%	0.13%	0.03%
125 (DBD)	57.8%	2.7%	8.6%	21.6%	2.67%	6.4%	0.23%	0.02%	0.16%	0.04%

Calendrier / situation politique

(transparents volés à F.Lediberder)

Inaugural Speech by PM Abe
(Japanese version of 'State of the Union')
Feb 28, 2013

- 'Japan is driving global innovation in cutting-edge areas, including among others the world's first production test of marine methane hydrate, a globally unparalleled rocket launch success rate, and our attempts to develop the most advanced accelerator technology in the world.'

PM Abe at the 83rd session of Diet

Q&As at the Diet
Mar 4, 2013

PM Abe's answer on the ILC

'We will pull along the innovations through accelerator technologies that are at the global state-of-the-art. The ILC is part of it and it is a project that inspires great dreams. On the other hand, it requires a large amount of funding.'

'As the government, we will proceed checking the progress of the international design activities at researchers' level .'

Science-Industry Alliance

- 'Advanced Accelerator Association for promoting science and technology (AAA)'
  - Established in 2008
  - Headed by a former CEO of Mitsubishi Heavy Industries: Mr. Nishioka
  - Hitachi, Toshiba, Mitsubishi, etc.
  - ~90 industries + ~30 universities

Intensive activities:
- Lecture series, symposiums
- Civil engineering study
- Studies on large projects
- Science-industry cooperation
- …

Activities of the new Federation (Diet)

- General meetings
  - Feb 1. 2013 : re-establishing the federation
    Huge attendance:
    45 diet members and 25 proxies + researchers/companies
  - Feb 26, 2013 : re-organization
  - March 25, 2013 : talk by Lyn Evans (LC collaboration director).
  - Apr : two general meetings planned

- Mini-lecture series
  - eg: March 13, by Sakue Yamada etc.

- Visit Washington DC w/ two Ministers
  - Apr 30, 2013
  - goal : enlarge US-Japan collaboration on the ILC
  - Joint symposium US-Japan w/industries planned

Machine

Coûts

- Evaluation détaillée dans le TDR
  - Exprime en ILCU (=1$ 1er janvier 2012)

The Value estimate for the cost of the ILC design as presented in this *Technical Design Report*, averaged over the three regional sites, is 7,780 MILCU. This may be compared with the escalated RDR estimate of 7,266 MILCU.

- Machine:
  - Linac 68% -> cout précis grâce à XFEL
  - Béton -> 30% du cout ?
- Détecteur

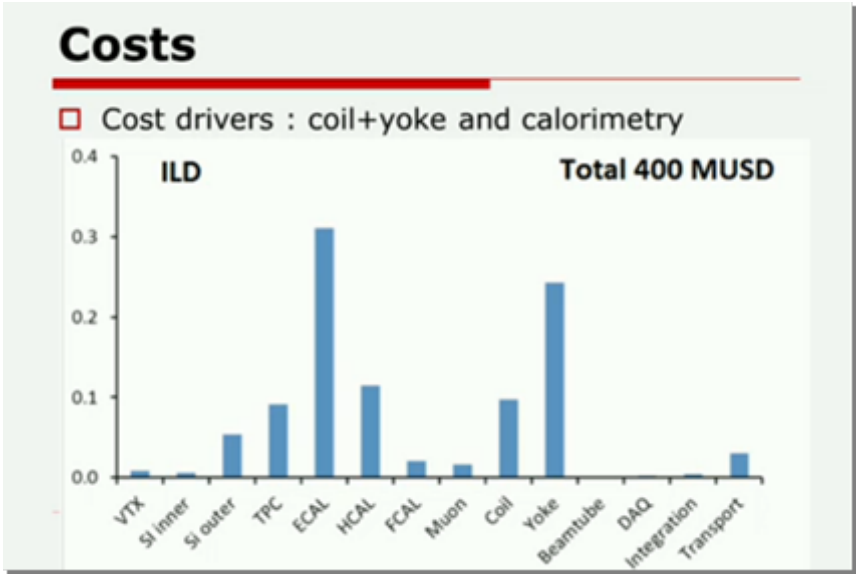

Included	Excluded
Construction, installation, and hardware commissioning costs for a 500 GeV machine	Beam commissioning, operations, decommissioning
Tooling-up industry, final engineering designs and construction management	Engineering, design, or preparation activities that can be accomplished before construction starts, such as research & development, and prototype systems tests
Construction of all conventional facilities, including the tunnels, surface buildings, access shafts and other facilities	Pre-construction costs (e.g. architectural engineering, conceptual and construction drawings, component and system designs), surface land acquisition and underground easement acquisition costs
Construction of the detector-assembly building, underground experimental halls and detector-access shafts	Experimental detectors
Explicit labour, including that for management and administrative personnel.	Taxes, contingency and escalation
Costs for upgrading the machine to 1 TeV which would be very difficult to provide after construction of the 500 GeV machine (e.g., beam dumps, BDS length).	Additional costs due to potential overheads related to management of in-kind contributions

Sites possibles

- Un site approprié
  - Site stable géologiquement sur 31km (50km)
  - Profondeur 50-400m
  - Absence de failles, sol granitique
  - Infrastructures (accès, etc.)
  - Soutien local et politique
- Un peu d'électricité...
  - 161MW @ 500GeV (286MW @ 1TeV)
- TDR: 5 sites envisagés:
  - Dubna
  - CERN
  - Kitakami (Sendai)
  - Sefuri (Fukuoka)
  - Fermilab
- Japon:
  - Choix entre les 2 sites: juillet 2013

- Kitakami site: located in Iwate prefecture (Tohoku district);
- Sefuri site: located in Fukuoka & Saga prefecture (Kyushu district).

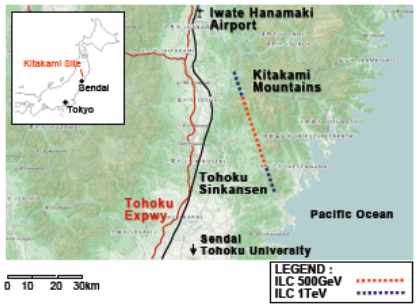

(a)

(b)

Figure 11.17
The potential location of ILC in the Geneva region.

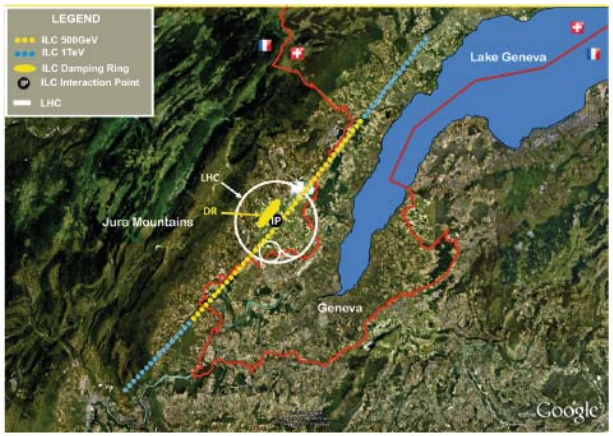

Real-World Challenges: Cost

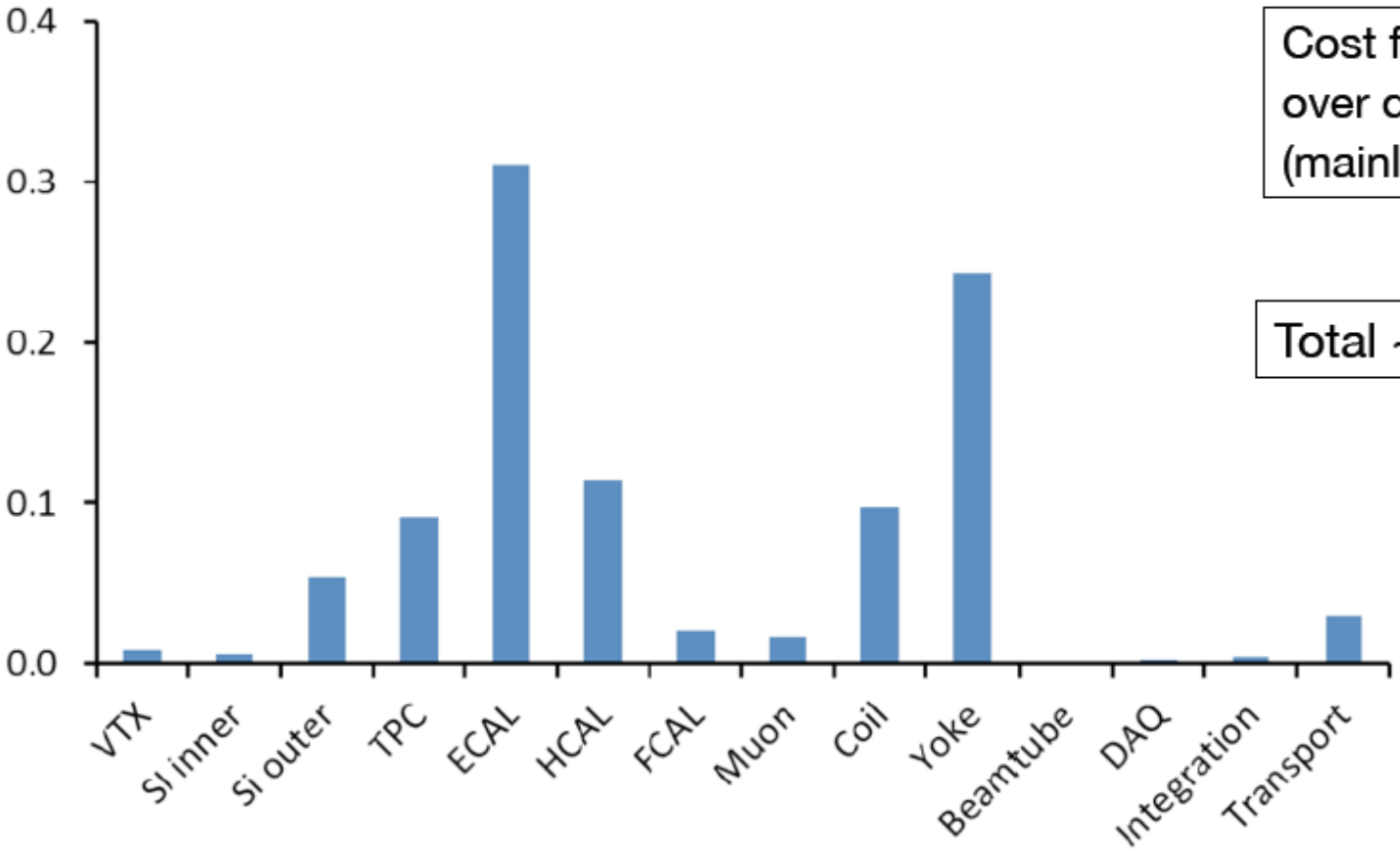

Cost fractions are averages over different options (mainly relevant for ECAL)

Total ~ 400 MUSD

- The distribution of the cost reflects the importance of particle flow in the detector design - Calorimeters account for ~ 50% of total cost

Remark on Photon collider Higgs factories

Photon collider can measure
$\Gamma(H\to\gamma\gamma)*Br(H\to bb, ZZ, WW)$, $\Gamma^2(H\to\gamma\gamma)/\Gamma_{tot}$, CP properties (using photon polarizations). In order to get $\Gamma(H\to\gamma\gamma)$ one needs $Br(H\to bb)$ from e+e-. This gives also Γ_{tot}.

e+e- can also measure Br(bb, cc, gg, ττ, μμ, invisible), Γ_{tot},
less backgrounds due to tagging of Z.

Therefore PLC is nicely motivated in combination with e+e-:
parallel work or second stage.

Physics motivation for PLC

(independent on physics scenario)
(shortly)

In $\gamma\gamma$, γe collisions compared to e^+e^-

1. the energy is smaller only by 10-20%
2. the number of events is similar or even higher
3. access to higher particle masses (H,A in $\gamma\gamma$, charged and light neutral SUSY in γe)
4. higher precision for some phenomena ($\Gamma\gamma\gamma$, CP-proper.)
5. different type of reactions (different dependence on theoretical parameters)

(Telnov, ECFA-DESY 2013)

Le tunnel

Figure 11.6
Equipment layout in the ML tunnel

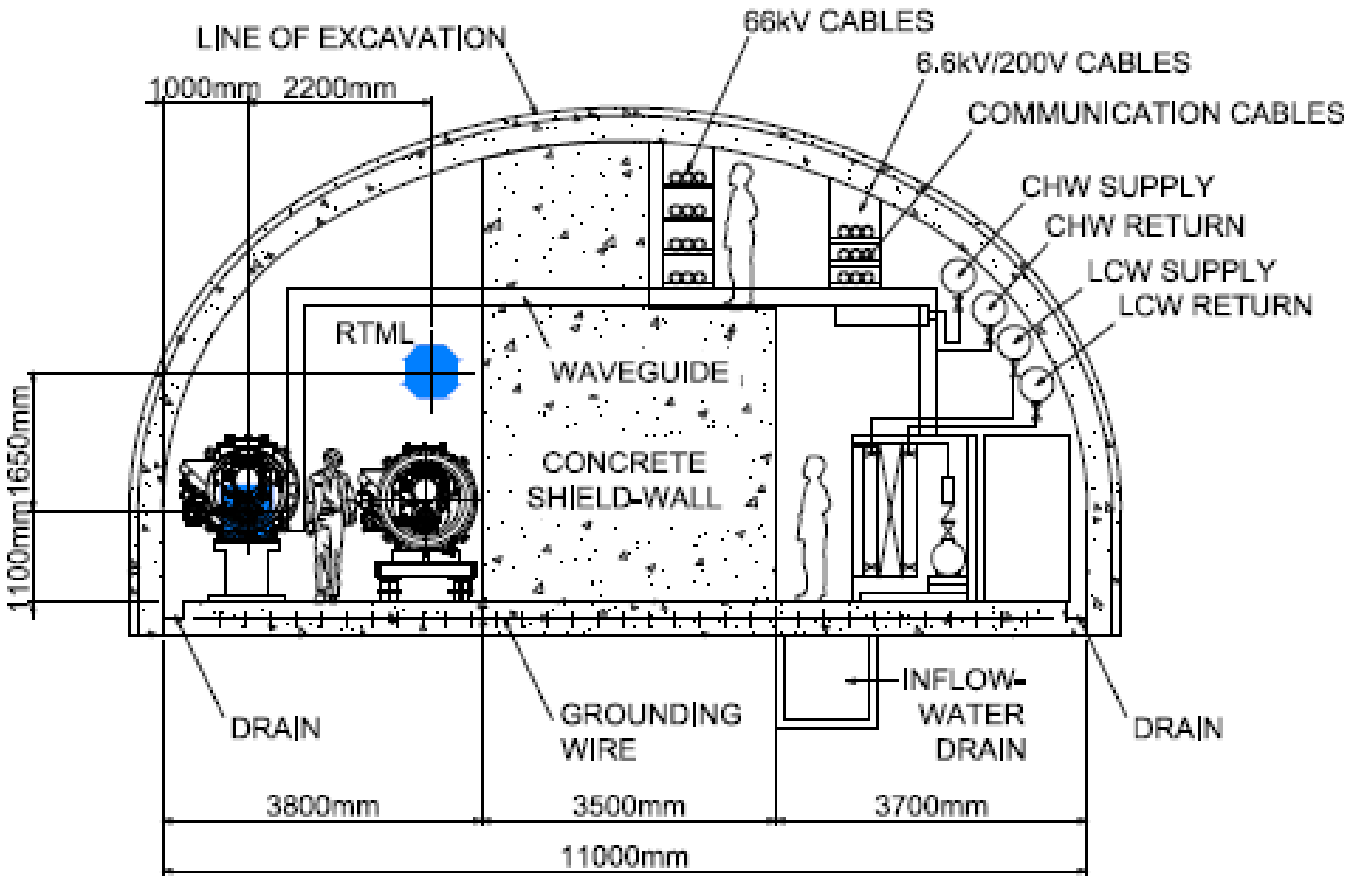

Calendrier Machine (TDR 2013)

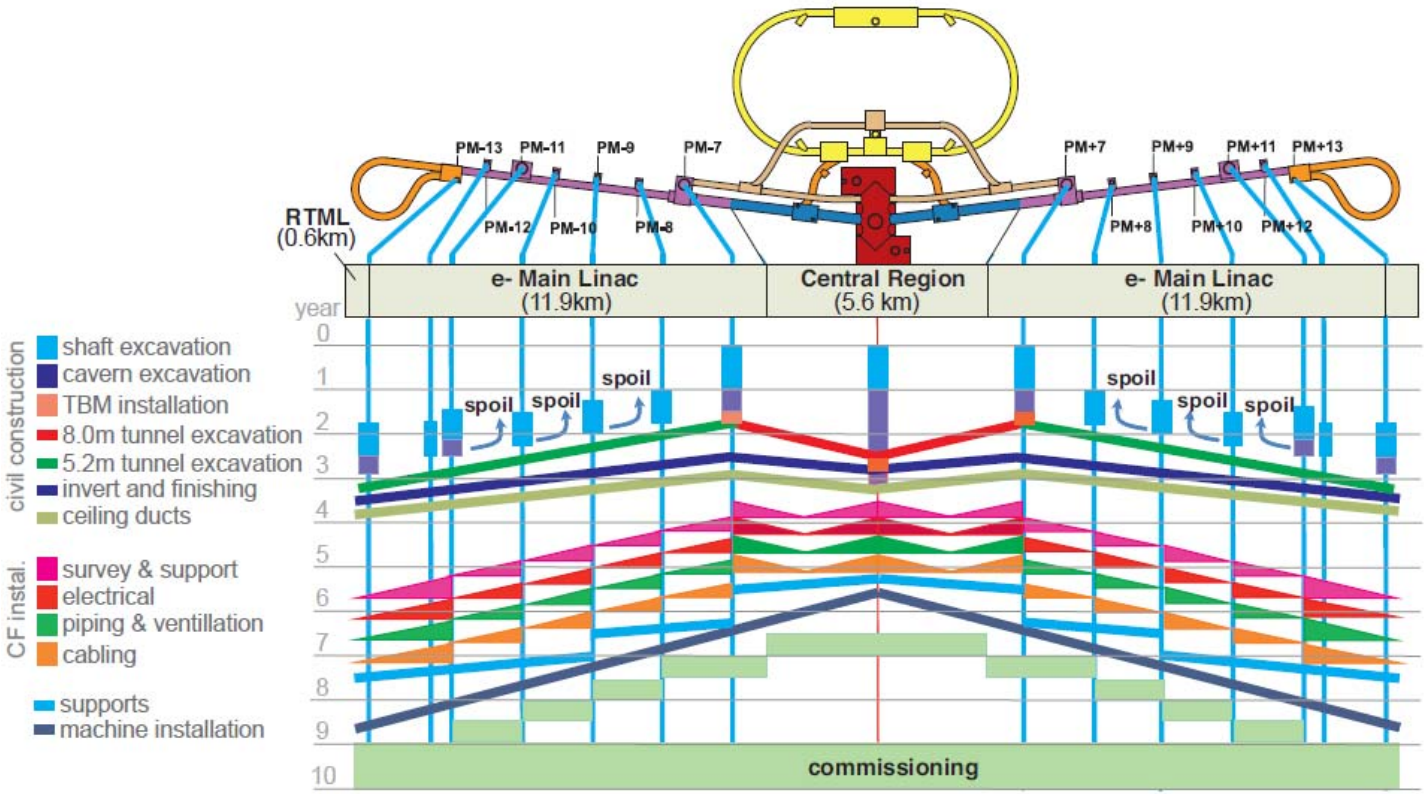

Table 14.7
The fourth set of level-1 milestones.

Milestone	Flat topography	Mountainous region
Civil Engineering work complete	Y4, Q4	Y5, Q1
Common Facilities installed	Y7, Q3	Y8, Q2
Accelerator ready for early commissioning (BDS and ML up to PM7/AH1)	Y7, Q2	Y8, Q2
ILC ready for full commissioning (whole accelerator available)	Y9, Q4	Y9, Q4
ILC ready for physics programme	Y10, Q4	Y10, Q4

Calendrier Zone d'interaction et detecteurs

Using the CMS concept, the ILD detector is to be assembled in a surface hall before being lowered to the underground facilities. This allows work underground to proceed unaffected by the construction of the detector.

Table 14.8
The fifth set of level-1 milestones.

Milestone	Flat topography	Mountainous region
Civil Engineering work complete	Y4, Q4	Y5, Q1
Common Facilities installed	Y7, Q3	Y8, Q2
Accelerator ready for early commissioning (BDS and ML up to PM7/AH1)	Y7, Q2	Y8, Q2
ILC ready for full commissioning (whole accelerator available)	Y9, Q4	Y9, Q4
ILC ready for beam	Y10, Q4	Y10, Q4
Caverns ready for beneficial occupancy	Y7, Q1	
Detector ready to be lowered	Y7, Q1	
Detector ready for commissioning with beam	Y8, Q3	

ILC

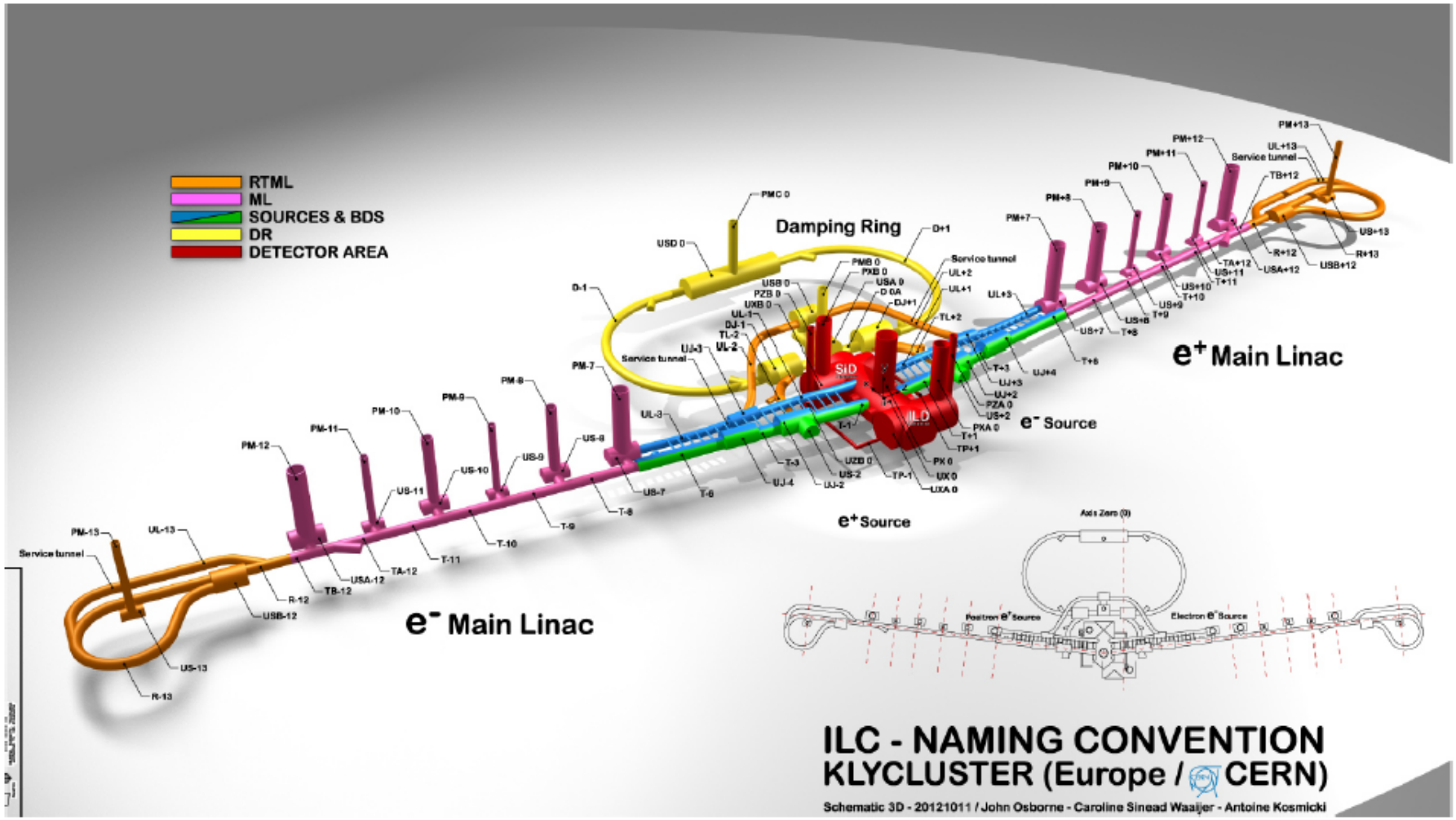
RTML
ML
SOURCES & BDS
DR
DETECTOR AREA
Damping Ring
e+ Main Linac
e- Main Linac
e- Source
e+ Source
SiD
ILD
Service tunnel
ILC - NAMING CONVENTION
KLYCLUSTER (Europe / CERN)
Schematic 3D - 20121011 / John Osborne - Caroline Sinead Waaijer - Antoine Kosmicki

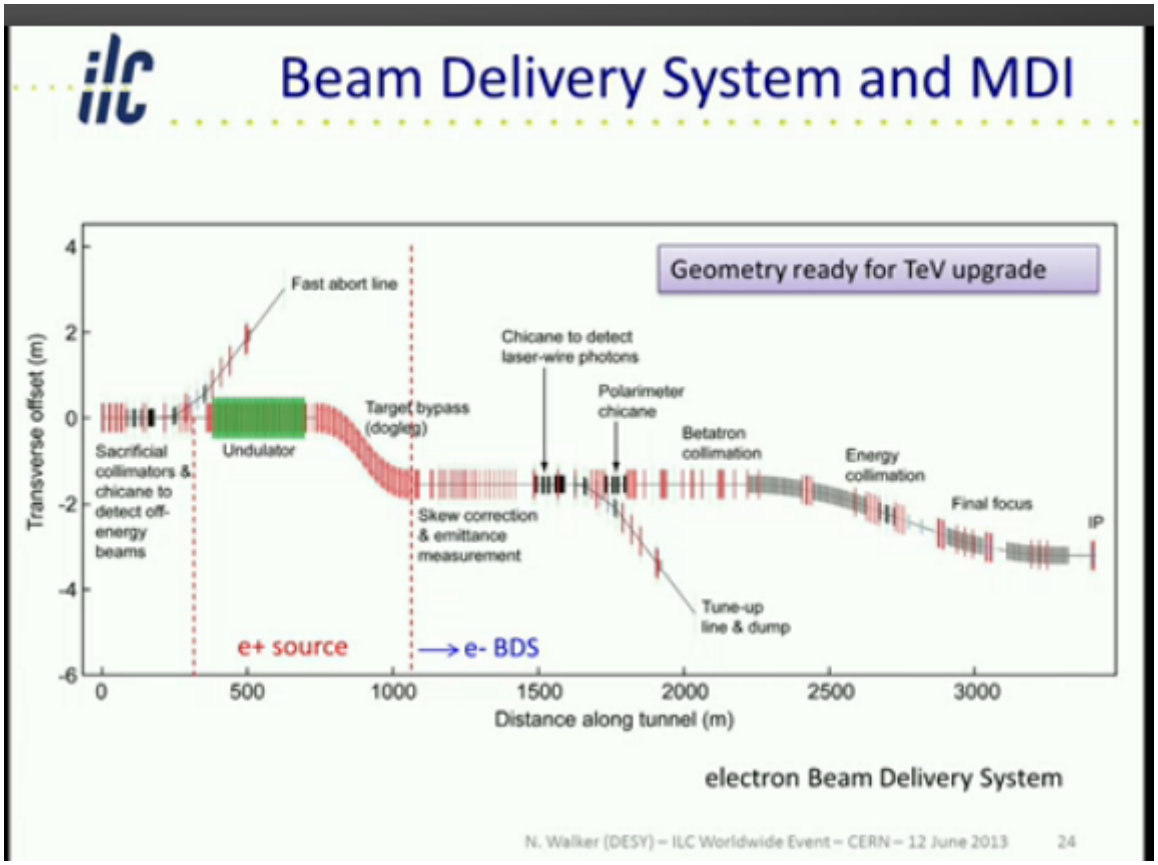
Beam Delivery System and MDI
Geometry ready for TeV upgrade
Fast abort line
Chicane to detect laser-wire photons
Polarimeter chicane
Target bypass (dogleg)
Betatron collimation
Energy collimation
Final focus
IP
Undulator
Sacrificial collimators & chicane to detect off-energy beams
Skew correction & emittance measurement
Tune-up line & dump
e+ source
e- BDS
Transverse offset (m)
Distance along tunnel (m)
electron Beam Delivery System
N. Walker (DESY) – ILC Worldwide Event – CERN – 12 June 2013
24

Gradient maximal

Quand on crée un champ accélérateur E_{acc} dans la cavité, on crée également des champs sur la surface interne de la cavité, qui prennent des valeurs maximales notées B_{pk} et E_{pk}

Pour que le niobium reste dans l'état supraconducteur, il faut que $\mathbf{B_{pk} < Bc_{RF}}$, sinon la cavité perd son caractère supraconducteur, et c'est le « quench »


shield wall removed
©Rey.Hori/KEK

Positron Source (central region)

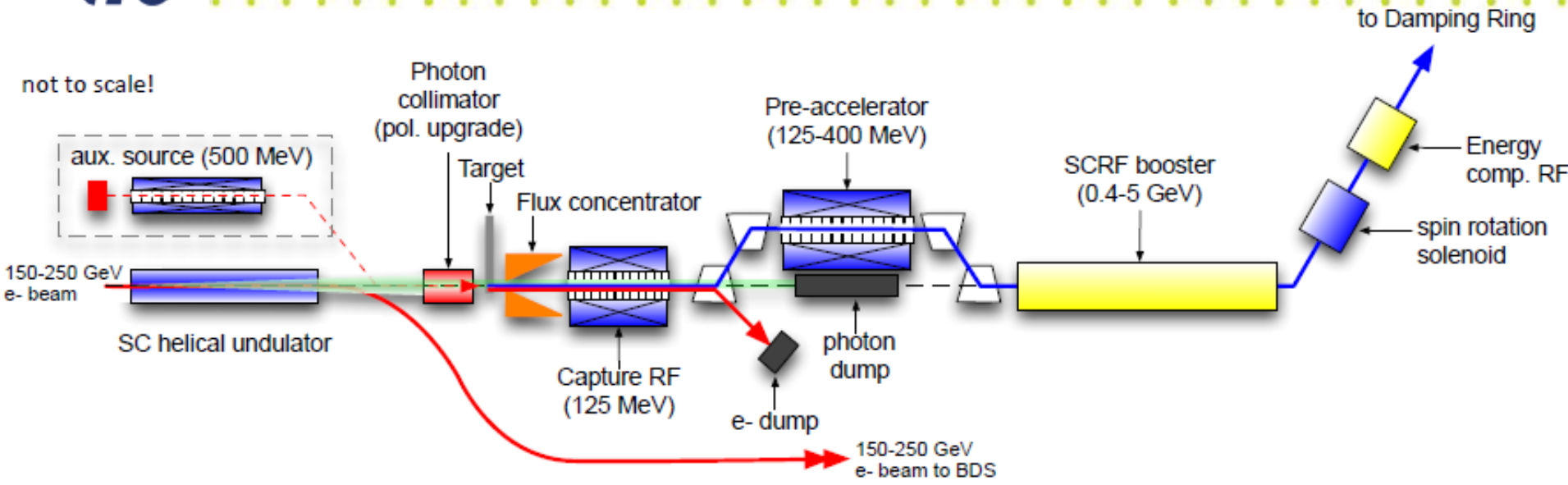

- located at exit of electron Main Linac
- 147m SC helical undulator
- driven by primary electron beam (150-250 GeV)
- produces ~30 MeV photons
- converted in thin target into e+e- pairs

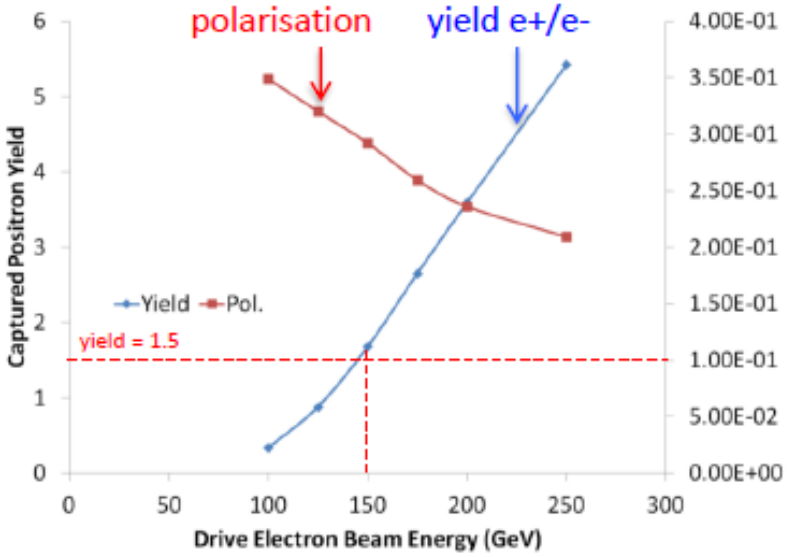

Damping Rings

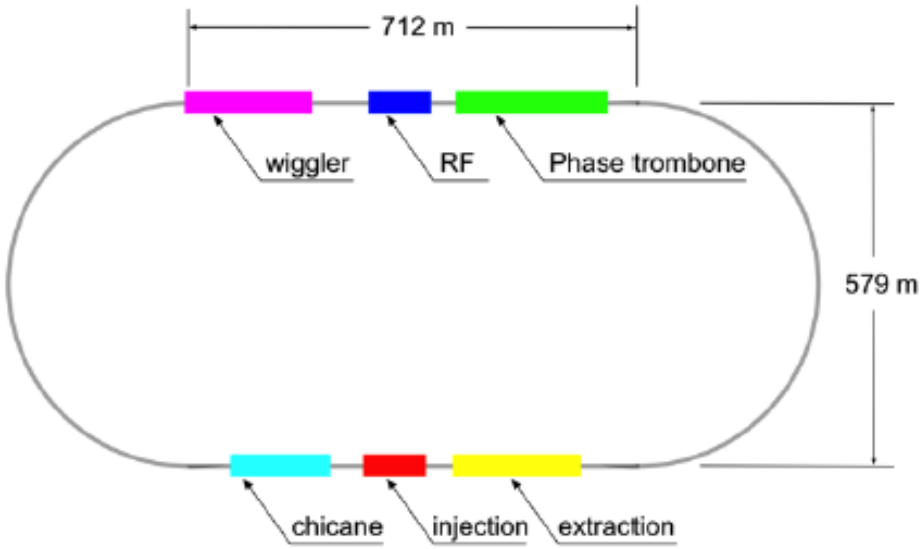

Circumference		3.2	km
Energy		5	GeV
RF frequency		650	MHz
Beam current		390	mA
Store time		200 (100)	ms
Trans. damping time		24 (13)	ms
Extracted emittance	x	5.5	μm
(normalised)	y	20	nm
No. cavities		10 (12)	
Total voltage		14 (22)	MV
RF power / coupler		176 (272)	kW
No.wiggler magnets		54	
Total length wiggler		113	m
Wiggler field		1.5 (2.2)	T
Beam power		1.76 (2.38)	MW

Values in () are for 10-Hz mode

Positron ring (upgrade)

Electron ring (baseline)

Positron ring (baseline)

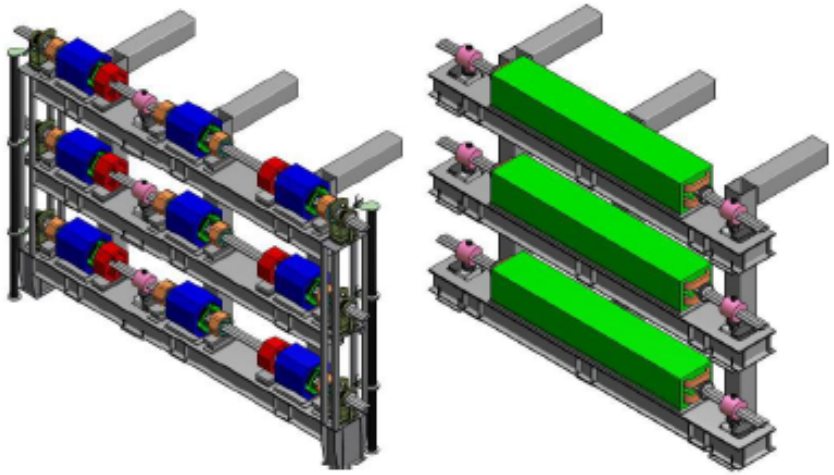

Arc quadrupole section

Dipole section

Many similarities to modern 3rd-generation light sources

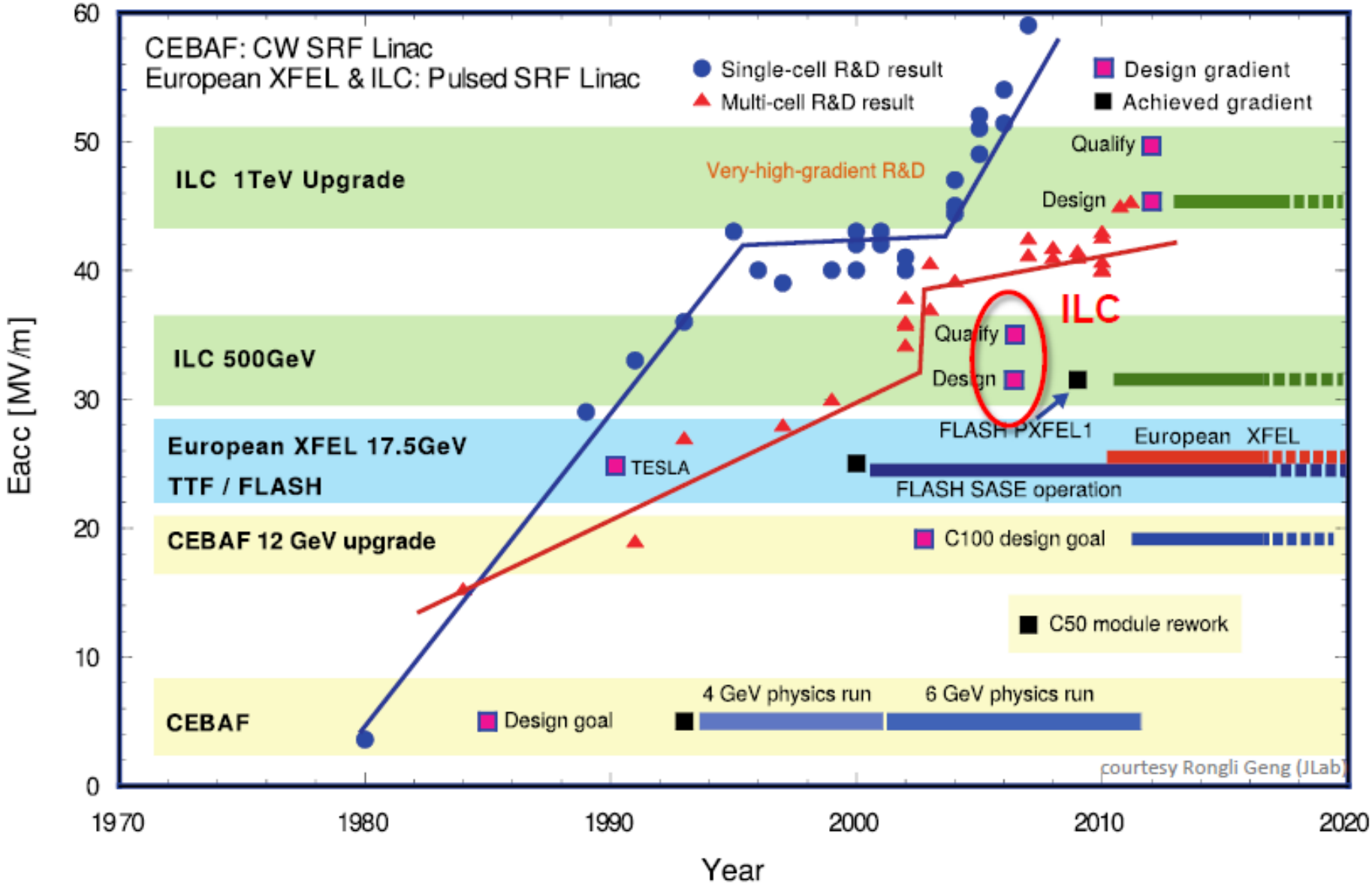
CEBAF: CW SRF Linac
European XFEL & ILC: Pulsed SRF Linac
Single-cell R&D result
Multi-cell R&D result
Design gradient
Achieved gradient
ILC 1TeV Upgrade
Very-high-gradient R&D
Qualify
Design
ILC
ILC 500GeV
Qualify
Design
European XFEL 17.5GeV
TTF / FLASH
TESLA
FLASH PXFEL1
European XFEL
FLASH SASE operation
CEBAF 12 GeV upgrade
C100 design goal
C50 module rework
CEBAF
Design goal
4 GeV physics run
6 GeV physics run
courtesy Rongli Geng (JLab)
Eacc [MV/m]
Year
0
10
20
30
40
50
60
1970
1980
1990
2000
2010
2020

the Big Jump from SLC to ILC:

In Beam Power (P_{beam}) X 100,
collision beam size (σ^*_y) 1/100
and Luminosity (L) X 10^4

SLC / ILC Comparison

	SLC	ILC	
E_{cm}	100	500	GeV
P_{beam}	0.04	5	MW
σ^*_y	500	6	nm
$\delta E/E_{bs}$	0.03	4	%
L	**3×10^{-4}**	**1.8**	**10^{34} cm^{-2}s^{-1}**

détecteurs

ILD - Dimensions

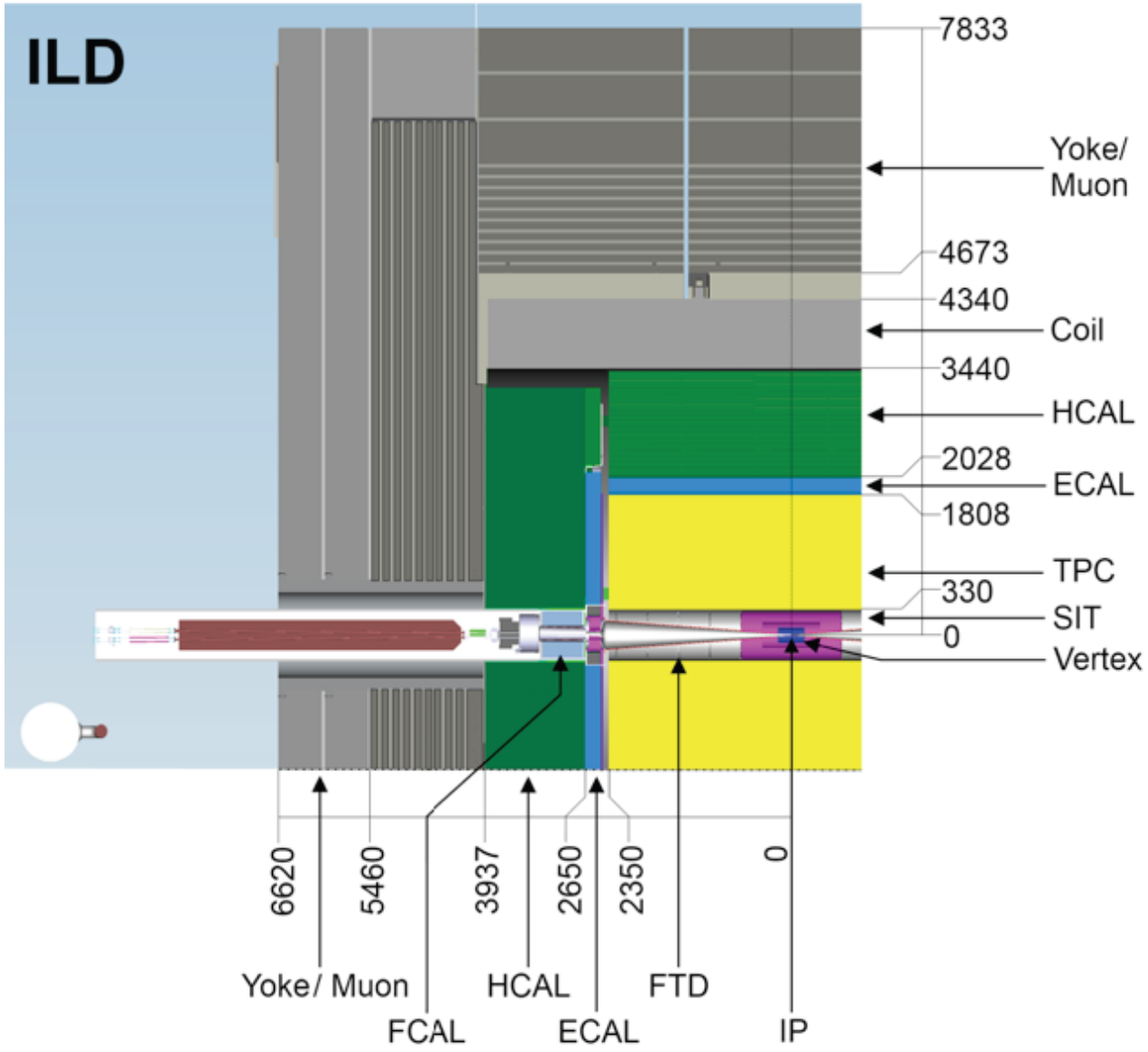

SiD / ILD

Common features

- Full **angular coverage** including for flavor tagging
- Large SC solenoidal magnetic field 'a la CMS' B>3 T ensuring excellent **momentum resolution**
- Almost 'transparent' trackers with calorimeters included inside the coil **minimizing material effects**
- **Imaging calorimetry** for PFA with a very large number of electronic channels($>10^8$)
- **Push-pull** philosophy insuring scientific and technical safety

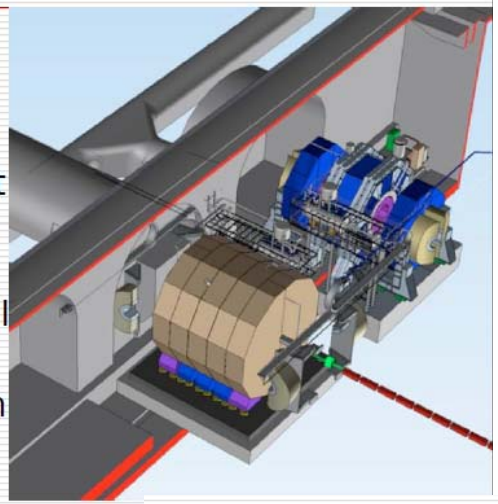

Differences

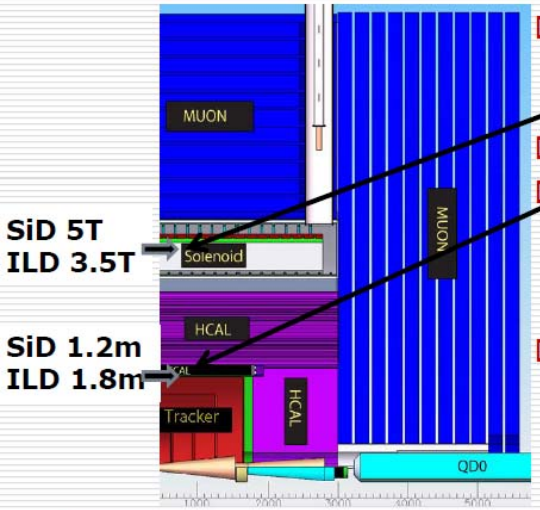

- Different B field & tracker radius achieving similar energy/momentum resolution
- 100% Silicon tracker for SiD
- ILD has a large volume gaseous tracker (TPC >>LEP) supplemented by silicon tracking
- Various calorimeter technologies are considered, ILD leaving open its final choice

Calorimetry Tree

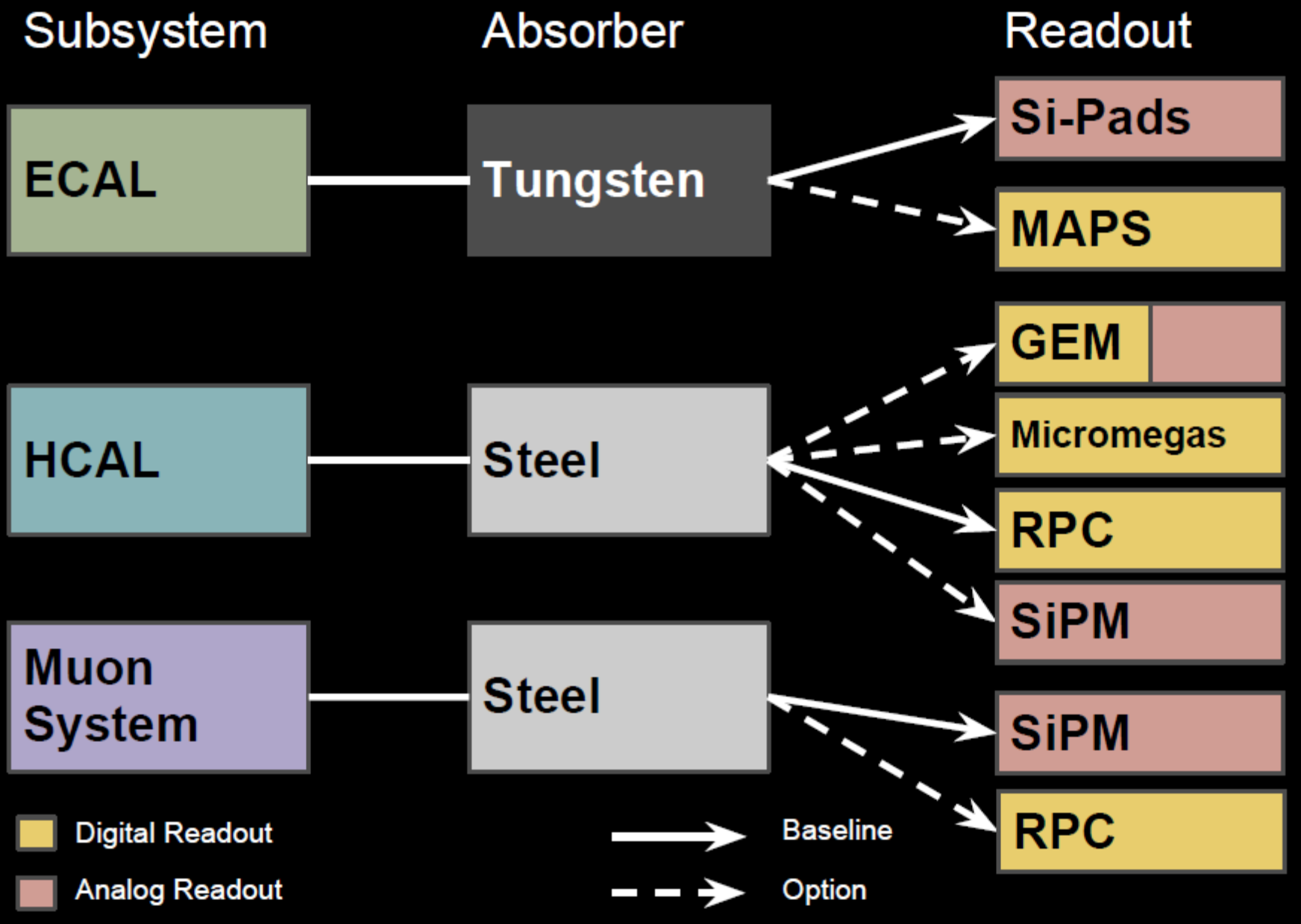

Capteurs CMOS pour le détecteur de vertex de l'ILD

- Cahier des charges:
  - Résolution spatiale/budget de $\sigma_b < 5 \oplus 10/p\beta \sin^{3/2}\theta \ \mu m.$
  - Occupation 1e couche: ~ 5 part/cm^2/BX ⇨ occupation de qqs % max
  - Radiations: O(100 krad) et O(1x10^{11} $n_{eq\ (1MeV)}$) / an
  - Puissance dissipée: 600W/12W (Power cycling, ~3% duty cycle)

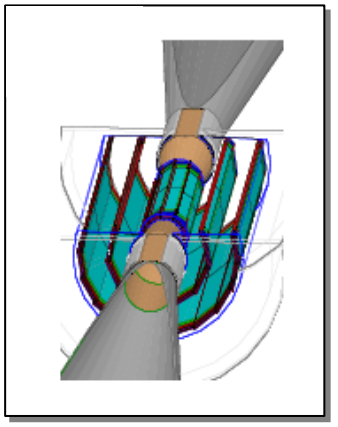

- Concept de base:
  - 3 x double couches
    - Gain budget matière / alignement.
- 2 lignes de développement:
  - Double Couche interne : priorité à la vitesse / résolution
    - Compromis vitesse vs résolution spatiale
    - 2 faces: optimisée resolution / optimisée vitesse (pixels allongés)
    - Pitch 16x16μm^2/ 16x64μm^2 + encodage binaire de la charge
    - $t_{read\text{-}out}$ ~ 50μs/10μs ; σ_{res} ~ 3 μm/6μm
  - Couches externes: priorité à la puissance dissipée
    - Compromis P_{diss} vs résolution spatiale
    - Pitch ~ 35x35 μm^2 + ADC 3-4 bits
    - $t_{read\text{-}out}$ ~ 100 μs

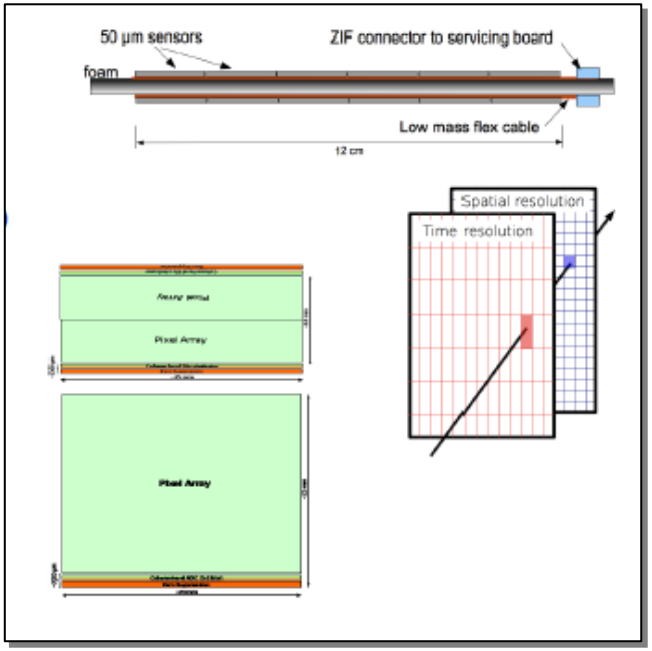

Détecteur de vertex

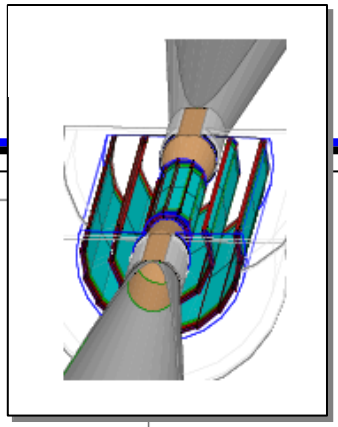

- Résolution sur le paramètre d'impact

$$\sigma_b < 5 \oplus 10/p\beta \sin^{3/2}\theta \ \mu m.$$

  - Résolution spatiale première couche
    - ~ 3 μm

- A spatial resolution near the IP better than 3 μm ;
- A material budget below 0.15%X_0/layer;
- A first layer located at a radius of $\sim$ 1.6 cm;
- A pixel occupancy not exceeding a few %, including backgrounds.

Table 2.1.1: ILD vertex detector parameters. The resolution and readout times are for the CMOS sensor option.

	R (mm)	$\|z\|$ (mm)	$\|\cos\theta\|$	σ (μm)	Readout time (μs)
Layer 1	16	62.5	0.97	2.8	50
Layer 2	18	62.5	0.96	6	10
Layer 3	37	125	0.96	4	100
Layer 4	39	125	0.95	4	100
Layer 5	58	125	0.91	4	100
Layer 6	60	125	0.9	4	100

Capteurs CMOS: Principes et état de l'art.

- Principes
  - Signal créé dans une couche épitaxiale
    - ~10-20 μm, faible dopage, faible résistivité
    - ~ 80 e- / μm ⇨charge totale ~ O(1000 e-)
  - Diffusion thermique des e-
    - zone déplétée limitée
  - Réflexion aux interface
    - substrats et P-well au dopage eleve
  - Charge collectee par des puits-N
    - Partage des charges entre les puits ⇨ résolution
  - Collecte continue des charges
    - pas de temps mort
- Avantages
  - Granularité
    - Pixels pitch jusqu'à 10 x 10 μm^2 si nécessaire (⇨résolution spatiale ~ 1 μm)
  - Budget de matière
    - Partie active ~ 10-20 μm
    - Amincissement jusqu'à 50 μm routinier
  - Prétraitement du signal dans le pixel
    - Compacité, flexibilité, flux de données
  - Fonctionnement
    - Jusqu'à ~30-40 °C si nécessaire
  - Production industrielle
    - Couts, rendements
    - rythme des soumissions (runs multiprojets)
    - évolution de la technologie

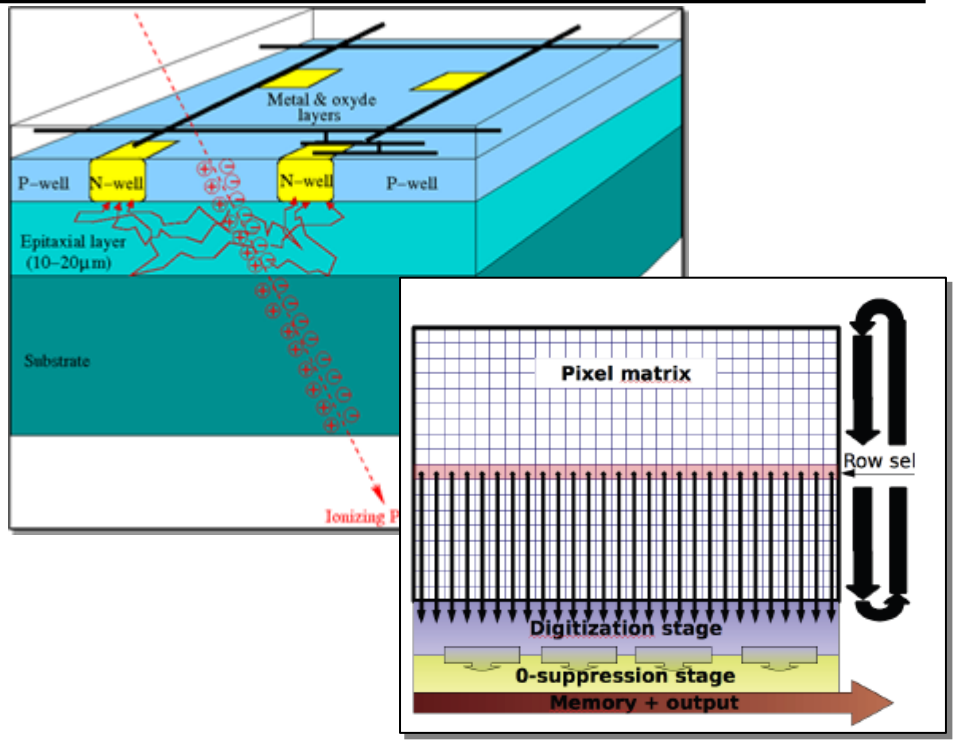

- Mode de lecture « volet roulant »
  - –Double échantillonnage corrélé dans le pixel (CDS)
  - –Préamplification dans le pixel
  - –Lecture parallèle des colonnes
    - ➢Temps de lecture = #lignes x $t_{r.o.}$ d'une ligne
  - –Discriminateurs en bout de colonne
  - –Sparsification en bout de colonne

⇨ Préserve granularité / budget matière

Etiquetage des saveurs b/c

- Etiquetage des b et de c
  - Simulation ILD.
  - Arbre de décision boosté
  - Echantillons
    - Z→qq et ZZZ→qqqqqq (tous de la même saveur)
  - 3 étiquetages: b (%udsc); c(udsb); c(%b)

- Major breakthroughs with respect to existing detectors with many available new technologies
- 1st layer at R<2cm (5cm at LEP)
- Detectors with very low material budget ~0.2% X0 per layer (~0.2mm Si) possible at ILC with low radiation
- Easy cooling with power pulsing
- Not only b/c separation is optimal but **b charge** determination becomes possible and very useful to measure t/b asymmetries

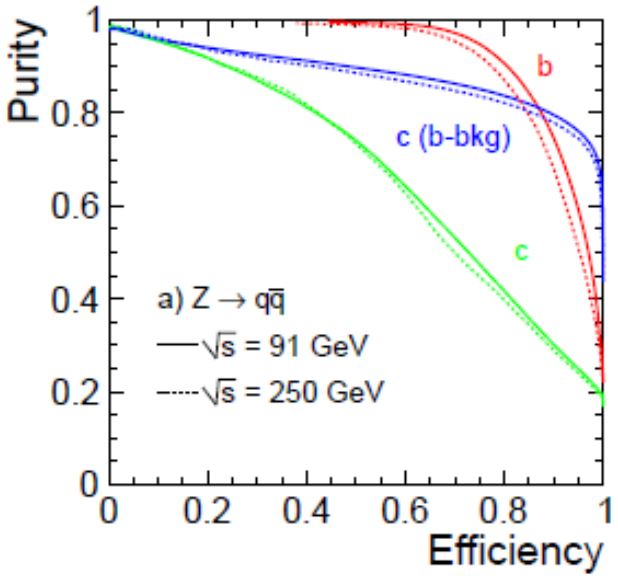

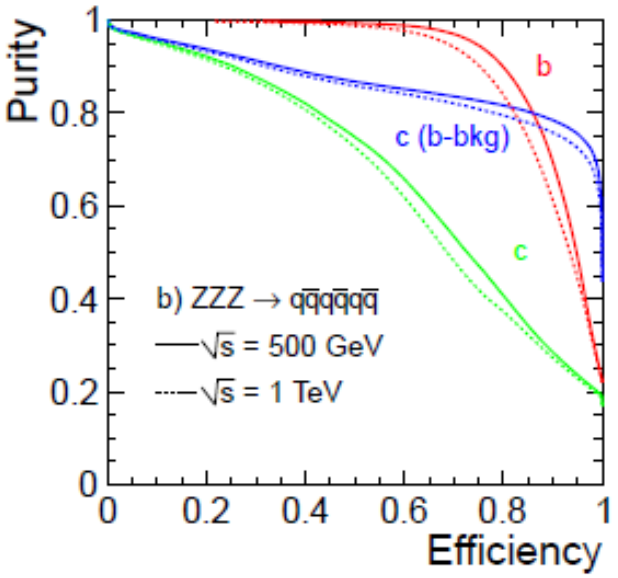

Dégradation modeste vs multiplicité et √s

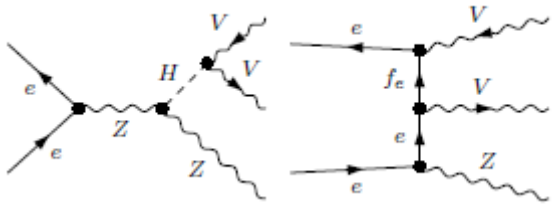

ILC Detectors Have Advanced Through This Development Process

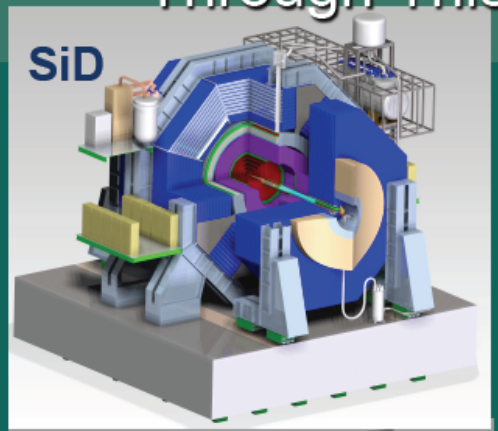

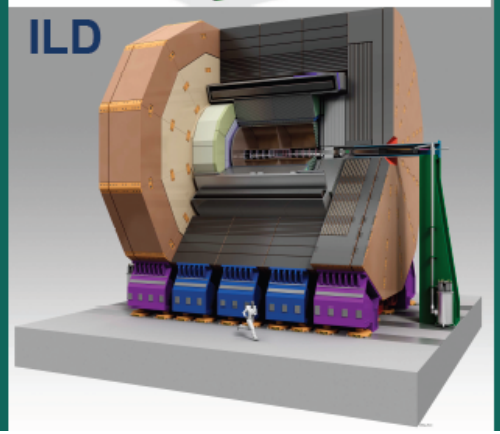

* Evolution of ILC detector concepts is captured in a series of documents

Detector Outline Document	2006
Detector Concept Report	2007
Letters of Intent (LoI)	2009
Detailed Baseline Design	2012

* Detector LoI (2009)

  Detailed detector description
  Status of critical R&D
  Full GEANT4 simulation
  Benchmark analyses
  Costs

* NOW– Detailed Baseline Design

  volume 4 of the ILC TDR

Beamstrahlung et occupation des détecteurs (ILD)

Sub-detector	Units	Layer	500 GeV	1000 GeV
VTX-DL	hits/cm^2/BX	1	6.320 ± 1.763	11.774 ± 0.992
		2	4.009 ± 1.176	7.479 ± 0.747
		3	0.250 ± 0.109	0.431 ± 0.128
		4	0.212 ± 0.094	0.360 ± 0.108
		5	0.048 ± 0.031	0.091 ± 0.044
		6	0.041 ± 0.026	0.082 ± 0.042
SIT	hits/cm^2/BX	1	0.0009 ± 0.0013	0.0016 ± 0.0016
		2	0.0002 ± 0.0003	0.0004 ± 0.0005
FTD	hits/cm^2/BX	1	0.072 ± 0.024	0.145 ± 0.024
		2	0.046 ± 0.017	0.102 ± 0.016
		3	0.025 ± 0.009	0.070 ± 0.009
		4	0.016 ± 0.005	0.046 ± 0.007
		5	0.011 ± 0.004	0.034 ± 0.005
		6	0.007 ± 0.004	0.024 ± 0.006
		7	0.006 ± 0.003	0.022 ± 0.006
SET	hits/BX	1	0.196 ± 0.924	0.588 ± 2.406
		2	0.239 ± 1.036	0.670 ± 2.616
TPC	hits/BX	-	216 ± 302	465 ± 356
ECAL	hits/BX	-	444 ± 118	1487 ± 166
HCAL	hits/BX	-	18049 ± 729	54507 ± 923

Etiquetage taus

- Taus

A neural network approach based on nine input variables is used to identify the tau decays modes. The variables include: the total energy of the identified photons, the invariant mass of the track and all identified photons (Figure III-6.7a); and electron and muon particle identification variables based on calorimetric information and track momentum.

Table III-6.3
Purity and efficiency of the main tau decay mode selections.

Mode	Efficiency	Purity
$e\nu\nu$	98.9 %	98.9 %
$\mu\nu\nu$	98.8 %	99.3 %
$\pi\nu$	96.0 %	89.5 %
$\rho\nu$	91.6 %	88.6 %
$a_1\nu$ (1-prong)	67.5 %	73.4 %
$a_1\nu$ (3-prong)	91.1 %	88.9 %

Table III-6.3 shows the efficiency and purity achieved for the six main tau decay modes. The selection efficiency is calculated with respect to the sample of $\tau^+\tau^-$ after the requirement that the two tau candidates are almost back-to-back. The purity only includes the contamination from other $\tau^+\tau^-$ decays. The high granularity and the large detector radius of ILD results in excellent separation.

ILD: TPC

Table III-2.4 Performance and design parameters for the TPC with standard electronics and pad readout.

Parameter	
Geometrical parameters	r_{in} r_{out} z 329 mm 1808 mm $\pm$ 2350 mm
Solid angle coverage	up to $\cos\theta \simeq 0.98$ (10 pad rows)
TPC material budget	$\simeq 0.05\ X_0$ including outer fieldcage in r $< 0.25\ X_0$ for readout endcaps in z
Number of pads/timebuckets	$\simeq$ 1-2 $\times\ 10^6$/1000 per endcap
Pad pitch/ no.padrows	$\simeq 1\times$ 6 mm^2 for 220 padrows
σ_{point} in $r\phi$	$\simeq$ 60 μm for zero drift, $<$ 100 μm overall
σ_{point} in rz	$\simeq 0.4 - 1.4$ mm (for zero – full drift)
2-hit resolution in $r\phi$	$\simeq 2$ mm
2-hit resolution in rz	$\simeq 6$ mm
dE/dx resolution	$\simeq 5$ %
Momentum resolution at B=3.5 T	$\delta(1/p_t) \simeq 10^{-4}$/GeV/c (TPC only)

Higgs

Higgs sector parameters

The Higgs mass and the vacuum expectation value of the Higgs field can be written in terms of the two free parameters of the Higgs potential $V = \frac{1}{2}\mu^2\Phi^2 + \frac{1}{4}\lambda\Phi^4$:

$$v^2 = \frac{\mu^2}{2\lambda} \qquad M_H^2 = 2v^2\lambda$$

Also, since $$\frac{G_F}{\sqrt{2}} = \frac{g^2}{8M_W^2} = \frac{1}{2v^2}$$

the well measured value of G_F gives: $v = (\sqrt{2}G_F)^{-1/2} = 246\ \text{GeV}$

$\Rightarrow$ typical scale of EW symmetry breaking!

After choosing the vacuum: $M_{W^\pm} = gv/2$ and $M_Z = \frac{1}{2}v(g'^2+g^2)^{1/2}$

$$\Rightarrow \quad \frac{M_W}{M_Z} = \frac{g'}{(g^2+g'^2)^{1/2}} = \cos\theta_W \qquad \text{(prediction!!)}$$

Higgs Br

A. Denner, S. Heinemeyer, I. Puljak, D. Rebuzzi and M. Spira, Eur. Phys. J. C 71, 1753 (2011) [arXiv:1107.5909 [hep-ph]].

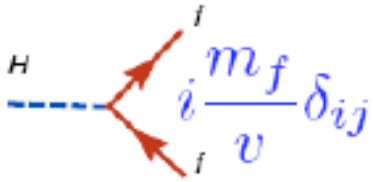

$$i\frac{m_f}{v}\delta_{ij}$$

$$\Gamma\left(H \to f\bar{f}\right) = \frac{M_H}{8\pi}\left(\frac{M_f}{v}\right)^2 N_c \left(1 - \frac{4M_f^2}{M_H^2}\right)^{\frac{3}{2}}$$

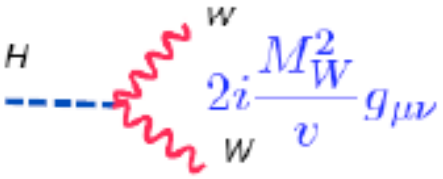

$$2i\frac{M_W^2}{v}g_{\mu\nu}$$

$$\Gamma\left(H \to WW\right) = \frac{M_H}{16\pi}\left(\frac{M_H}{v}\right)^2 \left(1 - \frac{4M_W^2}{M_H^2}\right)^{\frac{1}{2}} \times \left[1 - 4\left(\frac{M_W^2}{M_H^2}\right) + 12\left(\frac{M_W^2}{M_H^2}\right)^2\right]$$

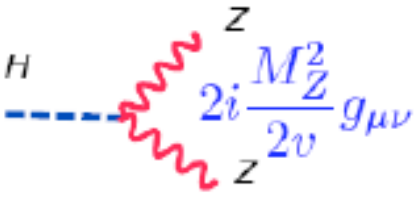

$$2i\frac{M_Z^2}{2v}g_{\mu\nu}$$

$$\Gamma\left(H \to ZZ\right) = \frac{M_H}{32\pi}\left(\frac{M_H}{v}\right)^2 \left(1 - \frac{4M_Z^2}{M_H^2}\right)^{\frac{1}{2}} \times \left[1 - 4\left(\frac{M_Z^2}{M_H^2}\right) + 12\left(\frac{M_Z^2}{M_H^2}\right)^2\right]$$

Higgs self coupling

$$\mathcal{L} = \mathcal{L}_{free} + \mathcal{L}_{int} \tag{10}$$

The free lagrangian contains the terms,

$$\mathcal{L}_{free} = \frac{1}{2}\partial_\mu H \partial^\mu H - m_H^2 H^2 - \frac{1}{4} F_{\mu\nu} F^{\mu\nu} + q^2 v^2 A_\mu A^\mu \tag{11}$$

while the lagrangian that includes the interactions is,

$$\mathcal{L}_{int} = q^2 A_\mu A^\mu \left(\sqrt{2} v H + \frac{1}{2} H^2 \right) - \lambda \left(\sqrt{2} v H^3 + \frac{1}{4} H^4 \right) \tag{12}$$

From the free lagrangian in eq. (11) we see that the Higgs boson H has a mass proportional to the quartic self coupling λ. In addition, a mass has been generated for the gauge boson $m_A = 2q^2 v^2$, which is proportional to the Higgs vev. Notice that this mass cannot be included by hand in the lagrangian since it is not gauge invariant.

Schematically, the interactions in eq. (12) are represented by the following Feynman rules,

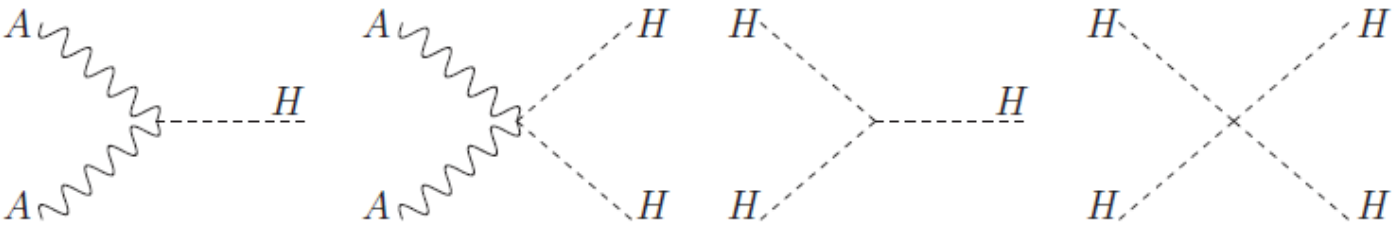

200-500 GeV baseline parameters (TDR 2013)

Table 2.1. Summary table of the 200–500 GeV baseline parameters for the ILC. The reported luminosity numbers are results of simulation [12]

Centre-of-mass energy	E_{CM}	GeV	200	230	250	350	500
Luminosity pulse repetition rate		Hz	5	5	5	5	5
Positron production mode			10 Hz	10 Hz	10 Hz	nom.	nom.
Estimated AC power	P_{AC}	MW	114	119	122	121	163
Bunch population	N	$\times 10^{10}$	2	2	2	2	2
Number of bunches	n_b		1312	1312	1312	1312	1312
Linac bunch interval	Δt_b	ns	554	554	554	554	554
RMS bunch length	σ_z	μm	300	300	300	300	300
Normalized horizontal emittance at IP	$\gamma\epsilon_x$	μm	10	10	10	10	10
Normalized vertical emittance at IP	$\gamma\epsilon_y$	nm	35	35	35	35	35
Horizontal beta function at IP	β_x^*	mm	16	14	13	16	11
Vertical beta function at IP	β_y^*	mm	0.34	0.38	0.41	0.34	0.48
RMS horizontal beam size at IP	σ_x^*	nm	904	789	729	684	474
RMS vertical beam size at IP	σ_y^*	nm	7.8	7.7	7.7	5.9	5.9
Vertical disruption parameter	D_y		24.3	24.5	24.5	24.3	24.6
Fractional RMS energy loss to beamstrahlung	δ_{BS}	%	0.65	0.83	0.97	1.9	4.5
Luminosity	L	$\times 10^{34}$ cm^{-2} s^{-1}	0.56	0.67	0.75	1.0	1.8
Fraction of L in top 1% E_{CM}	$L_{0.01}$	%	91	89	87	77	58
Electron polarisation	P_-	%	80	80	80	80	80
Positron polarisation	P_+	%	30	30	30	30	30
Electron relative energy spread at IP	$\Delta p/p$	%	0.20	0.19	0.19	0.16	0.13
Positron relative energy spread at IP	$\Delta p/p$	%	0.19	0.17	0.15	0.10	0.07

„Required“ accuracy

$$\frac{g_{hVV}}{g_{h_{\rm SM}VV}} \simeq 1 - 0.3\% \left(\frac{200\ {\rm GeV}}{m_A}\right)^4$$
$$\frac{g_{htt}}{g_{h_{\rm SM}tt}} = \frac{g_{hcc}}{g_{h_{\rm SM}cc}} \simeq 1 - 1.7\% \left(\frac{200\ {\rm GeV}}{m_A}\right)^2$$
$$\frac{g_{hbb}}{g_{h_{\rm SM}bb}} = \frac{g_{h\tau\tau}}{g_{h_{\rm SM}\tau\tau}} \simeq 1 + 40\% \left(\frac{200\ {\rm GeV}}{m_A}\right)^2 . \qquad (13)$$

At the lower end of the range, the LHC experiments should see the deviation in the hbb or $h\tau\tau$ coupling. However, the heavy MSSM Higgs bosons can easily be as heavy as a TeV without fine tuning of parameters. In this case, the deviations of the gauge and up-type fermion couplings are well below the percent level, while those of the Higgs couplings to b and τ are at the percent level,

$$\frac{g_{hbb}}{g_{h_{\rm SM}bb}} = \frac{g_{h\tau\tau}}{g_{h_{\rm SM}\tau\tau}} \simeq 1 + 1.7\% \left(\frac{1\ {\rm TeV}}{m_A}\right)^2 . \qquad (14)$$

$$\frac{g_{hVV}}{g_{h_{\rm SM}VV}} \simeq 1 - 3\% \left(\frac{1\ {\rm TeV}}{f}\right)^2$$

$$\frac{g_{hff}}{g_{h_{\rm SM}ff}} \simeq \begin{cases} 1 - 3\% \left(\frac{1\ {\rm TeV}}{f}\right)^2 & ({\rm MCHM4}) \\ 1 - 9\% \left(\frac{1\ {\rm TeV}}{f}\right)^2 & ({\rm MCHM5}). \end{cases}$$

$$\frac{g_{hgg}}{g_{h_{\rm SM}gg}} \simeq 1 + 1.4\% \left(\frac{1\ {\rm TeV}}{m_T}\right)^2 , \qquad \frac{g_{h\gamma\gamma}}{g_{h_{\rm SM}\gamma\gamma}} \simeq 1 - 0.4\% \left(\frac{1\ {\rm TeV}}{m_T}\right)^2 , \qquad (17)$$

and for a fermionic top-partner,

$$\frac{g_{hgg}}{g_{h_{\rm SM}gg}} \simeq 1 + 2.9\% \left(\frac{1\ {\rm TeV}}{m_T}\right)^2 , \qquad \frac{g_{h\gamma\gamma}}{g_{h_{\rm SM}\gamma\gamma}} \simeq 1 - 0.8\% \left(\frac{1\ {\rm TeV}}{m_T}\right)^2 . \qquad (18)$$

b-tagging CMS vs ILD

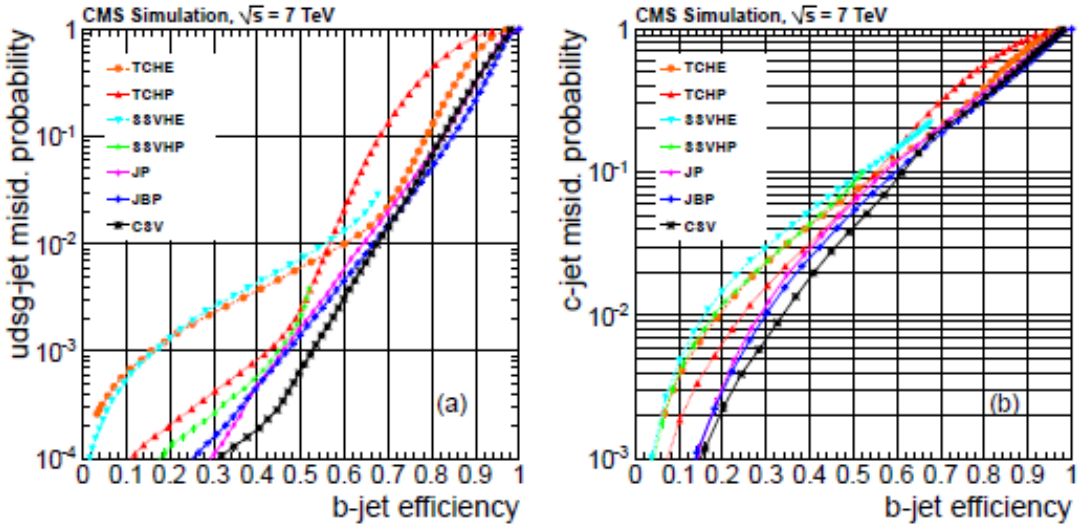

Figure 6. Performance curves obtained from simulation for the algorithms described in the text. (a) light-parton- and (b) c-jet misidentification probabilities as a function of the b-jet efficiency. Jets with $p_T >$ 60 GeV/c in a sample of simulated multijet events are used to obtain the efficiency and misidentification probability values.

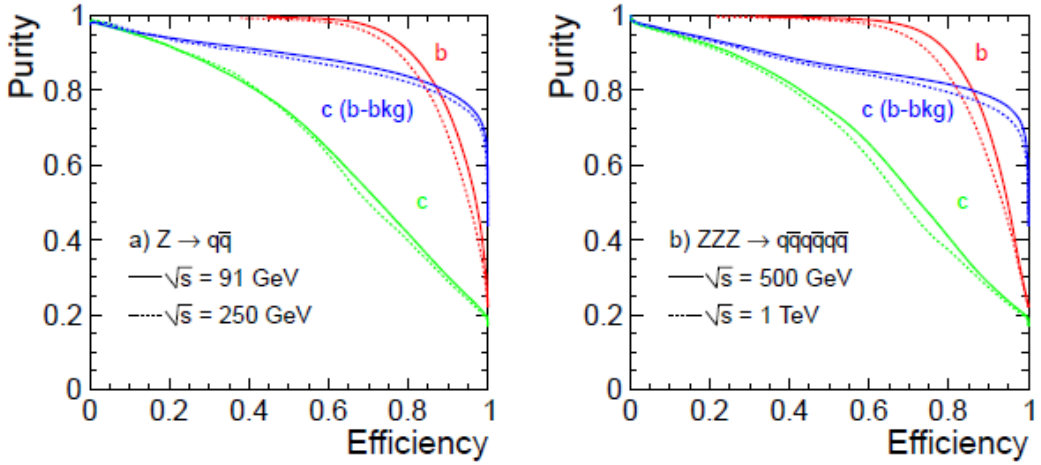

Higgstrahlung: theta distribution

$$\frac{\mathrm{d}\sigma(\mathrm{e}^+\mathrm{e}^- \to ZH)}{\mathrm{d}cos\theta} \sim \lambda^2 sin^2\theta + 8M_Z^2/s \ ,$$

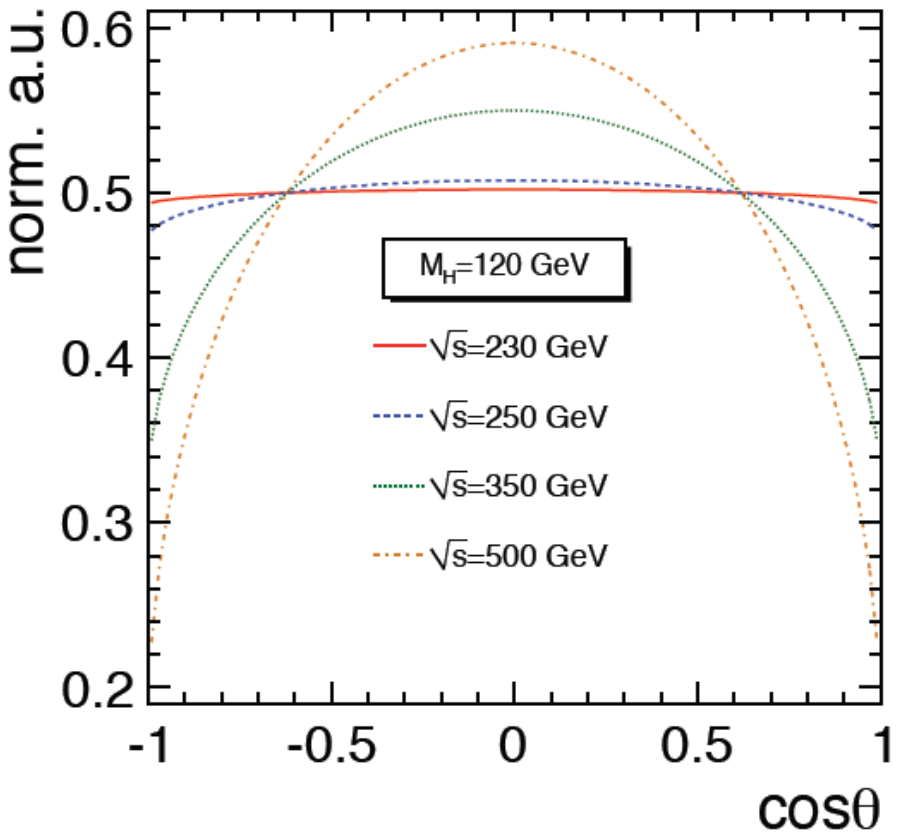

Electro-weak fit with Giga-Z

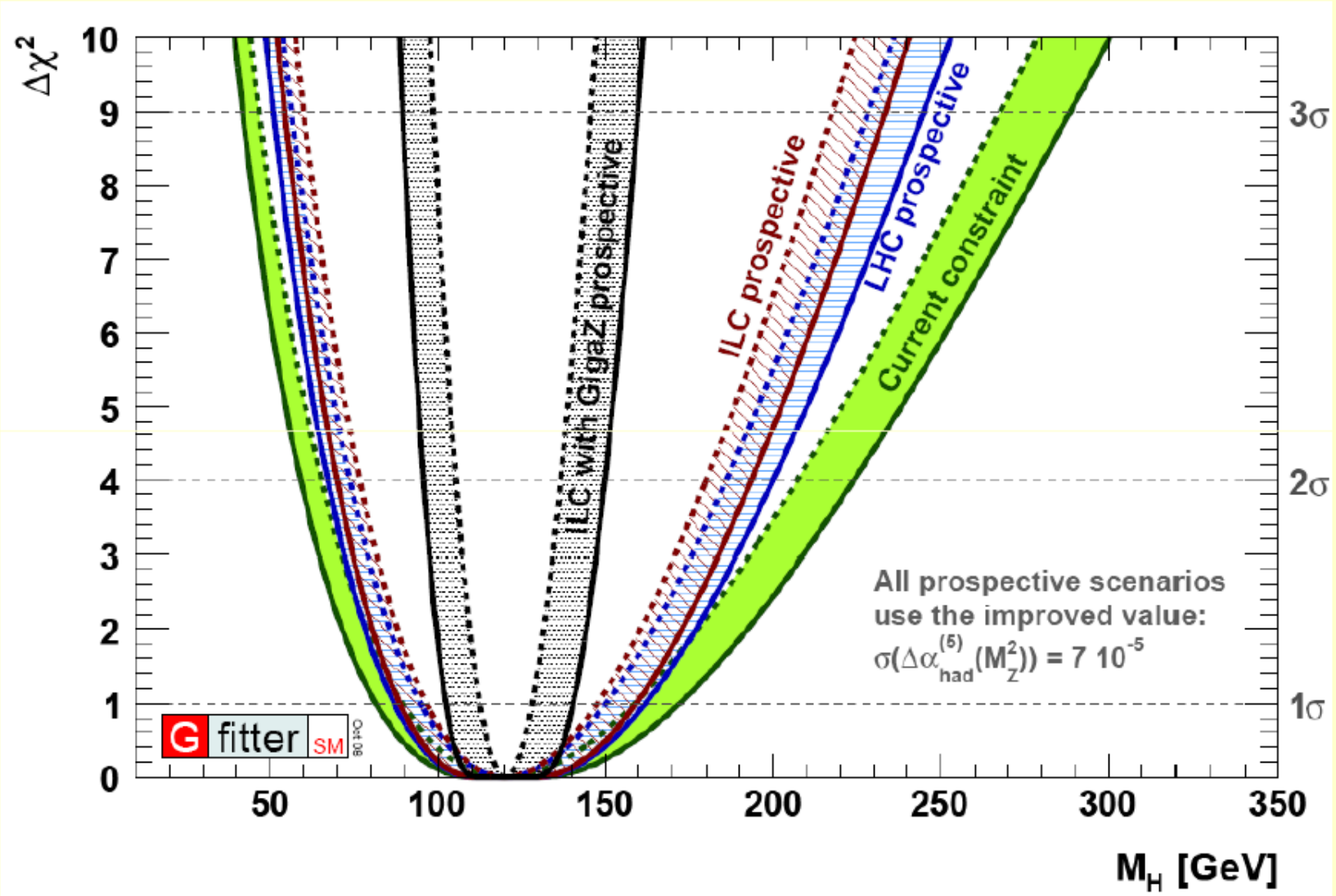

[Flächer, Goebel, Haller, Höcker, Mönig, Stelzer 08]

Triple Higgs coupling et λ

Sensitivity to triple Higgs coupling λ: [taken from K. Fujii '13]

$ZHHH$@500 GeV

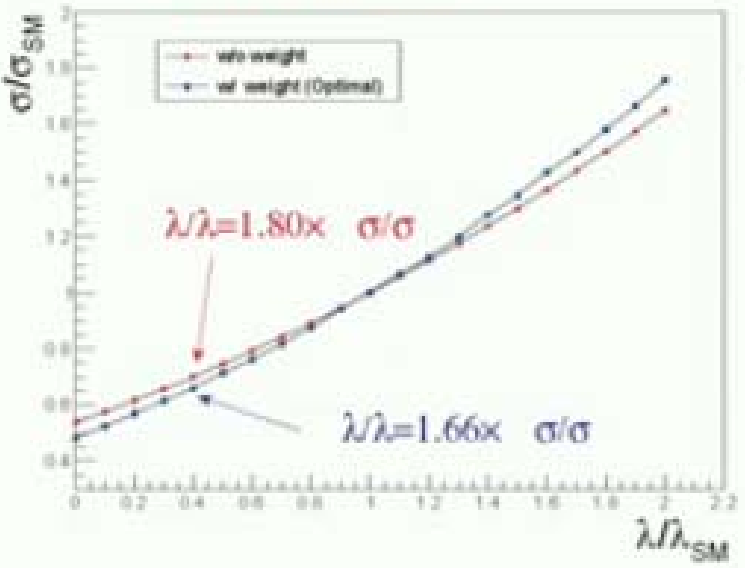

$\nu\bar{\nu}HHH$@1000 GeV

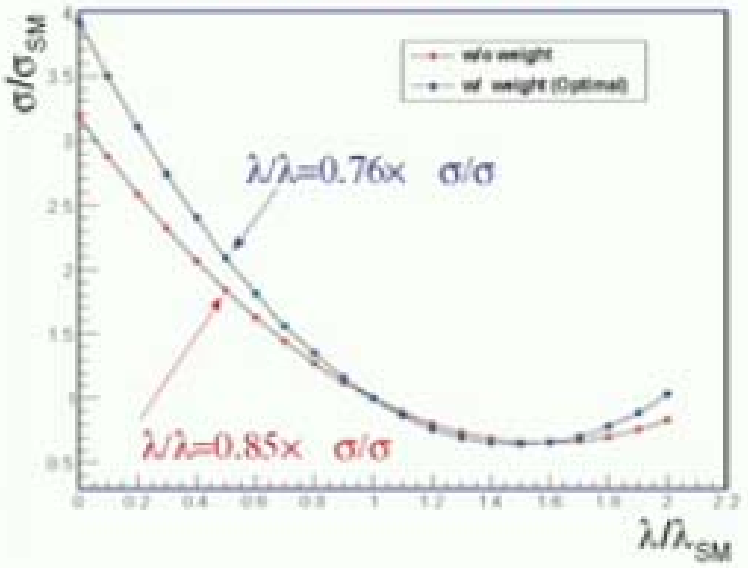

⇒ currently full simulations are performed

Expected sensitivity on λ: ~21% ($2\,ab^{-1}$ @ 1000 GeV) [ILC TDR '13]

Sven Heinemeyer (CSIC, Spain) ILC TDR Launch, CERN, 12.06.2013 14

Top

Top: Pole mass

What is the top mass?

Particle masses are not direct physical observables
one can only measure cross sections, decay rates, ...

Additional problem for the top mass:

what is the mass of a colored object?

Top pole mass is not IR safe (affected by large long-distance contributions), cannot be determined to better than $\mathcal{O}(\Lambda_{QCD})$

Measurement of m_t:

- At Tevatron, LHC:
  kinematic reconstruction, fit to invariant mass distribution
  $\Rightarrow$ "MC" mass, close to "pole" mass?
- At the ILC: unique possibility
  threshold scan $\Rightarrow$ threshold mass $\Rightarrow$ **SAFE!**
  transition to other mass definitions possible, $\delta m_t \lesssim 100$ GeV

Sven Heinemeyer (CSIC, Spain) ILC TDR Launch, CERN, 12.06.2013 *18*